



UNIVERSITÀ DEGLI STUDI DI MILANO

University of Milan

Department of Agricultural and Environmental Sciences

Production, Landscape, Agroenergy

PhD Course of:
Agriculture, Environment and Bioenergy
(XXIX cycle)

Insight into grapevine (*Vitis vinifera*) genetic resources from Caucasus using an integrative approach

Thesis supervisor

Dr. Osvaldo Failla

Università degli studi di Milano

Thesis co-supervisor

Dr. Maria Stella Grando

Fondazione Edmund Mach, San Michele all'Adige



Ph.D student

Maria Lucia Prazzoli

Matr. n° R10455

CONTENTS

Riassunto		ii-iii
Abstract		iv-v
Abbreviations		vi-viii
Chapter 1	General introduction	1-11
Chapter 2	Phylogenetic reconstruction of Caucasian germplasm	12-36
Chapter 3	Genetic mapping and QTL analysis in Mgaloblishvili Noir	37-63
Chapter 4	Gene expression assays	64-91
Chapter 5	General discussion	92-93
Appendix		94-96
References		97-105
Acknowledgements		106

RIASSUNTO

La vite europea, *Vitis vinifera* L., è una delle colture arboree più importanti al mondo sia per il valore economico che per la superficie coltivata. Negli ultimi anni una maggiore sensibilità alle problematiche ambientali insieme alle opportunità di mercato hanno stimolato l'avvio di nuovi programmi di miglioramento genetico per ottenere cultivar resistenti alle malattie, in particolare peronospora e oidio. Questo ha comportato anche una maggiore attenzione verso la conservazione delle risorse genetiche come fonti di caratteri utili. Allo stato attuale, i metodi tradizionali di miglioramento genetico, che includono l'utilizzo di altre specie di *Vitis* per la produzione di varietà ibride resistenti, possono essere complementati dalle nuove tecnologie quali la selezione assistita da marcatori molecolari (MAS) e la possibilità di identificare geni di interesse agronomico tramite analisi di popolazioni sperimentali (QTL mapping) o naturali (GWAS, association mapping).

Recentemente una maggiore attenzione è stata volta alla valorizzazione dei vitigni coltivati e delle viti selvatiche del Caucaso, considerato il centro primario di domesticazione della vite e contraddistinto da un'elevata diversità genetica dei materiali.

Il presente progetto di ricerca è improntato sulla caratterizzazione di un germoplasma ancora inesplorato di origine caucasiaca composto da 25 accessioni di *Vitis vinifera*, sia coltivate che selvatiche, che presentano una bassa suscettibilità alla peronospora, come descritto in Toffolatti et al., 2016 [1]. Al fine di definire una eventuale introgressione di tratti di resistenza provenienti da viti americane o asiatiche, è stato condotto un primo screening con marcatori molecolari associati ai loci *Rpv* noti, che apparentemente ha escluso tale evenienza. Una prima analisi filogenetica, tramite l'utilizzo di 21 marcatori microsatelliti, ha permesso di comparare queste accessioni con una collezione di cultivar di varia provenienza geografica precedentemente descritte (Vv1, Vv2, Vv3, Vv4) insieme ad altre varietà Georgiane e ad alcuni portainnesti, posizionandole all'interno della specie *V. vinifera*. Utilizzando un più ampio database composto da accessioni provenienti dall'Europa, Caucaso, Israele, America ed Asia, una seconda analisi ha permesso di collocare queste accessioni all'interno della regione Georgia caratterizzata da una forte diversità genetica, un numero elevato di varianti alleliche e di alleli privati. L'analisi delle componenti principali (PCoA) e l'analisi di struttura di popolazione hanno inoltre identificato all'interno del germoplasma georgiano una certa percentuale di "admixture" tra le varietà coltivate e le accessioni selvatiche. Allo scopo di approfondire questi risultati, è stata impostata un'analisi filogenetica basata su marcatori plastidiali descritti in letteratura, suddividendo la collezione sulla base dei diversi clorotipi. In accordo con i dati ottenuti, alcune cultivar georgiane, di particolare interesse per la loro bassa suscettibilità alla peronospora hanno mostrato una elevata omozigosità e un clorotipo molto simile a quello delle viti *sylvestris* Europee, lasciando presupporre la presenza di caratteri ancestrali tipici di varietà ibride di viti coltivate ed accessioni selvatiche.

Tra queste accessioni una cultivar georgiana, nota come 'Mgalobshvili N.', è stata maggiormente approfondita per la sua bassa suscettibilità alla peronospora. Al fine di studiare questa tolleranza, è stata costruita una mappa genetica derivata da una popolazione segregante, composta da 154 genotipi, ottenuta da un'autofecondazione della cultivar. Nonostante l'alta omozigosità della cultivar, sono stati ottenuti tutti i 19 cromosomi, utilizzando 177 marcatori molecolari (SSRs e SNPs). La mappa ottenuta è stata integrata a dati fenotipici della popolazione segregante al fine di elaborare una preliminare analisi QTL. La popolazione mantenuta in vaso è stata valutata in anni differenti: 2013, 2014, 2015 (maggio e luglio) e 2016 in seguito a infezioni artificiali di peronospora. Tuttavia il comportamento delle piante non è risultato riproducibile nelle diverse annate e andrà valutato in condizioni di maggiore stabilità sulla popolazione adulta. L'analisi QTL effettuata ha individuato tre QTLs nel 2014 sui cromosomi 1, 7 e 11 ed un QTL minore nel 2016 coincidente con il locus *Rpv11*. Su tali cromosomi è stato effettuato un fine mapping per poter circoscrivere il più possibile i geni di interesse. All'interno di questi QTL sono stati identificati prevalentemente geni legati al pathway dell'etilene.

È stato inoltre intrapreso un approccio integrativo basato su uno studio di espressione genica. Sono stati selezionati due genotipi della popolazione che durante gli anni hanno mostrato un comportamento differente in risposta all'infezione con *P. viticola* ed insieme alla linea parentale sono stati micropropagati, partendo da internodi. In un arco di sette mesi, sono state ottenute piantine sufficientemente grandi per poter effettuare un esperimento di espressione genica. Allo scopo di testare l'efficienza dell'inoculo e la risposta dei vari

genotipi a tale inoculo, sono stati eseguite delle valutazioni fenotipiche su dischetto fogliare indicative delle differenze di sporulazione tra i genotipi. Successivamente lo stesso inoculo è stato testato sulle diverse repliche biologiche delle intere piante e sono stati effettuati campionamenti a diversi tempi dopo l'inoculo (0h, 8h, 24h, 48h). Mentre la valutazione fenotipica su dischetto ha definito una chiara differenza tra i genotipi, quella sull'intera pianta ha evidenziato delle differenze significative tra repliche biologiche che hanno influenzato anche la successiva espressione genica. Una volta ottenuti i cDNA opportunamente restrotrascritti, è stata valutata l'espressione di diversi geni scelti sia sulla base dei geni individuati nelle regioni dei QTL, sia sulla base della letteratura con riferimento alle resistenze studiate nella vite selvatica, date le caratteristiche ancestrali della cultivar. Ogni esperimento è stato condotto in qRT-PCR e ne è stata confermata la significatività tramite appositi test statistici quali ANOVA e Tukey. I risultati ottenuti dall'esperimento di espressione genica hanno confermato, nel genotipo più resistente all'infezione da *P. viticola*, una risposta HR associata ad un'induzione di geni coinvolti nel pathway dell'etilene. Inoltre l'elevata espressione di fattori di trascrizione MYB e VvWRKY ha evidenziato una risposta immune legata alla produzione di fitoalessine e metaboliti secondari.

In conclusione, questo lavoro ha permesso di caratterizzare un germoplasma di *V. vinifera* meno suscettibile alla peronospora rispetto alle cultivar commerciali e proveniente dalla Georgia, centro di domesticazione della vite, composto da alcune varietà filogeneticamente molto vicine a accessioni di viti selvatiche Europee. Questo ha suggerito una possibile natura "ibrida" di tali accessioni con tratti ancestrali molto accentuati. Le successive analisi sulla cultivar 'Mgalobshvili N.' fanno ipotizzare che questo interessante fenotipo (Toffolatti et al., 2016) [1] sia controllato da geni che inducono la produzione di fitoalessine e quindi prettamente legati ad un sistema di difesa basale influenzato dalla produzione di etilene. Questa ricerca evidenzia la presenza di caratteri di resilienza nelle viti coltivate che hanno mantenuto tratti ancestrali e che hanno, presumibilmente, assunto un ruolo primario nel processo di domesticazione, migliorando anche il processo di difesa della pianta dal patogeno.

ABSTRACT

European grapevine, *Vitis vinifera* L., is one of the most important tree crops worldwide for both economic value and cultivated area. The social-economic significance of *Vitis vinifera* led to the development of new cultivation techniques in order to produce hybrids characterized by the resistance to diseases like downy and powdery mildews typical of American and Asian *vitis* and at the same time characterized by the quality of European grapevines. During the last years, a major sensitivity to environmental issues along with market demand led the research towards the crops genetic improvement and the greater attention over the biodiversity conservation. The advent of new technologies and the improvement of crop farming and winemaking made the wine growing activity very profitable. Indeed, traditional methods of breeding, which include the employment of rootstocks for the resistant hybrids production, together with the advent of new techniques such as marker assisted selection (MAS) and the chance to isolate gene of agronomic interest throughout experimental populations (QTL mapping) or natural populations (association mapping, GWAS) represent, to date, the best method to produce and study grapevine. Recently, a major attention was turned to the exploitation of cultivated and wild genetic resources from Caucasus, primary center of grapevine domestication, characterized by a high genetic diversity.

The present research project was focused on the characterization of a previously unexplored Caucasian germplasm collection composed by 25 accessions of *Vitis vinifera*, both cultivated and wild, with a low susceptibility to downy mildew based on Toffolatti et al., 2016 [1] evaluations. In order to exclude any possible introgression of resistant traits from American and Asian species, a screening with markers linked to the major *Rpv* loci has been performed, apparently confirming the absence of introgressions. A first phylogenetic analysis, performed with 21 microsatellites, allowed to compare these accessions with a collection of cultivars of various geographic origin previously described (Vv1, Vv2, Vv3, Vv4) together with other Georgian cultivars and some rootstocks classifying them in *V. vinifera* clade. Enlarging the databases with European, Caucasian, Israeli, American and Asian accessions, a second classification allowed to place these genotypes within the Georgia region, characterized by a strong genetic diversity, a high number of alleles and private alleles. PCoA analysis and STRUCTURE analysis identified a certain amount of admixture between wild and cultivated grapevine species. In order to deepen these results, a new phylogenetic analysis based on plastid markers described in literature has been performed to classify the entire collection on the base of chlorotype. In agreement with obtained data, a few Georgian cultivars, particularly interesting for their low susceptibility to downy mildew, showed a high homozygosity and a chlorotype similar to the ones of European *sylvestris*, suggesting ancestral features typical of hybrids between wild and cultivated varieties.

Among these ancestral grapevine accessions a Georgian cultivar, known as 'Mgalobshvili N.', was mainly deepened for its low susceptibility to downy mildew (Toffolatti et al., 2016) [1]. In order to study this tolerance, a genetic map derived from a segregating mapping population, composed by 154 offspring and obtained by selfing, was constructed. Despite the high homozygosity, all the 19 chromosomes have been reproduced, using 177 molecular markers (SSRs and SNPs). The obtained map has been integrated with phenotypic data to perform a preliminary QTL analysis. The population, maintained in pots, has been evaluated after artificial infections with *P. viticola* during different years: 2013, 2014, 2015 (May and July) and 2016. However, plants behavior has not been reproducible in the various seasons and it should be evaluated in conditions of greater stability on adult population. QTL analysis detected three QTLs in 2014 on chromosome 1, 7 and 11 and a minor QTL in 2016 corresponding to *Rpv11* locus. A fine mapping has been performed on these chromosomes in order to restrict the region of interest. Within these regions, genes mainly involved in ethylene pathway have been identified.

Moreover, an integrative approach based on the study of gene expression has been started. Two genotypes of the offspring, which showed a contrast behavior to *P. viticola* infection among the years have been selected and, together with the parental line, have been micropropagated, starting from internodes. In the time frame of seven months seedlings, grown enough to carry out a gene expression experiment, have been obtained. In order to test the efficiency of inoculum and the response to infection of each genotype, a few phenotypic evaluation on leaf discs, indicating the differences among the rates of sporulation, were carried out. Subsequently, the same inoculum was tested on the different biological replicas of the whole plants and

various samplings were performed at four time points post infection (0hpi, 8hpi, 24hpi and 48hpi). If the phenotypic evaluation on leaf discs defined a clear differentiation among genotypes behaviors, the ones performed on the entire plant highlighted significant differences among biological replicas which influenced also the further gene expression. Once obtained reverse transcribed cDNAs, samples were tested with candidate genes, chosen both on the base of detected QTL regions and literature reports mainly based resistance traits studied in wild species, given the ancestral features of the cultivar. Each experiment was carried out in qRT-PCR and statistical test like ANOVA and Tukey confirmed the significance levels. Results revealed, in the most resistant accession, an HR response associated to a considerable induction of genes involved in ethylene pathway. Moreover the high expression of MYB and VvWRKY transcription factors marked out an immune response linked with the production of phytoalexins and secondary metabolites.

In conclusion, this research work allowed to characterize a *V. vinifera* germplasm collection with a low susceptibility to downy mildew and originated from Georgia, the cradle of grapevine domestication, composed by a few cultivar, phylogenetically very similar to European *sylvestris* varieties. This suggested the probable “hybrid” nature of these accessions marked out by ancestral features. Further analyses on ‘Mgalobshvili N.’ suggested that this interesting phenotype (Toffolatti et al., 2016) [1] could be controlled by genes which induce production of phytoalexins therefore strictly associated to a basal immunity system influenced by ethylene production. This work allowed to stress the presence of interesting resilience features in cultivated grapes which maintained ancestral traits and which, presumably, assumed a central role in the domestication process, improving the plant’s defense process from the pathogen.

ABBREVIATIONS**Units**

°C	Celsius degree
cM	centimorgan
dpi; hpi	day post infection; hours post infection
g; ug; ng	gram(s); microgram(s); nanogram(s)
h; m; s	hour(s); minute(s); second(s)
Klx	Kilolux
LOD	Log of Odds
M; mM; uM	molar (moles per liter); millimolar; micromolar
Mb; Kb; bp	mega base(s); kilo base(s); base pair(s)
ml; ul	milliliter(s); microliter(s)
cm; mm	centimeter; millimeter
rpm	revolution per minute
U	units
w/v; v/v	weight per volume; volume per volume

General

4CL	4-Coumarate-CoA Ligase
AVR	Avirulence gene
BLAST	Basic Local Alignment Search Tool
C4H	Cinnamate 4-Hydroxylase
CaM	Calmodulin
cDNA	complementary DNA
CG	Candidate Gene
Chr	Chromosome
CHS	Chalcone Synthase
D/ND	Deletion/Non Deletion
DM	Downy Mildew
DNA	deoxyribonucleic acid
dNTP	Dinucleotide Triphosphate
EDTA	ethylenediaminetetraacetic acid
ERF	Ethylene-Responsive Factor
ET	Ethylene
ETI	Effector-Triggered Immunity
ETS	Effector-Triggered Susceptibility
GF	Geilweilerof
HLH	Helix-Loop-Helix
HR	Hypersensitive Response
ITP	Italian Peninsula

Abbreviations

JA	Jasmonic Acid
KW	Kruskall Wallis
LG	Linkage Group
MEA	Middle East
MQM	Multiple QTL Mapping
mRNA	messenger RNA
NBS-LRR	Nucleotide Binding Site Leucine Rich Repeat
NCBI	National Center for Biotechnology Information
NEA	Near East
NLS	Nuclear Localization Signal
PAL	Phenylalanine Ammonia-Lyase
PAMP	Pathogen Associated Molecular Patterns
PCD	Programmed Cell Death
PCoA	Principal Coordinate Analysis
PP	phenylpropanoids
PPR	Pentatricopeptide Repeats
PR	Pathogenesis Related
PRR	Pattern Recognition Receptors
PTI	PAMPs-Triggered Immunity
qRT-PCR	Quantitative Real Time PCR
QTL	Quantitative Trait Loci
R	Resistance
RAD	Restriction site associated DNA
Ren/Run	Resistance to <i>Erysiphe necator</i> / <i>Uncinula necator</i>
RGA	Resistance Gene Analogs
RLK	Receptor Like Kinase
RNA	ribonucleic acid
ROS	Reactive Oxygen Species
Rpv	Resistance to <i>Plasmopara viticola</i>
RRTF1	Redox Responsive Transcription Factor 1
RT/PCR	Retro Transcriptase/Polymerase Chain Reaction
SA	Salicylic Acid
SAR	Systemic Acquired Resistance
SD	Segregation Distortion
SE	Standard Error
SIM	Simple Interval Mapping
SNP	Single Nucleotide Polymorphism
SPCS3	Signal Peptidase Complex Subunit 3b
SSR	Simple Sequence Repeats
STS	Stilbene Synthase

Abbreviations

StSy	Stilbene Synthase
TBE/TAE	tris-boric acid-EDTA/tris-acetic acid-EDTA
TF	Transcription Factors
TM-LRR	Transmembrane Leucine Rich Repeat
UFGT	UDP-glycosyl: Flavonoid-3-O-GlycosylTransferase
Vv	<i>Vitis vinifera</i>

Chapter 1

GENERAL INTRODUCTION

Introduction

Grapevine (*Vitis vinifera* L.) represents one of the major crop species on a world-wide scale mainly used for wine and spirits production and fresh and dry fruit consumption, with a harvested area of over 7.5 million hectares, yielding 73.7 million tons of grapes in 2014 (OIV, 2015 – Organization International de la Vigne et du Vin). In the last decade, the will to increase the economic competitiveness related to this cultivation in terms of quality and productivity and the requirement to adapt it to the new geographical areas depletion, climate changes, the advent of new diseases and the market demands, led to a remarkable intensification of physiology and pathology studies on this species, together with a strong development of tools and genetic resources aimed at its improvement.

The whole genome sequence

A great step in the field of grapevine research was achieved through the publication of the first draft of the grapevine reference genome by the French-Italian Consortium (Jaillon et al., 2007) [2] in which is described how the highly homozygous (93%) line PN40024, derived from Pinot noir by successive selfings, was sequenced through the whole-genome shotgun strategy, gaining an 8.4-fold coverage of the genome. When considering only one of the haplotypes in each heterozygous region, the assembly consists of 19,577 contigs and 3,514 supercontigs. About 69% of the assembled 487Mb were anchored along the 19 linkage groups and the 41.4% of the genome consisted of repetitive/transposable elements (TEs). A comparative analysis with other fully sequenced plant genomes revealed the contribution of three ancestral ones (*P. trichocarpa*, *A. thaliana* and *O. sativa*) to the grapevine haploid content, suggesting an ancestral hexaploidization event occurred after divergence from monocotyledons and before the radiation of the Eurosids (Jaillon et al., 2007) [2]. A second genome draft (Velasco et al., 2007) [3] was obtained by the Pinot Noir clone ENTAV 115 clone, through Sanger sequencing. The genome sequence was slightly larger, with a size for the haploid genome estimated at 504.6 Mb and a total number of 29,585 gene predictions. The variation within this clone of grape consisted largely of chromosome-specific gaps and hemizygous DNA.

Together with these research works, additional essential data about *V. vinifera* chloroplast genome are reported in Jansen et al., 2006 [4]. The complete chloroplast genome of grape is 160,928 bp in length, including a pair of inverted repeats of 26,358 bp that are separated by small and large single copy regions of 19,065 bp and 89,147 bp, respectively. The gene content and order of *Vitis* is identical to many other unrearranged angiosperm chloroplast genomes. There is a recent interest in using complete chloroplast genome sequences for resolving phylogenetic relationships among angiosperms. Unlike the diploid nuclear genome, which displays two microsatellite alleles per locus and individual, the chloroplast genome is haploid, with only one allele per locus in each individual and is maternally inherited in grapevine.

Taxonomy

Grapevine belongs to the *Vitaceae* family which consists of perennial plants spread across all over the world, especially in temperate and inter-tropical climates. It's an economically important family of angiosperms whose phylogenetic placement is currently unresolved. The phylogeny of *Vitaceae* was reconstructed using several plastid (rbcL, trnL-F intron and spacer, atpB-rbcL spacer, rps16, trnCpetN spacer [5] [6] [7] and nuclear (GAI1, [8]) genes, identifying five major clades in the family: the *Ampelocissus-Vitis-Nothocissus-Pterisanthes* clade, the *Parthenocissus-Yua* clade, the core *Cissus* clade, the *Cayratia-Cyphostemma-Tetrastigma* (CCT) clade and the *Ampelopsis-Rhoicissus-Clematicissus* clade.

According to Kubitzki et al., 2007 [9], around 900 species from 15 different genera are documented in *Vitaceae* family and, among them, *V. vinifera*, belonging to the genus *Vitis*, represents the only species to be extensively used in the wine industry and is the only one indigenous to Eurasia. *Vitis* is composed of two very distinct subgenera: *Muscadinia* Planch. (2n =40) and *Vitis* Planch. (2n =38). Subg. *Vitis* contains about 60 species distributed primarily in eastern Asia and North America to Central America, while subg. *Muscadinia* consists

of only three species, *V. rotundifolia*, *V. munsoniana* and *V. popenoei* mainly distributed in North America, the West Indies to Mexico. The two subgenera are reproductively isolated, while the species within subgenus *Vitis* are interfertile. All species are dioecious except for *V. vinifera* L., which has hermaphroditic flowers, and *V. rotundifolia*, which segregate for this traits [10]. Recently molecular methods have been introduced to resolve the various taxonomic controversies due to the morphological variations within species and three clades have been identified in *Vitis* genus reflecting the geographic distribution: Europe, Asia and North America. According to Hewitt et al., 2000 [11], the genetic diversity among these three major groups dates back to Pliocene and Pleistocene cooling cycles, which caused the isolation of some North America and Asia species leading to a primary division within *Vitis*. After the glacial period, these species expanded and adapted to their range, acquiring a remarkable diversity in morphological traits, which has been maintained by geographical, ecological and phenological barriers.

Domestication of *V. vinifera*

The history and the vineyard cultural practices have largely determined the genetic diversity that exists today in grapevines. The Eurasian species *V. vinifera* is the only one extensively used in the global wine industry. Two forms still coexist in Eurasia and North Africa: the cultivated form, *V. vinifera* subsp. *sativa* and the wild form *V. vinifera* subsp. *sylvestris*. The wild form is rare and it is believed to be the ancestor of present cultivars. The two species present morphological differences due to the domestication process, during which the biology of grapes underwent several changes to ensure a greater yield and a more regular production. In this process the changes in berry and bunch size, in seed morphology, in sugar content and the change from dioecious wild plants to hermaphroditic cultivated plants were crucial even if the biological significance is still unknown. Still remain unpredictable whether this changes occurred through sexual crosses and natural or human selection, or via mutation, selection and subsequent vegetative propagation [12] and moreover, major questions about grapevine domestication concern the number of domestication events and their geographic locations [13]. Surely, both sexual crossing and natural mutations have been the drivers during the grapevine evolution. Since much of grapevine propagation is performed through cuttings, mutations can accumulate over time leading morphological and agronomical differences. Even though the south of Caucasus together with eastern Anatolia, has been considered for a longtime as the cradle of domestication with the earliest examples of wine-making, a 1998 census showed the presence of wild grapevine in different places such as Spain, Italy, Switzerland, Romania, Bulgaria, Hungary, Austria and in the balkan countries (Figure 1). In light of this it has been questioned if the current wild vines are real *sylvestris* individuals that have never been cultivated or if they are naturalized cultivated forms escaped from vineyards as well as hybrids derived from spontaneous hybridizations among those two subspecies. The total genetic diversity values found in wild grape individuals from Anatolia region is higher than of wild type accessions from other regions described for Mediterranean basin [14] [15] [16] [17], in particular the comparison of the genetic diversity values with the autochthonous grape cultivars from Anatolia region indicated that diversity is greater in the wild grapes than in the cultivated ones. On the other hand the wild populations from the Mediterranean basin showed a lower genetic diversity values and suffered from inbreeding depression. The discovery of two genetic groups within *sylvestris* accessions from Spain suggests some level of isolation among those genetic lineages [13]. One possible scenario implies an isolation created by the last Pleistocene glaciations as reviewed by Gómez et al., 2007 [18], alternatively these groups can represent different colonization events. In conclusion, molecular marker analysis have shown clear divergence between wild and cultivated grapes and low level of introgression, providing evidences of the complex pedigree of *sativa*, due to a number of spontaneous and inter-generation crosses between cultivars compared to the absence of inter-wild population gene flow and small size of intra-population flow of wild populations, characterized by a potential inbreeding depression.

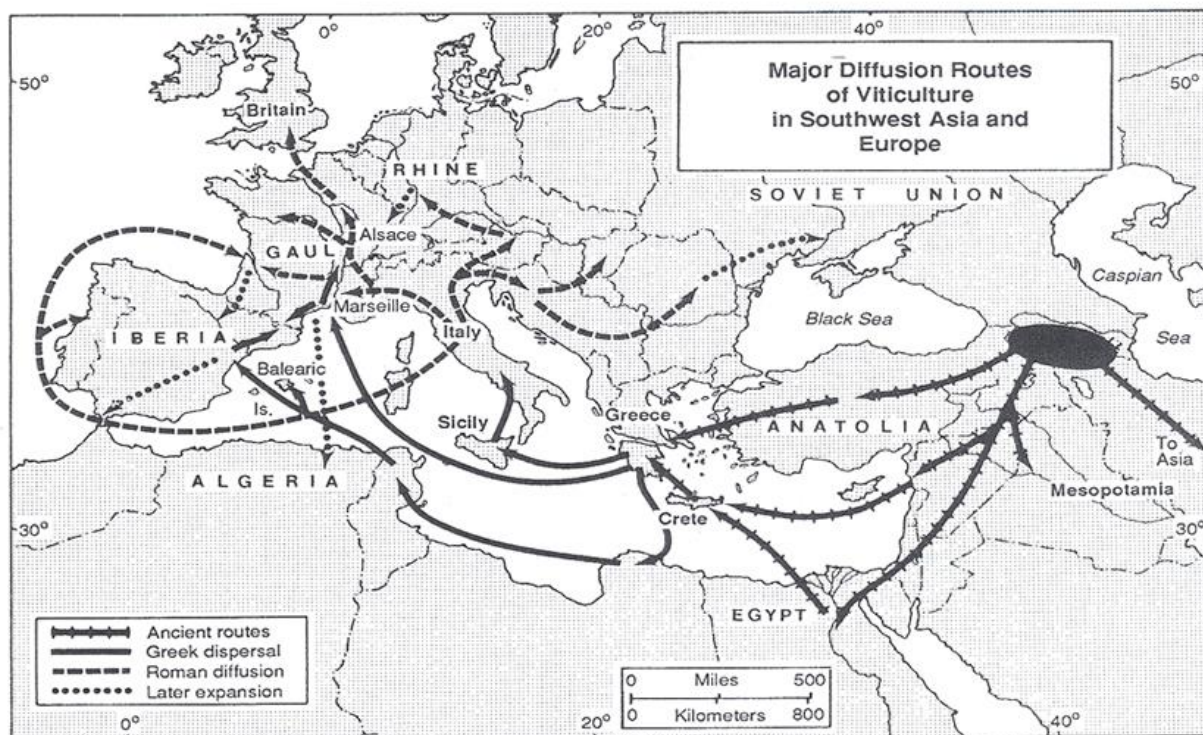


Figure 1 **Domestication process.** Major diffusion routes of viticulture in southwest Asia and Europe [19] and Georgia as center of domestication process.

Historical background of grapevine diseases and wild grapes as phylogenetic resources

A few information about the place and the period of the original domestication are available, and despite wild grapes were present in many places across Europe during the Neolithic period, archeological and historical evidence suggest that the first domestication process occurred in the Near East. In particular seeds of domesticated grapes dated from ~8000 BP (Before Present) were found in Georgia and in Turkey. From the primo-domestication sites, a gradual spread to adjacent regions such as Egypt and Lower Mesopotamia occurred, followed by a further distribution around the Mediterranean, following the main civilizations. Under the influence of the Roman Empire, *V. vinifera* expanded in the most of the European locations where they are grown today. Following the 16th century, *V. vinifera* colonized the New World countries where it was not native. The missionaries of Catholic Church introduced it to America, first as seeds and then by cuttings from their places of origin. At the end of 19th century disease-causing agents from America reached Europe resulting in a massive death of many European vineyards, drastically changing the diversity of this species. To date, it is well known that *V. vinifera* is prone to numerous diseases requiring intense plant protection, on the other hand, most of the pathogens have evolved together with wild grapes in North America that can cope with them. The situation was resolved through the introduction of several American non-*vinifera* species used as rootstocks and for breeding disease resistant interspecific hybrids, in order to combine the resistant traits of American wild species with the quality of *V. vinifera* cultivars.

The introduction of international vine varieties had rapidly displaced the traditional ones resulting in a loss of genetic variability and an increase of vulnerability of the different cultivars to new environmental changes and the appearance of new pests and diseases. Wild forms represent a rich genetic resource which still conserve an overall important genetic diversity and some interesting characteristics could be transferred, throughout the breeding, to cultivars suitable of wine making, table grapes and also rootstocks. Gene flow between crops and their wild relatives is an important process that has major implications both for in situ conservation of genetic diversity and for plant breeding. Most domesticated plants are able to spontaneously hybridize with wild relatives present in their distribution area [20]. In particular, an overwhelming gene flow from crops may deplete genetic diversity in wild populations through the loss of some specific or rare alleles of the wild

subspecies, reducing the adaptability and finally leading to the extinction of the wild populations. Conversely a moderate gene flow between wild populations may help maintain genetic variation and reduce the risk of inbreeding depression [21]. Most of the works in the past years has been devoted to the development of methods for the analysis of many traits from compositions of berries to disease resistance and abiotic stresses tolerance [22] [23] often found in resilient wild plants able to overcome diseases and characterized by several gene variants. Recently, novel immunity genes were discovered in a pool of *V. vinifera* subsp. *sylvestris* which were able to trigger the basal immunity very efficiently, demonstrating that they could be able to activate the formation of defense compounds resveratrol and viniferin faster and stronger, arising the interest on these almost extinct species [24].

Multi-level plants defense mechanisms

Understanding plant responses to different kind of pathogens may show some light on the co-evolution of plant and pathogen strategies, and their impact on resistance or susceptibility to infections. Plants has evolved different level of mechanisms against pathogens which included a first defense line induced by physical barriers (trichomes, cell walls, waxy epidermal cuticles) and a second line carried by the innate immune system of plants because when pathogens manage to overcome these physical barriers, chemical barriers are installed. The interactions between a plant and its pathogens involved two-way communication, through which both plant and pathogen have evolved a suite of genes that enable this interaction. Currently, the active defense responses of plant are considered to operate at two levels. The first PTI or PAMPs-Triggered Immunity, is a basal immune response, common in plants, activated after recognition of pathogens and it is mediated by plasma membrane localized pattern recognition receptors (PRRs), which are composed of an extracellular domain able to detect PAMPs (structural components of the pathogen). Often, it happens that pathogens are able to suppress the different component of PTI by virulence factors delivered into the plants with a type of interaction known as Effector-Triggered Susceptibility (ETS). In particular, some pathogens can successfully break through this second line of defense and enter the cytoplasm to suppress chemical plant defense responses and reprogram their host to provide the nutrients for their own survival. Therefore, a third line of plant defense involves the recognition of specific effectors (AVR) through receptors known as resistance proteins (R), triggering what is often perceived as a stronger resistance response and referred to as Effector-Triggered Immunity (ETI) (Figure 2). Both PTI and ETI initiate massive transcriptional reprogramming and the major differences appear more quantitative rather than qualitative, suggesting that most pathogens trigger a common or interconnected plant signaling network. Very little is known about the biochemical signals and how they are relayed and linked to nuclear components and despite five major families of plant transcription factors, including bZIP, WRKY, MYB, ERF and homeodomain protein, have been shown to play roles in the regulation of the plant defense response, a few is known about the exact function or mechanism of individual TFs.

All these mechanisms are regulated by hormone-mediated signaling pathways. Ethylene (ET), jasmonic acid (JA) and salicylic acid (SA) play a central role in the regulation of plant immune responses; in addition, other plant hormones, such as auxins, abscisic acid, cytokinins, gibberellins and brassinosteroids, that have been thoroughly described to regulate plant development and growth, have recently emerged as key regulators of plant immunity. Although, SA and JA/ET defense pathways are mutually antagonistic, evidences of synergistic interactions have also been reported [25] [26] [27] [28]. This suggests that the defense signaling network activated and utilized by the plant is dependent on the nature of the pathogen and its mode of pathogenicity. The essential roles of SA and ET/JA-mediated signaling pathways in resistance to pathogens are well described in [29]. SA signaling positively regulates plant defense against biotrophic pathogens that need alive tissue to complete their life cycle, whereas ET/JA pathways are commonly required for resistance to necrotrophic pathogens that degrade plant tissue during infection, and to herbivorous pests [30] [31]. Several exceptions for this general rule have been described, and thus SA pathway is also required for plant resistance to particular necrotrophic pathogens, whereas ET/JA pathways were found to be essential for resistance to some biotrophic pathogens [32] [29].

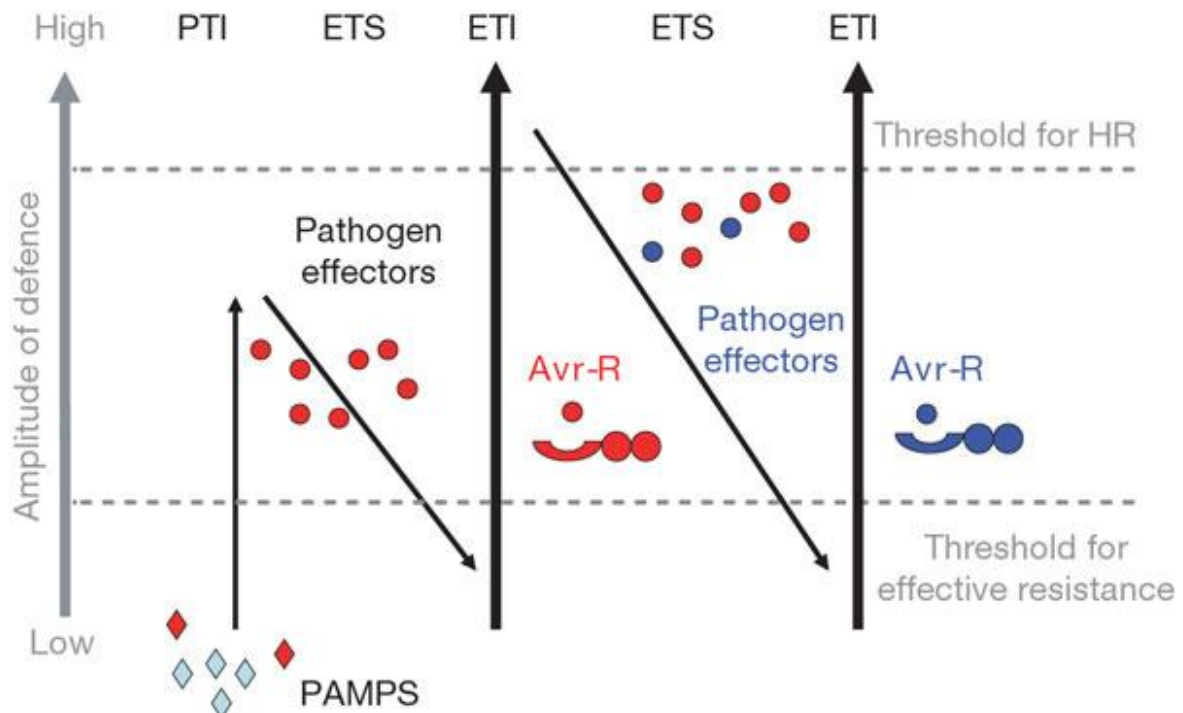


Figure 2 **Model of plant immune system.** Phase1) Plants detect microbial/pathogen-associated molecular patterns (MAMPs/PAMPs, red diamonds) via PRRs to trigger PAMP-triggered immunity (PTI). Phase 2) Successful pathogens deliver effectors that interfere with PTI, or otherwise enable pathogen nutrition and dispersal, resulting in effector-triggered susceptibility (ETS). Phase 3) One effector (indicated in red) is recognized by an NB-LRR protein, activating effector-triggered immunity (ETI), an amplified version of PTI that often passes a threshold for induction of hypersensitive cell death (HR). Phase 4) Pathogen isolates are selected that have lost the red effector, and perhaps gained new effectors through horizontal gene flow (in blue) - these can help pathogens to suppress ETI. Selection promotes new plant NB-LRR alleles that can recognize one of the newly acquired effectors, resulting again in ETI [33].

The constitutive basal plant defenses or race non-specific resistance, involves the production of secondary metabolites that can be considered as markers for disease resistance in plants and they include a large spectrum of compounds, mainly phenolics such as flavonoids, anthocyanins, phytoalexins, tannins, lignin, and furanocoumarins. An important precursor for biosynthesis of phenolics is the amino acid phenylalanine; after pathogen attack it is converted to *trans*cinnamic acid (CA) and then enters in phenylpropanoid pathway, which is responsible also for the formation of many phytoalexins. The starting point for this pathway involves the deamination of phenylalanine to *trans*cinnamic acid, in a reaction catalyzed by the enzyme phenylalanine ammonia lyase (PAL). Moreover, additional enzymes known as polyketide synthases, such as chalcone synthases (CHS) and stilbenes synthases (STS), leads to the flavonoid and stilbenoid families of phytoalexins, respectively (Figure 3). Flavonoid pathway leads to the production of anthocyanins that provide antiviral and antimicrobial activities in plants [34]. Stilbenes, instead, are scarcely expressed under normal conditions, but strongly accumulated in response to a wide range of biotic and abiotic stresses, as result of an increased transcription of stilbene synthase (STS) genes and coordinate activation of upstream genes belonging to the general phenylpropanoid pathway, such as PAL and C4H. Downy mildew-resistant cultivars, for instance, accumulate a much higher level of stilbenes than susceptible ones and, in particular, rapidly convert resveratrol into the much more toxic viniferin compounds, which inhibits the pathogen growth [35]. Malacarne et al., 2011 [36] used a combination of metabolic and transcriptional analyses to investigate *P. viticola* resistance in a population of Merzling x Teroldego. According to their results, infection induces transcripts related to the accumulation of phytoalexins, suggesting that gene expression analysis could be an alternative method to study defense mechanism in grapevine. On the other hand, if phytoalexins are important factors in the resistance of a plant, the ability of a pathogen to degrade these compounds could be an important feature in the success of a fungal pathogen. Indeed, as described in Sbaghi et al., 1996 [37], a few isolates of *B. cinerea* cultured under the same conditions showed different abilities to degrade the grapevine phytoalexins resveratrol and pterostilbene. Regulation of gene expression at the level of transcription is predominant way

by which plants control the production of these secondary metabolites. This is achieved thanks a class of proteins, referred as “transcription factors” (TFs) that are able to recognize DNA in a sequence specific manner and to regulate the transcription of genes. The principal structure of TFs is composed at least of four domains: DNA-binding domain, nuclear localization signal (NLS), transcription activation domain and oligomerization site. On the basis of similarities in the DNA binding-domain, TFs are grouped into different families such as MYBs, helix-loop-helix (HLH), zinc finger, helix-turn-helix, leucine zipper, scissors, MADS cassettes etc [38]. In the recent years a growing number of TFs responsible for the regulation of flavonol, lignin or anthocyanins biosynthesis have been isolated including the R2R3-MYBs, and the basic bHLH transcription factors [39] [40].

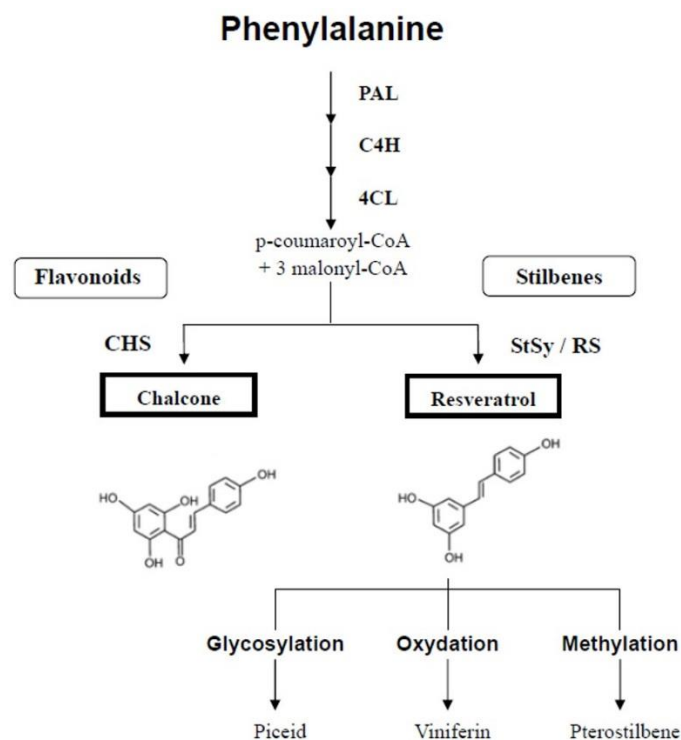


Figure 3 **Phenylpropanoid pathway**. Simplified representation of the phenylpropanoid pathway with the positions of phenylalanine ammonium lyase (PAL), stilbene synthase (StSy), resveratrol synthase (RS), and chalcone synthase (ChS).

On the other hand, the race specific-resistance is conferred by a single or a few major genes that operate in a gene-for-gene fashion. Resistance gene analogs (RGAs) are a large class of potential R-genes that have conserved domains and structural features. RGAs can be grouped as either nucleotide binding site leucine rich repeat (NBS-LRR) or transmembrane leucine rich repeat (TM-LRR). Recently, other modes of plant resistance mechanisms including pentatricopeptide repeats (PPRs) and peroxidases have been identified. NBS-LRR can be further classified as toll/interleukin receptor (TIR)-NBS-LRR (TNL) or non-TNL/coiled-coil-NBS-LRR (CNL) and both of them specifically target pathogenic effector proteins inside the host cell, termed ETI response. Likewise, TM-LRRs can be subdivided in receptor like kinases (RLKs) class and in receptor like proteins (RLPs) class and both of them are PPRs that mediate PTI to allow recognition of a broad range of pathogens. To date, a large number of resistance gene loci have been identified in plants using linkage mapping or association studies, most of them correspond to flanking molecular markers or quantitative trait loci.

Downy mildew (DM) disease

The history of European grape-growing can be summarized in three periods, the first defined by the absence of major phytosanitary problems, a second concerning a troubles half century during which European grape crops were faced with the arrival of new diseases (phylloxera, downy and powdery mildews) followed by the last one characterized by a search of solutions. *Plasmopara viticola* is a biotrophic pathogenic oomycete responsible for grapevine downy mildew and is endemic on wild *Vitis* species of North America and spread to Europe by the year 1878. Although European *V. vinifera* cultivars are highly susceptible to *P. viticola*,

Muscadinia species and several American and Asian *Vitis* species exhibit varying levels of resistance to this pathogen.

The infection occurs specifically throughout stomata. It starts in early season, when oospores in fallen leaves or mycelium in dormant twigs are activated by adequate climate conditions to produce sporangia. In presence of water, mature sporangium releases self-motile biflagellate zoospores that infect plant tissues. Zoospores are able to place on the abaxial surface of leaves close to stomata, then germinate and penetrate throughout stomatal cavity, forming substomatal vesicle. Vesicle gives rise to the primary hyphae and mycelium, which grows enclosed by the veins of the leaf and enters to the cell of mesophyll by its cell-wall penetrating and feeding haustoria, which invaginates the plasma membrane of the parenchyma cells. As result, the adaxial surface of the leaf displays a typical oil-spot lesion visible in plants affected to this pathogen. The mycelium also develops to produce sporangiophores emerging from the stoma and releasing sporangia to the surrounding susceptible tissues, activating the secondary infection. Production of sporangiophores and sporangia requires 95 to 100% relative humidity and at least 4 h of darkness at temperatures initially exceeding 13°C. Stomata remains abnormally open and unresponsive to abscisic acid in grapevine leaves infected by DM [41]. Although all green parts of the grapevine are susceptible, the first symptoms of downy mildew of grapes, caused by *Plasmopara viticola*, are usually seen on the leaves as soon as 5 to 7 days after infection. On the foliage, small yellow spots develop on the upper sides of the leaf while white to bluish-white fluffy growth forms on the underside of the leaf. As the leaf spot dies, the fluffy growth darkens to gray in color. Conversely, mature berries, although they may be symptomatic and harbor the pathogen, may not support sporulation even when provided with ideal conditions. Infected parts of young fruit bunches turn brown, wither, and die rapidly. If infections occur on the young bunch stalk, the entire inflorescence may die (Figure 4).



Figure 4 **Downy mildew symptoms.** i) Sporulation on the lower side and oil spots on the upper side of the same leaf ii) Sporulation on inflorescences iii) Withering of bunches

In Yu et al., 2012 [42] different immunity levels to DM in grapevine are well explained: i) if accumulation of callose deposits around the stomata and inhibition of zoospores germination early in infection process are observed; ii) emergence of callose deposits around and in the stomata but unable to inhibit the formation of hyphae; iii) with callose near the stomata and around haustoria, incapable to stop infection; iv) with more development of hyphae than in (iii); v) with hyphae in all mesophyll tissue intercellular spaces. According to classification, *M. rotundifolia* was classified as level i), several Chinese species as level iii), except *V. amurensis* as level iv) and some Chinese species and *V. vinifera* as level v) (Figure 5).

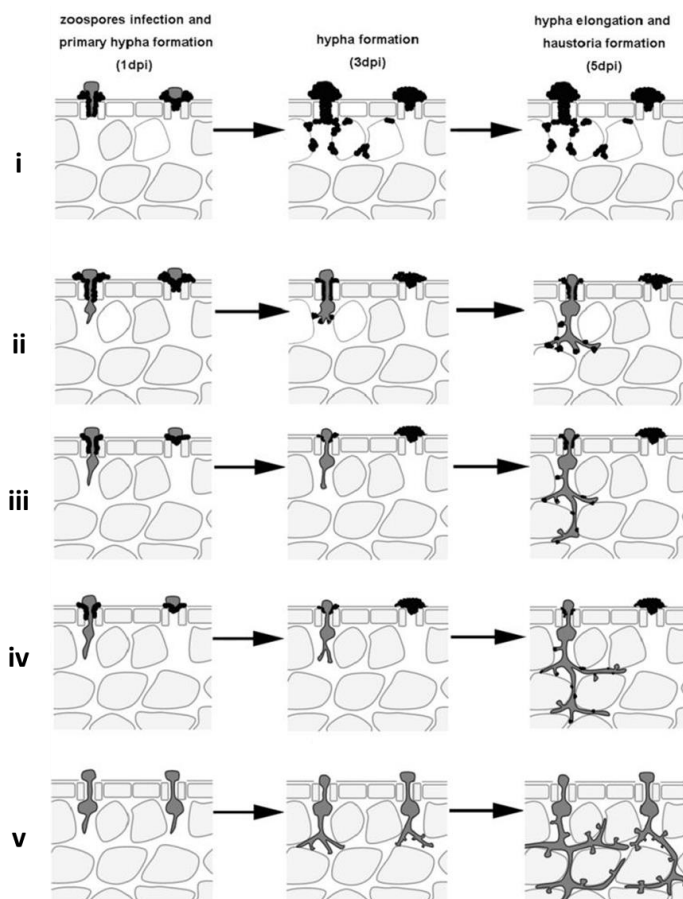


Figure 5 **Illustration of interaction between the *Plasmopara viticola* and grapevines with different downy mildew (DM) resistant levels.** i) DM immune grapevine ii) Extremely resistant grapevine iii) Resistant grapevine iv) Partially resistant grapevine and v) Susceptible grapevine. Black spots indicate callose deposits [42].

The lack of characterized isolates of *Plasmopara viticola* is a very limiting issue in the management of downy mildew of grapevine. Although molecular studies have previously confirmed a high diversity of this pathogen, there are still no phenotypically characterized pathotype strains or races available which could be used to study the mechanisms of interaction with host genotypes of different resistance. If differences in morphological characteristics such as size and branching of the sporangiophores result inadequate to identify possible biological races, biotypes or forms [43], variability of physiological traits are highly influenced by the temperature and humidity. A recent study (Gómez-Zeledón et al., 2013) [44] revealed a high pathogenic diversity between accessions from different geographical, but also depending on the host cultivar from which the isolate was collected. Only in the last years, as described in Dussert et al., 2016 [45] and in the more recent paper Yin et al., 2017 [46], a first draft of the *P. viticola* genome was published, allowing a better understanding of the molecular interactions governing this pathosystem and facilitating the identification of genes involved in gene-for-gene interactions with grapevine. The availability of a reference genome will also be helpful for population genomics studies addressing the worldwide invasion of this pathogen and the mechanisms responsible for its rapid adaptation to fungicides and to resistant grapevine cultivars.

Molecular maps and QTL analysis in grapevine

Linkage mapping in grape is based on the pseudo-testcross strategy [47] and starting from 1995 several linkage maps have been developed with the goal of locating the genetic determinants of target traits and identifying markers to assist breeding. The first maps was based on random amplified polymorphic DNA (RAPD) [48] and amplified fragment length polymorphism (AFLP) [49] markers which allowed the rapid generation of LGs, but not easily permit their comparison. The increasing interest in the comparison of genes and QTLs detected in different crosses encouraged the development of simple sequence repeats (SSRs) [50], which are co-dominant, highly polymorphic and easily transferable across related *Vitis* species. The first large set was produced by *Vitis* Microsatellite Consortium (VMC), a cooperative effort of 21 research groups in 10 countries

that was coordinated by AgroGene S.A. in Moissy Cramayel, France. Merdinoglu et al., 2005 [51] reported the first map based on 152 SSRs, mostly from VMC, which has been adopted as a reference to harmonize LGs resulting from individual mapping projects (www.vitaceae.org). Successively, two additional sets of microsatellite-based markers (VVI and UDV) were developed by Merdinoglu et al., 2005 [51] and Di Gaspero et al., 2005 [52], respectively and positioned on the map published by Adam-Blondon et al., 2004 [53], which became the second international grape reference map. In 2006 Doligez et al., 2006 [54] reported an integrated genetic map of grapevine based on the segregation data from five mapping populations [55], [56], [53], [52] filling in the major gaps present in individual maps and becoming the most complete reference map. The subsequent step in the development of genetic maps was the introduction of markers related to transcribed regions of the genome such as expressed sequence tags (ESTs) [57], [58], [59], [60], [61]. Finally, the advent of high-throughput single nucleotide polymorphism (SNP) arrays allowed to generate saturated genetic linkage maps from set of different samples, although the production of a high-quality array still requires a substantial investment of resources. Genotyping-by-sequencing (GBS) is a Next Generation sequencing (NGS)-based method that could represent an alternative to microarrays because it enables markers discovery and genotyping in one single step at significantly lower per sample cost [62].

Grape genetic maps were applied in several cases for the detection of genetic factors controlling target traits. In grapevine, some Quantitative Trait Loci (QTLs) for resistance to DM have been identified and molecular maps based on populations segregating for this trait are available. QTLs with major effects on downy mildew resistance were identified through comparative genetic mapping and were named Resistance to *P. viticola* (Rpv). Examples of these are *Rpv1* and *Rpv2* located on linkage groups (LGs) 12 and 18, respectively and derived from *M. rotundifolia* [63] [64], as a QTL identified in the same region in *V. riparia* [65]. The *Rpv3* locus is found on LG18 in the resistance grapevine Bianca [66], [67], [68], while *Rpv8* and *Rpv12* located on LG 14 together with *Rpv10* found on LG 9 derived from *V. amurensis* [69], [70], [71]. Nearby these major QTLs, additional ones with minor effects have been identified but never examined in depth. Among these loci, *Rpv1* is the only one to be cloned and functionally characterized [63], [72].

Quantitative (horizontal) resistance to downy mildew

The mode of inheritance of resistance to downy mildew in grapevine is controlled by several genes each one of which contributes a small amount to the variation of the character and is termed as polygenic/quantitative inheritance. Being a polygenic trait, downy mildew resistance is highly sensitive to environmental changes, therefore often characterized by low heritability. Polygenic variation of a genetic population is measured in terms of phenotypic, genotypic and environmental variances. While the genotypic variance remains unaltered by environmental conditions and consists of additive, dominance and epistatic components useful in plant breeding, the environmental ones refers to non-heritable variation. The phenotypic variance instead represents the total variability which is observable. Polygenic inheritance is characterized by continuous segregation at a large number of loci, affecting the trait, referred to a quantitative trait loci. Quantitative characters have been a major area of study in genetics for over a century and the genetic factors responsible for their variation could be localized as QTLs on the basis of the association between quantitative phenotypic variation and specific alleles of molecular markers. QTs are greatly affected by genetic backgrounds (gene interaction) or environmental factors or both. As explained in Figure 6, three types of QTLs can be described: i) major QTL, ii) major QTL linked to a minor QTL and iii) minor QTL. Usually, the major QTLs exhibit Mendelian inheritance, whereas other two types deviate from Mendelian nature of inheritance, making them difficult to trace. Indeed, sometimes can be the chance of losing a QTL with a minor effect during the phenotypic selection.

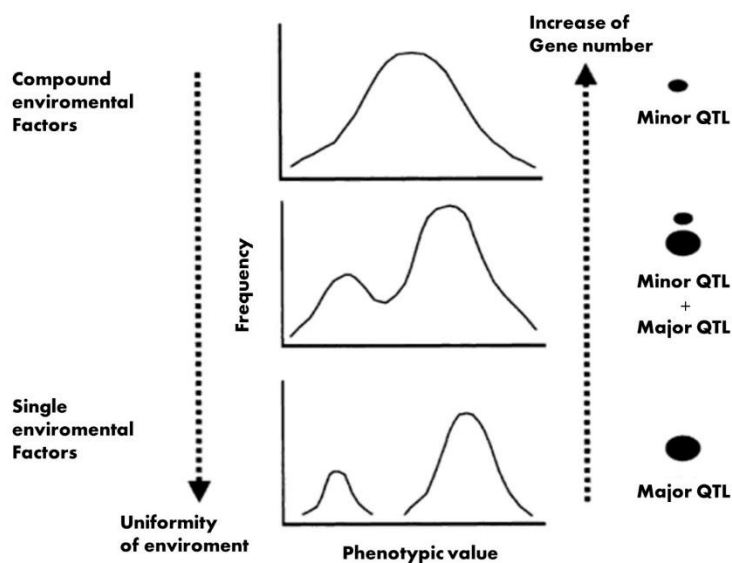


Figure 6 Relationship between phenotypes, genes and environments. Discrete phenotype distribution for qualitative traits arises from major genes, bimodal distribution for qualitative-quantitative traits from the joint effect of a major QTL and some minor QTL, and normal distribution for typical quantitative traits from many minor QTL [73].

Grapevine breeding

Plant breeding may be considered to have begun with the domestication of a small number of promising wild species. Hybridization has been used to access genes present in the wild relatives but not available in the cultivated germplasm. Sequencing of grapevine genome has opened up new opportunities in grape breeding, genetics and genomics research, by the analysis of genetic diversity, development of hybrids, comparative and functional genomics and molecular breeding for the introduction of desirable traits. Major improvement efforts have been directed toward enhancing fungal disease resistance in table and wine grape cultivars. The introduction of American hybrids and the rapid improvement of rootstocks by selection and hybridization led to a continuous recovery of European vineyards, reducing the chemical control which still remains the most efficient mean to prevent severe mildew epidemics and to obtain good quality grapes.

Although European *V. vinifera* cultivars are highly susceptible to *P. viticola*, *Muscadinia* species and several American and Asian *Vitis* species exhibit variable levels of resistance to the pathogen. Some American resistant genotypes efficiently halt hyphal growth in mesophyll, and neither visible symptoms nor sporulation are observed on these plants [74], while some Asian grapes can tolerate hyphal growth on the outer sides of the leaf laminae while preventing stomatal penetration [75].

To date, several studies regarding the genome sequencing and the realization of genetic maps by using different molecular markers and high-throughput technologies have been published; this has allowed to undertake advanced research aimed at localization of genes of agronomic interest and identification of QTLs. Molecular crop breeding use the DNA based markers as handle for the mining and tagging of novel alleles. Marker-Assisted Breeding (MAB) aims at the introgression those alleles, which control the trait to be improved, in the desirable cultivars and it involves several type of markers including restriction length RAPDs, AFLPs, microsatellites, ESTs, and SNPs. From a breeding point of view, it is highly preferred to combine as many resistance as sustainable as possible and MAB provides a new tool for breeders to gain this goal. For this reason, repeatability of field tests are required to characterize the effects of QTLs and the genetic interactions ant to evaluate their stability across environments. Breakdown of disease or pest resistance conferred by single major genes is a common phenomenon in several crops, due to the emergence of new pathogenic races or biotypes after its wide cultivation, therefore pyramiding stress resistance genes is a useful mean to develop durable resistant variety [76]. The concept of gene pyramiding was proposed by Nelson et al., 1978 [77] to develop crop varieties with durable resistance to diseases by combining together desirable QTLs through conventional crossing using molecular markers. Recently, significant advancements in cell culture, gene discovery and gene insertion technologies merged to fully unable precision breeding for genetic improvement of grapevine, overcoming the conventional breeding as reviewed by Gray et al., 2014 [78].

OBJECTIVES

An integrative approach was used in this research to characterize an unexplored Caucasian germplasm collection of *Vitis vinifera*, aiming to determine the phylogenetic context and to identify and mine genes and defense pathways associated to the lower susceptibility to downy mildew (DM) previously reported in this grapevine population. First of all **Chapter 1** allows to better understand the context of this research work through a general introduction.

Chapter 2 presents the genetic characterization of 25 unexplored Caucasian genotypes by using both nuclear and plastid molecular markers. The genetic relationship among the investigated germplasm collection and other grapevine accessions from Europe and neighboring countries was also defined through phylogenetic and PCoA approaches. A specific attention was placed on the Caucasian accession 'Mgaloblishvili Noir', which displayed the most interesting phenotype in previous seasons as regard to DM infection.

Chapter 3 describes the construction of a genetic linkage map based on a self-cross population (S1) obtained from this Georgian cultivar by the colleagues of the Department of Agricultural and Environmental Sciences – Production, Landscape and Agroenergy (DISAA) of the University of Milan which also evaluated each plant under artificial inoculations of *Plasmopara viticola* (Downy mildew, DM). The genetic map was built essentially with SSR markers and enriched with RAD-derived SNPs chosen to fill in several gaps. The preliminary association analysis for DM resistance identified only a few putative minor QTLs due to the poor repeatability of the plant response to DM among the different phenotyping years.

Chapter 4 describes a gene expression analysis during the *P. viticola* inoculation on the individuals of the S1-progeny showing different levels of DM tolerance. This work was carried out at Julius Kuhn Institute (JKI) of Geilweilerhof (Germany).

Finally, a general discussion (**Chapter 5**) concludes this research work by integrating results of preceding chapters and by estimating their implications in breeding programs.

Chapter 2

PHYLOGENETIC RECONSTRUCTION OF CAUCASIAN GERMPLASM

Abstract

According to historical and archeological findings, Georgia, in the South of Caucasus, was widely defined the 'cradle' of grapevine domestication and this hypothesis made the germplasm resources of the region particularly fascinating from a genetic point of view. Recently, some grapevine accessions from Georgia have attracted attention because of their low susceptibility to several diseases, including downy mildew (DM) caused by *Plasmopara viticola* (*Pv*). This suggested that there may be potential genetic variation within *Vitis vinifera* to be exploited for resilient viticultural system, in addition to breeding resources from other *Vitis* species. Here we present the genetic characterization of 25 previously unexplored Caucasian grapevine accessions aiming to understand the eventual genetic basis of less susceptible phenotypes observed under natural field infection by DM. Screening at major Rpv loci didn't find any SSR markers of the expected size for resistance traits that might have been introgressed from Asian or American resistant grapes, suggesting how the observed low susceptibility to *P. viticola* may be ascribed to novel genetic factors. A phylogenetic analysis including several hundred grapevine varieties, from across Eurasia placed this germplasm among Georgian *V. vinifera* populations. However, the assessment of genetic diversity and population structure confirmed the strong separation of the Georgian germplasm from the Middle Asia ones. Principal coordinate analysis (PCoA) has also identified special overlapping of the Caucasian wild compartment with some cultivated varieties, better described through the investigation of the chlorotype variation and distribution. Generated data proved the importance of phylogenetic characterization of this germplasm and supported the presence of interesting traits of tolerance to diseases in ancestral cultivated grapevines.

Background

It is widely accepted that the cultivated form of *V. vinifera* subsp. *sativa* derived from its wild form *V. vinifera* subsp. *sylvestris*, which was spread across Western Europe, the Mediterranean, the Caucasus and Central Asia. The South of Caucasus together with the eastern Anatolia, has been considered for a long time the heart of viticulture with the earliest examples of winemaking [12], [79], [80] as also supported by historical, ethnographical, religious and toponymical evidences [81], [82], [83], [84], [85]. Georgia has been considered the cradle of the domestication process. Despite it was not so easy to determine the exact number of autochthonous varieties (both table and wine) for this country, recent local ampelographic books provided morphological description of the plants, defining the most important Georgian varieties and their old putative regions of origin, such as Kakheti, Kartli, Imereti, Racha, Lechumi, Samegrelo, Guria, Adjara, Abkazeti, Saingilo and Meskheta (Appendix).

Transitional types of grapes that included wild forms of the subsp. *sylvestris*, feral and cultivated land races and ancient local varieties were once common in this region [86], [87]. One of the most important features separating the domesticated grapes from the wild ones is still their reproductive system. Indeed, wild grapevines are dioecious while cultivated varieties are hermaphroditic in nature. It is still unknown whether hermaphroditism evolved through sexual recombination or as a mutation of wild form subsequently introgressed into cultivated one. To date, a great amount of cultivars has been found worldwide and the existence of morphological differentiation between cultivars from eastern and western ends of the modern distribution of the Eurasian grape may reflect the existence of different contribution from local *sylvestris* populations. Eurasian grapes had a complex history of movement over growing regions, which hampered the identification of clear geographic trends in their distribution [88]. Chloroplast markers are powerful tools to reconstruct the evolutionary relationships between wild and cultivated grapevines as showed by Arroyo-García et al., 2006 [13]. Indeed, the chloroplast are haploid and inherited uniparentally, and the variations in their genome are potentially informative characters [89].

Historical records report that the most widely cultivated European grapevine varieties are highly susceptible to various pathogens such as downy and powdery mildew, in contrast with the American and Asian varieties which show a strong resistance to them, probably due to the coevolution with these pathogens. More importantly, the identification of powdery mildew resistance in accessions of *V. vinifera* indicated that some genetic resistances may be present in the germplasm. Several works that have exploited available genetic information on the powdery mildew genetic resistance have already been published [90], [91], [92], [93]. On the other hand no cultivated varieties, resistant to downy mildew, present in the domestication area of *V. vinifera*, has been detected.

Our investigation intended three major objectives in order to obtain a wider view of a Caucasian germplasm, composed by 25 unexplored accessions which show a low susceptibility to *P.viticola*. The first objective was to verify, through the genotyping at Rpv and Ren/Run major loci, the lack of introgression of resistance traits to *Plasmopara viticola* from already known American and Asian *vitis*, especially *V.amurensis*, *V. rupestris* and *Muscadinia rotundifolia*. Afterwards, the genetic diversity and population structure of the investigated germplasm collection as well as its phylogenetic relationships with genotypes reported in the European *Vitis* Database (www.eu-vitis.de) were evaluated. Finally, we expanded the research work by analyzing different chloroplast markers already described in Arroyo-García et al., 2006 [13] and Lózsa et al., 2015 [94] in order to investigate the connection among ancient grapevine cultivars and our germplasm collection and to elucidate the geographic trend of their distribution.

Methods

Plant material and DNA extraction

A total of 25 grapevine accessions from a Caucasian germplasm, grown in a collection vineyard established in 2006 at the Regional Research Station of Riccagioia in Lombardia (northern Italy), were selected as objects of study, for their low susceptibility to *Plasmopara viticola*. More detailed information about each genotype are available in Appendix. To perform a complete analysis, a set of 666 accessions, composed by 396 *V. vinifera* ssp. *sativa* (Sativa), 186 *V. vinifera* ssp. *sylvestris* (Sylvestris) and 84 accessions of rootstock varieties including wild non-*vinifera* *Vitis* species (Rootstocks) were used. The *V. vinifera* group included several genotypes (100 sativa and 94 sylvestris) from the FEM grape germplasm repository (ITA362), located in San Michele all'Adige (Italy), 79 accessions from UzRIPI germplasm collection (66 sativa and 13 sylvestris), which includes accessions from different Asiatic regions such as Uzbekistan, Tajikistan and Kirghizstan (Middle Asia), and a few derived from Israel (42 sativa and 64 sylvestris) and, Armenia (16 sativa), Azerbaijan (32 sativa) and Iran (10 sativa). Moreover, a germplasm collection from Georgia (COST ACTION FA1003) composed by 72 sativa and 8 sylvestris together with a second germplasm collection from Georgia composed by 40 sativa accessions (URZIPI database) were enclosed. For chloroplast analysis only a few genotypes of the previous list were chosen for the comparison with the chlorotype of Caucasian germplasm.

Young leaf tissue of greenhouse grown plant per accession was harvested, stored in 96-well microtube plate and freeze-dried. Total genomic DNA was isolated after grinding with MM 300 Mixer Mill system (Retsch., Germany). DNA extraction was performed employing the DNeasy 96 plant mini kit (QIAGEN, Germany) and suspended in AE buffer after digestion with RNase A (QIAGEN) at 65°C for 10 m. Finally, the DNA samples were diluted to approximately 4 ng/ul before using for successive analysis.

SSR amplification and genotyping at Rpv and Ren/Run major loci

A total of 14 markers linked to some of known downy mildew (*Rpv1*, *Rpv3*, *Rpv12* and *Rpv10*) and powdery mildew (*Ren1*, *Run1*) resistance loci were tested on the Caucasian germplasm collection in order to detect a possible introgression of resistance traits from well-studied American and Asian *Vitis*. Genotyping was performed according to already published protocols [63], [95], [66], [71], [92], [96], [70].

SSR selection for phylogenetic analysis and genotyping

Nineteen SSR markers previously developed for grape by Laucou et al., 2011 [97] and two additional markers VrZAG62 and VrZag79 [98], including at least one locus per chromosome, were chosen to profile the whole population. This set of markers includes the SSRs proposed by European Project GrapeGen06 for the characterization of regional cultivars [99].

Nine multiplex panels of fluorescent-labeled (6-FAM, HEX and NED) microsatellite loci were used, allowing simultaneous PCR amplifications. All the reactions were carried out in a final volume of 12.5 ul including 10 ng of genomic DNA, 0.25 mM of each dNTPs, 2 mM MgCl₂, 1X gold PCR buffer (Perkin Elmer) and 1.5 U Taq DNA Polymerase (AmpliTaQ, Gold™, Applied Biosystems, Foster City, CA). Depending on the locus, primer concentrations ranged from 0.2 to 0.6 uM. All SSR markers were amplified under the same thermocycler conditions: 7 m at 95°C, 30 cycles of 45 s at 95°C, 1 m at 54°C, 30 s at 72°C; with a final extension of 30 s at 72°C. Amplified fragments, generated by different fluorescent dye-labeled primers, were mixed with 9.45 ul of formamide and 0.05 ul of the GeneScan™ -500 ROX® Size Standard (Applied Biosystems) and, after a denaturation process, they were separated on an ABI 3130xl Genetic Analyzer (Applied Biosystems) and allele sizes were estimated by using GeneMapper v3.5 software. Rates of missing data were below 1.9%.

Genetic diversity assessment and relationships among and within populations

The final dataset of genetic profiles at the 21 SSR loci was used to estimate the main diversity statistics, such as a total number of different alleles per locus (Na), number of effective alleles (Ne, the number of equally frequent alleles required to give the observed level of heterozygosity), number of private alleles (Np) across populations, observed (Ho) and expected (He) heterozygosity, Shannon's Information Index (I) and fixation index (F, inbreeding coefficient) throughout GenAlex v6.502 software [100].

Genetic relationships among Caucasian genotypes and the entire collection were determined using the Darwin software package v6.0 [101]. A weighted neighbor-joining tree was created based on simple matching dissimilarity matrix with 100 bootstrap replicates.

Analysis of population structure

The genetic structure of the Central Asia germplasm collection was analyzed by using STRUCTURE 2.3.4 software [102], [103] and performing Principal Coordinate Analysis (PCoA) [104] implemented in the program GenAlex v6.502. STRUCTURE software uses the Bayesian clustering algorithm to identify subpopulations and estimate their allele frequencies. In particular, STRUCTURE sorted individuals into K clusters, according to their genetic similarity. The best K was chosen based on the estimated membership coefficients (Q) for each individual in each cluster. Ten independent runs for K values ranging from 1 to 12 were performed with a burn-in length of 500000 followed by 750000 interactions with 10 replicate runs for each value of K. The population structure was analyzed assuming admixture in the population and no prior population information was used. Taking results from STRUCTURE output file, the number of true clusters in the data (K) was determined using Structure Harvester [105], which identifies the optimal K based on Evanno method [106], plotting the log probability L(K) and ΔK of the data over ten runs.

Furthermore, a “hierarchical STRUCTURE analysis” was applied on these data by running the program on partitioned data, as suggested by Pritchard [102], employing only the accessions suspected of being subdivided into different clusters. For this approach the ΔK method [106] was used in adjudication for the best K and the individuals with a proportional membership $Q > 0.8$ in their primary population were considered in the subsequent analysis.

Moreover, different PCoAs, based on standardized covariance of genetic distances calculated for codominant markers, were performed to confirm the hierarchical analysis.

SSR selection for chloroplast analysis and genotyping

To characterize chloroplast genetic diversity within the Georgian germplasm collection, we studied the allelic variations at 6 chloroplast SSR polymorphic loci (cpSSR3 equal to NTCP8, cpSSR5 equal to NCTP12 and ccSSR5, cpSSR10 equal to ccSSR14, ccSSR9 and ccSSR23) compared with the ones of other accessions ($Q > 0.8$), located across Eurasia, in order to define the geographic distribution according to the chlorotype assignment described in Arroyo-García et al., 2006 [13]. Moreover, since several recent works described the reconstruction of phylogeny of Vitaceae using noncoding plastid markers as *trnC-petN*, *trnH-psbA*, and *trnL-F*, we investigated the presence/absence of one 54 nucleotide deletion in the *trnC-petN* region (Lózsa et al., 2015) [94]. After aligning seven different chloroplast genomes (EMBL-EBI database) related to *M. rutundifolia*, *V. aestivalis*, *V. amurensis*, *V.v. Maxxa*, *V.v. Saperavi*, *V.v. Meskhuri Mtsvane* and *V.v. Rkatsiteli*, using CLC Genomics Workbench 8.5 program (CLC bio, Aarhus, Denmark), we constructed an UPGMA phylogenetic tree (bootstrap 100) with the software MEGA 5.1. Finally, the obtained data were compared with the ones obtained from analysis of *trnC-petN* detection on Caucasian germplasm collection.

Genotyping was carried out with a modified EcoR1-tailed primer method [107]. Reactions of 11.5 μ l contained 5 ng of genomic DNA, 0.25 mM of each dNTPs, 2 mM $MgCl_2$, 1X gold PCR buffer (Perkin Elmer) and 1.5 U Taq DNA Polymerase (AmpliTaq, Gold™, Applied Biosystems, Foster City, CA) and 5 μ M EcoR1, with the following touch-down profile: 10 m at 95°C, followed by 10 cycles (1 m 95°C, 1 m 59°C minus 0.5°C each cycle, 2 m 72°C), 25 cycles (1 m 95°C, 1 m 54°C, 2 m 72°C), and a final extension of 10 m at 72°C. Forward primers were designed with an EcoR1 FAM-labeled tail and combined with reverse primer were added in the reaction in a ratio 1:5, respectively. Amplification protocol were optimized for each marker, but the touch-down profile described above was the most widely used. Dye labeled PCR products were visualized on an ABI 3130xl Genetic Analyzer and analyzed with GeneMapper v3.5 software, after a denaturation in a mix of formamide and GeneScan™ - 500 ROX® or -1200LIZ® standard.

Results

Genotyping at *Rpv* and *Ren/Run* major loci

The application of molecular markers associated with resistance loci allows to trace the introgression of the corresponding genes in plants at an early stage of development and thus to accelerate the breeding by early selection of the plants harbouring this trait. This approach led to achieve more information about our starting germplasm collection composed by 25 Caucasian genotypes, which showed a tolerance to downy mildew infection. We tested several markers on these accessions to discover a possible introgression of resistance from Asian and American *Vitis* species (supplementary tables S1, S2). In detail, we tested VVIm11, VMC1g3.2 associated to *Rpv1* (*M. rotundifolia*), UDV737 and VMC7f2 linked to *Rpv3* (*V. rupestris*), GF09_46 and GF09_47 linked to *Rpv10* (*V. amurensis*) and UDV370, UDV350 associated to *Rpv12* (*V. amurensis*). Moreover we tested also markers linked to powdery mildew resistance such as VMC8g9 and VMC4f3.1 for *Run1* locus and all the markers described in Riaz et al., 2013 [90] linked to *Ren1* locus and identified in the resistant Kishmish Vatkana *Vitis vinifera*. Our results highlighted the absence of the expected sizes linked to the different genes of interest, suggesting the presence of unexplored genetic traits underlying the low susceptibility observed in the investigated Caucasian population.

Phylogenetic analysis and Genetic variation assessment of Caucasian germplasm

A set of 21 microsatellites, including the standard set of markers for genetic identification, was used in a first step for the analysis of the starting plant material from Caucasus. The first analysis compared 100 *Sativa* accessions, including proles *pontica* (Vv1), proles *orientalis* sub-proles *antiasitica* (Vv2), proles *orientalis* sub-proles *caspiaca* (Vv3), proles *occidentalis* (Vv4), 129 Georgian and 25 Caucasus accessions, as well as 94 European *sylvestris*. Moreover 75 rootstocks were selected as outgroup. The phylogenetic tree (Figure 1) revealed four different clades, representing the *V. vinifera* proles, which were well separated from the Georgian *V. v.* subsp. *sativa* accessions including all the Caucasian genotypes. Only a few Georgian accessions were included in Vv1, Vv2 and Vv3 clades, probably due to a certain percentage of admixture. Rootstocks were instead classified in a distinct and well-separated group.

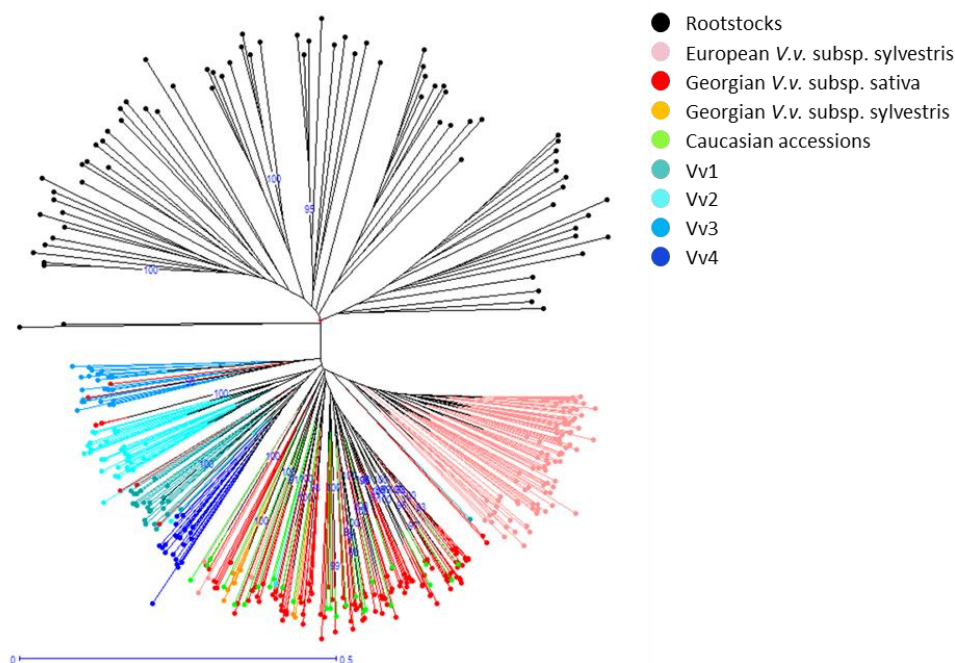


Figure 1 Neighbour-joining dendrogram based on simple matching dissimilarity matrix calculated from the dataset of 21 SSRs. Branch length is proportional to the distance between nodes. Only bootstraps superior to 90 are presented.

Afterwards, a second phylogenetic analysis was performed by adding genotypes derived from Iran, Israel region, Armenia, Azerbaijan and Middle Asia (UzRIPi germplasm). The dendrogram (Figure 2) confirmed the

membership of the Caucasian accessions to the *V. vinifera* group. Given the assigned membership of the Caucasian accessions investigated in this study to the Georgian group, we will refer hereafter only to Georgian clade. However, they splitted in two different clades, one comprising the most of the Georgian cultivars and one composed by a combination of wild and cultivated genotypes, showing a similarity to the European *sylvestris*. Moreover, the phylogenetic analysis showed a high rate of admixture among populations, in particular within Middle Asia accessions which derived from really close related regions such as Armenia, Azerbaijan, Iran, Uzbekistan, Tajikistan and Kyrgyzstan.

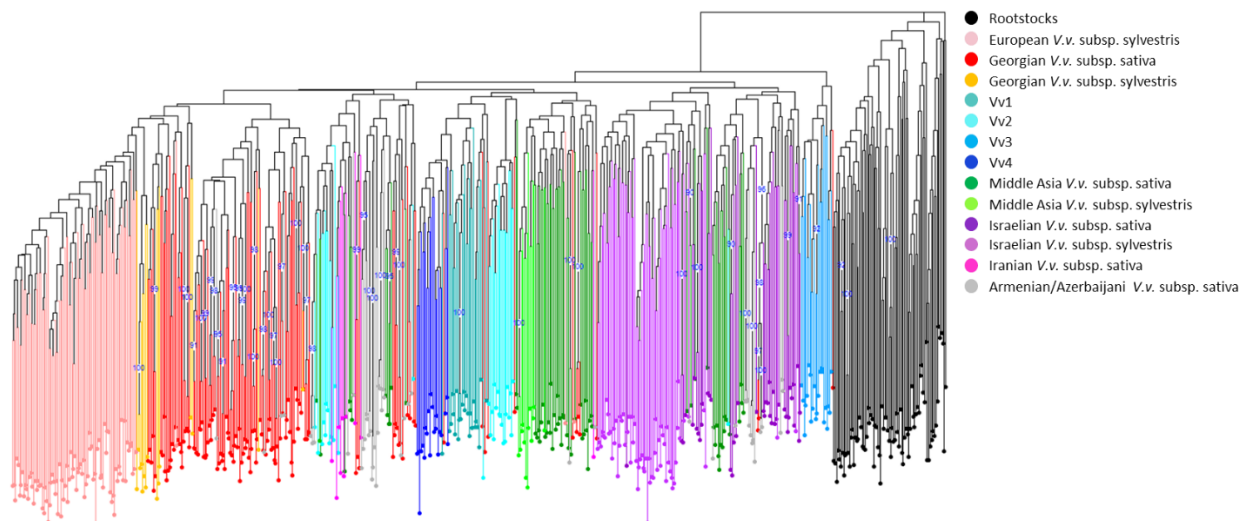


Figure 2 Neighbour-joining dendrogram based on simple matching dissimilarity matrix calculated from the dataset of 21 SSRs across 666 genotypes. Only bootstraps superior to 90 are presented. Georgian germplasm included all the 25 Caucasian accessions previously described.

Genetic variability within the different populations was studied by using a set of 21 SSRs. All the parameters are summarized in Table 1. Despite the different number of accessions per population, we observed a conserved trend with a higher level of observed heterozygosity (H_o) values within the cultivated subgroups compared to the *sylvestris*. This result suggests a higher degree of homozygosity of the wild populations, partially supported by the relative fixation indexes. In particular, the highest value of observed heterozygosity (H_o) was detected in Armenia region (0.818), followed by the Azerbaijan ones (0.774), whereas the lower H_o value was detected in European *sylvestris* population (0.595), followed by Middle Asia *sylvestris* accessions (0.645). Moreover, a lower F index in Israelian sativa (0.007) and European sativa (average value $Vv = -0.063$) compared with the *sylvestris* (0.076, 0.133, respectively) was observed, in agreement with Emanuelli et al., 2013 and Marrano et al., 2015 [108,109] surveys.

Conversely, we observed a higher F index within cultivated populations of Georgia (0.044) and Middle Asia (0.024) compared with wild groups (0.017, 0.008, respectively). This result suggested a higher degree of inbreeding among Georgian cultivated accessions, partially explaining the splitting of Georgian population described previously. Indeed presumably, Georgian sativa accessions clustered in two subgroups, one more isolated, conserved and linked to wild population and the other characterized by a greater rate of gene flow.

Table 1 Summary statistics for genotypes from different populations assessed using 21 SSRs. N-sample size; Na-N° of different alleles per locus; Ne-N° of effective alleles; Np-N° of private alleles; Ho-observed heterozygosity; He-expected heterozygosity; uHe-unbiased expected heterozygosity; I- Shannon's information index; F-fixation index.

Pop	Mean and SE over Loci for each Pop										
		N	Na	Ne	I	Ho	He	uHe	F	Np Mean	Np
Middle Asia <i>V.v. subsp. sativa</i>	Mean	66	9.571	4.928	1.739	0.750	0.770	0.776	0.024	0.286	6
	SE	0	0.709	0.386	0.080	0.025	0.020	0.020	0.022	0.122	2.6
Middle Asia <i>V.v. subsp. sylvestris</i>	Mean	13	4.857	3.362	1.262	0.645	0.651	0.677	0.008	0.000	0
	SE	0	0.398	0.310	0.089	0.041	0.032	0.034	0.035	0.000	0.0
Georgia <i>V.v. subsp. sativa</i>	Mean	130	13.190	5.312	1.849	0.738	0.773	0.776	0.044	1.905	40
	SE	0	0.830	0.395	0.092	0.032	0.029	0.029	0.022	0.292	6.1
Georgia <i>V.v. subsp. sylvestris</i>	Mean	15	6.810	4.208	1.558	0.711	0.726	0.751	0.017	0.333	7
	SE	0	0.466	0.303	0.085	0.038	0.029	0.030	0.047	0.126	2.6
Azerbaijan <i>V.v. subsp. Sativa</i>	Mean	32	8.952	4.712	1.730	0.774	0.762	0.774	-0.016	0.190	4
	SE	0	0.537	0.341	0.075	0.024	0.019	0.019	0.022	0.088	1.8
Armenia <i>V.v. subsp. Sativa</i>	Mean	16	6.857	4.472	1.587	0.818	0.735	0.759	-0.109	0.143	3
	SE	0	0.480	0.332	0.089	0.040	0.032	0.033	0.030	0.078	1.6
Iran <i>V.v. subsp. sativa</i>	Mean	10	5.476	3.676	1.415	0.724	0.700	0.736	-0.039	0.048	1
	SE	0	0.376	0.284	0.069	0.029	0.020	0.021	0.038	0.048	1.0
Israel <i>V.v. subsp. sativa</i>	Mean	42	8.905	4.864	1.700	0.748	0.749	0.758	0.007	0.286	6
	SE	0	0.672	0.382	0.100	0.041	0.035	0.035	0.030	0.122	2.6
Israel <i>V.v. subsp. sylvestris</i>	Mean	64	10.714	5.466	1.828	0.714	0.774	0.780	0.076	0.952	20
	SE	0	0.778	0.494	0.102	0.026	0.026	0.026	0.020	0.305	6.4
Vv1	Mean	25	7.238	3.829	1.511	0.739	0.704	0.718	-0.052	0.000	0
	SE	0	0.511	0.338	0.073	0.027	0.021	0.022	0.026	0.000	0.0
Vv2	Mean	33	7.429	4.070	1.535	0.750	0.713	0.724	-0.057	0.000	0
	SE	0	0.510	0.351	0.083	0.033	0.028	0.028	0.029	0.000	0.0
Vv3	Mean	22	6.238	3.811	1.443	0.742	0.695	0.711	-0.073	0.095	2
	SE	0	0.390	0.297	0.082	0.037	0.031	0.032	0.029	0.066	1.4
Vv4	Mean	20	6.095	3.380	1.364	0.717	0.664	0.681	-0.072	0.095	2
	SE	0	0.396	0.254	0.073	0.041	0.029	0.030	0.038	0.066	1.4
European <i>V.v. subsp. sylvestris</i>	Mean	94	9.905	3.464	1.509	0.595	0.681	0.685	0.133	0.667	14
	SE	0	0.746	0.238	0.074	0.029	0.023	0.023	0.029	0.252	5.3

Taking into account number of different alleles (Na) and number of private alleles (Np) as shown in Figure 3, recorded data showed a high genetic diversity within the Georgian population, confirming the main feature of the “cradle of domestication”. Similar results has been achieved by analyzing the Israel accessions, both wild and cultivated, which reported a peculiar genetic variation, probably due to the fact that, during the Muslim prohibition of winemaking, they would have survived uncontaminated in the wild owed to the high resilience of the grapevine [110]. Given that, private alleles have proven to be good indicators of gene flow, these results clearly demonstrates that Georgia, as center of domestication process, have preserved the most private alleles (40) and rare alleles, making them the most important reservoirs of genetic variation.

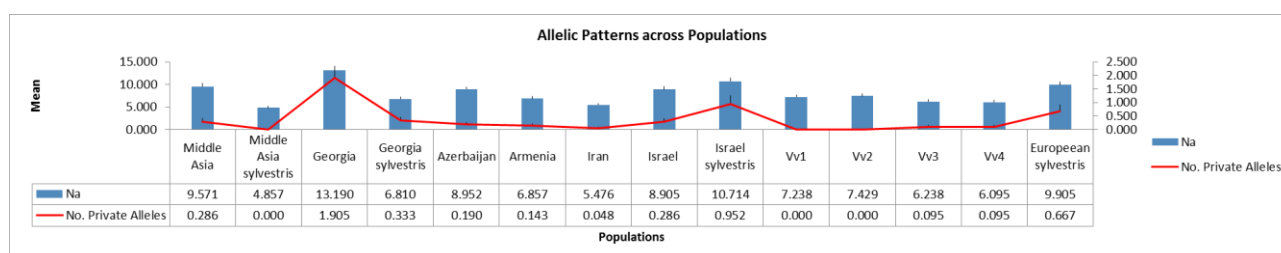


Figure 3 Allelic Patterns across Populations. Graph of private alleles (Np) and different alleles (Na) which characterized different populations.

Population structure

Inference of population structure from genetic data has been often used to understand underlying evolutionary and demographic processes experienced by populations. Such inference was mainly done by clustering individuals into groups, often referred to as subpopulations. Evaluation of population structure and gene flow levels between subpopulations allowed inference about migration patterns and their genetic consequences [111] [112]. The genetic structure of the whole Near East germplasm collection was analyzed using PCoA and STRUCTURE, compared with the four proles (Vv1, Vv2, Vv3, Vv4) and European *sylvestris* accessions. Despite the presence of some overlapping zones, the PCoA approach based on a genetic distance matrix with data standardization showed a clear differentiation between the subspecies derived from the Near East, which comprised regions of Middle Asia (including Iranian cultivated accessions), Georgia, Israel, Armenia and Azerbaijan, and European accessions, which included Vv4 and European *sylvestris* (Figure 4). The first axis accounted for 8% of the overall variance and well separated the genotypes derived from the Near East from the European ones. The second axis explained 4.26% of variance, distinguishing the Georgia region from the rest of Near East. An overlapping region was identified, including individuals from Vv1 and Vv3 subpopulations, which represented the proles *pontica* and *orientalis* respectively.

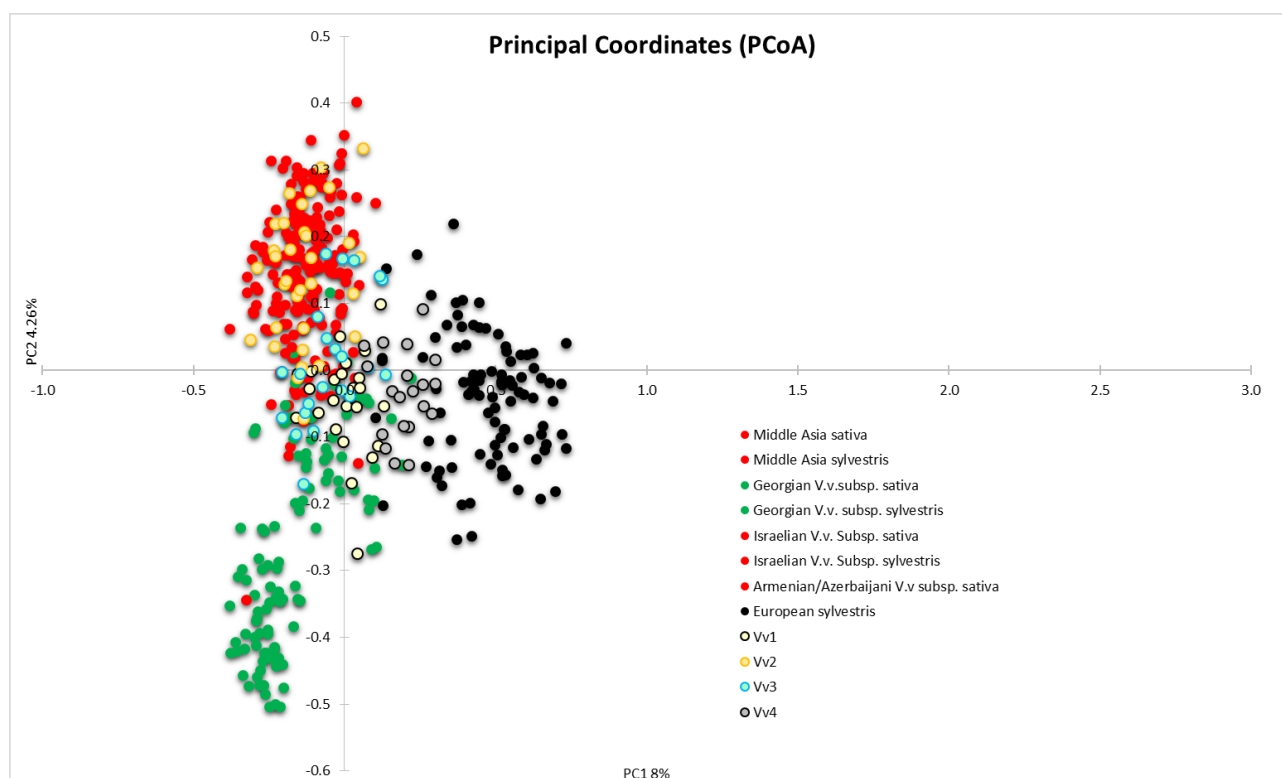


Figure 4 Scatter plot from a PCoA. Representation of the first two principal coordinate analysis axes for the SSR data.

The SSR dataset was used for the model-based Bayesian clustering analysis as implemented in STRUCTURE. The genetic structure of grapevines from Near East regions has been influenced by the historical migration, human selection and it has been understood as a complex pedigree, reflecting the domestication process, therefore the analysis was carried out only on the Near East germplasm collection, to better define its population structure. The number of cluster (K) that best fit the data, was evaluated by using STRUCTURE HARVESTER program, which is based on the “Evanno” method. As shown in Figure 5, the program discriminated two major clusters (K=2) as the best fit, although peaks of ΔK were found also at K=3 and K=5.

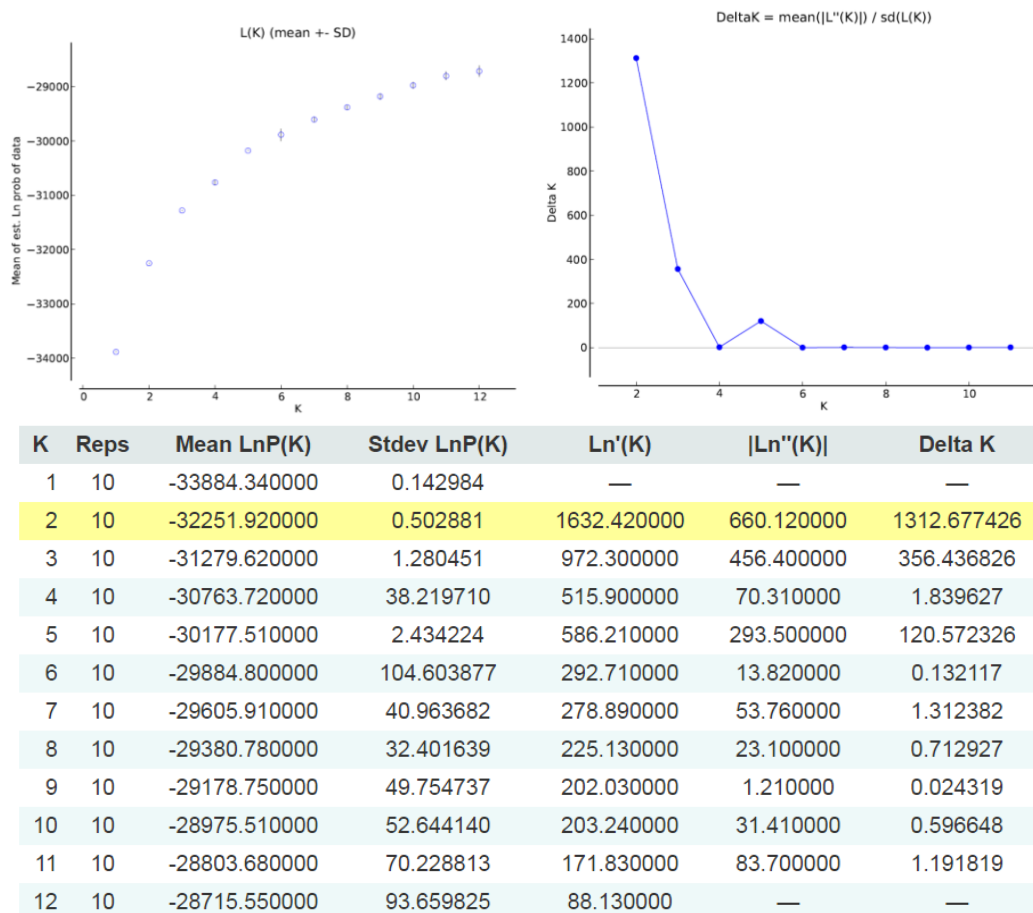


Figure 5 Plot of mean likelihood $L(K)$ and variance per K value from STRUCTURE on the studied dataset for 21 polymorphic microsatellite loci. The number of K groups that best fit the data was calculated with STRUCTURE harvester. Yellow highlight in the table output of the Evanno method results, is performed dynamically on the website and shows the largest value in the Delta K column

Running STRUCTURE at $K=2$ (Figure 6), the germplasm was clearly clustered in two subpopulations. The first one included Georgian and Caucasian accessions, confirming the membership of the 25 Caucasian genotypes to the Georgia region. The second subpopulation included all the other accessions, putting together Armenian, Azerbaijani, Israeli and Middle Asia individuals. Since these results highlighted a certain admixture proportions within the clusters, a second run of STRUCTURE was performed to reduce the admixture by screening only the individuals strongly assigned ($Q>0.8$) to the inferred populations.

Such hierarchical analysis allowed to detect an additional subpopulation ($K=3$), including the Israeli accessions.

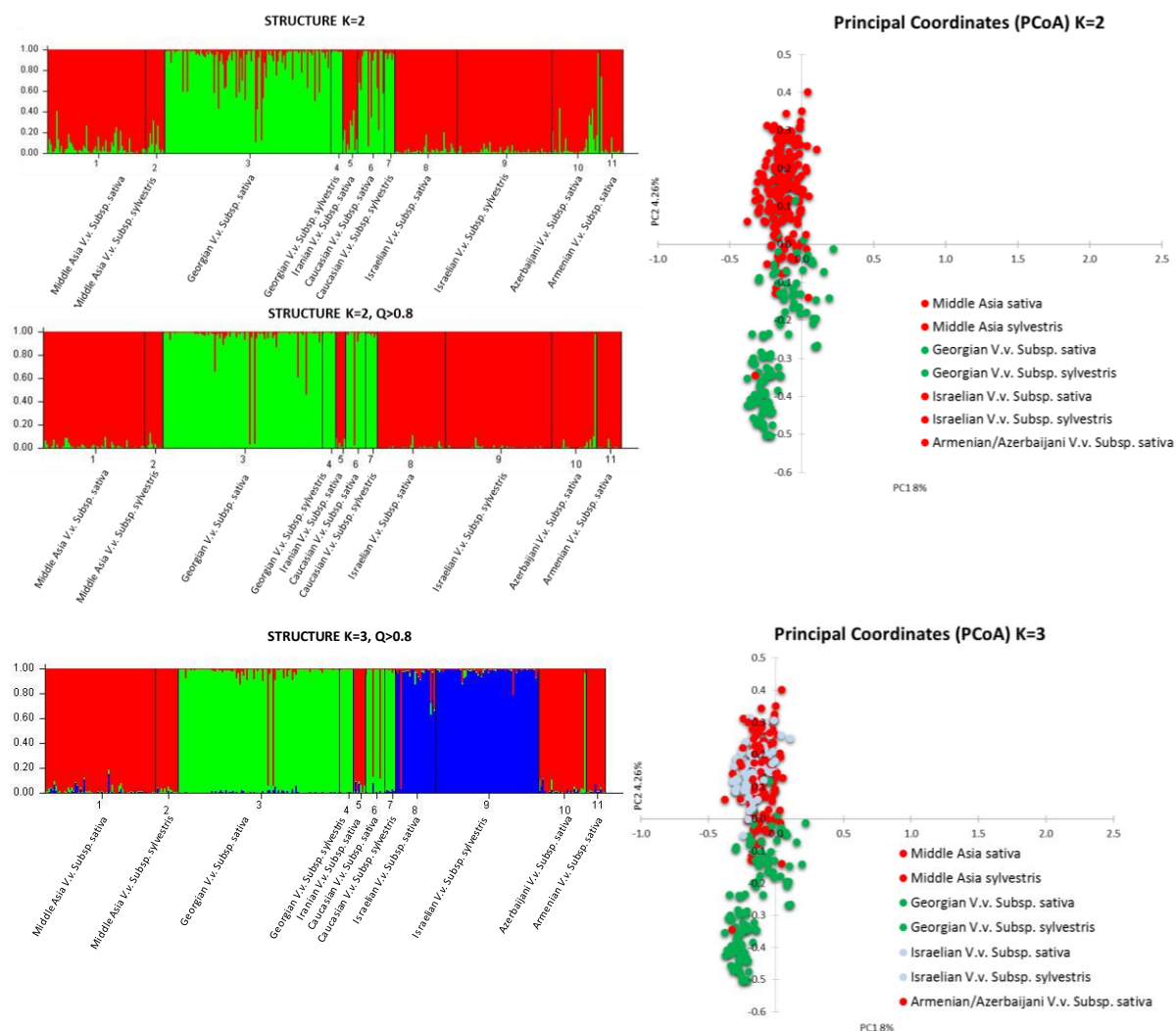


Figure 6 Inferred population structure using the model-based program STRUCTURE. Representation of population structure based on K=2, K=2 (Q>0.8) and K=3 (Q>0.8). Each accession is represented by a single vertical line, which is partitioned into colored segments in proportion to the estimated membership in to different subpopulations. The hierarchical clustering is represented also by PCoA analysis, with the relative different colors, Green used for Georgia and Caucasus regions, Red used for Middle Asia and Blue for Israelian accessions.

While at K=2 and K=3, the cultivated grapevine accessions were not separated from their wild relatives, at higher K value (K=5), all these accessions were re-sorted into different clusters (Figure 7). Indeed, at K=5 we were able to discriminate 5 subpopulations representing regions of Middle Asia, Israel, Armenia/Arzerbaijan and Georgia, separating the Georgian accessions in sativa and sylvestris. As shown in PCoA (Figure 7), the Georgian germplasm collection revealed a high rate of admixture, suggested by the overlapping zone between wild and cultivated species. In detail, 27 of 91 Georgian cultivars were assigned to the sylvestris cluster, suggesting the close relationship with wild progenitors (Supplementary table S3).

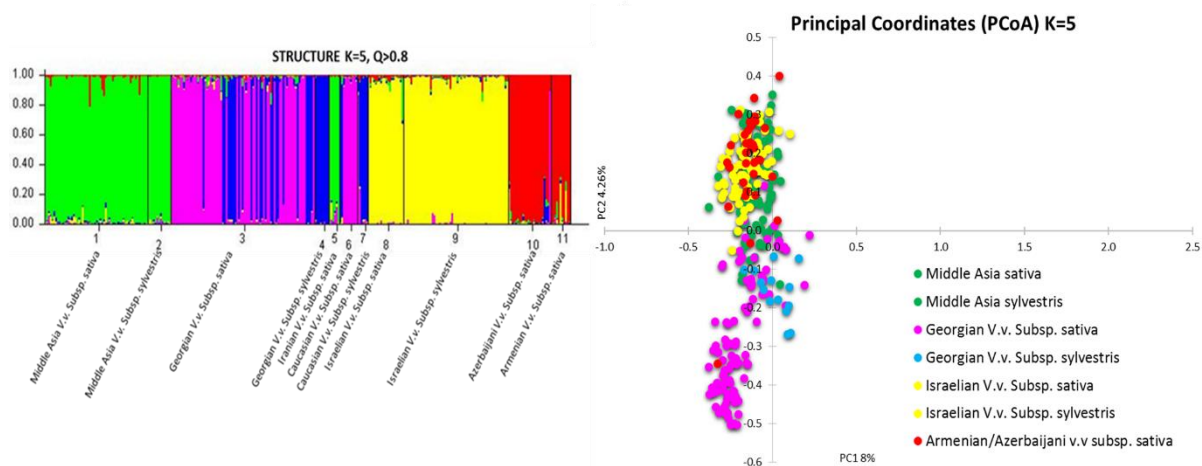


Figure 7 Inferred population structure using the model-based program STRUCTURE for $K=5$ ($Q>0.8$). Color legend: Green used for Middle Asia, Red for Armenia/Arzerbaijan, Yellow for Israeli accessions, Pink for cultivated accessions from Georgia and Blue for the wild ones.

Multiple origins detection of Georgian germplasm based on chloroplast analysis

To study in depth the origin of Georgian germplasm, we compared our Georgian accessions (NEA, Near East) with others derived from Middle Asia (MEA, Middle East) and a minority including European sylvestris and sativa (ITP). Since we analyzed those accessions previously selected for a Q value > 0.8 , we were not able to detect all the eight chlorotypes described in Arroyo-García et al., 2006 [13]. We performed a genotypic analysis for six polymorphic chloroplast microsatellite loci which identified five different chlorotypes as described in Figure 8. According to Arroyo-García et al., 2006 [13], three of the most frequent chlorotypes (A, B and D) corresponded to the three major chlorotype lineages ITP, NEA and MEA respectively. The results showed that chlorotype G was closely associated to chlorotype A, while chlorotype C was strictly related to chlorotype D, mostly represented within the Middle Asia accessions (including Iranian, Armenian, Azerbaijani genotypes). According to our analysis, the five chlorotypes (A, B, C, D, G) did not distinguish cultivated from wild forms. Moreover, in contrast with Arroyo-García et al., 2006 [13], chlorotype A was prevalent in the ITP population and in those accessions of NEA, located in the overlapping zone between wild and cultivated forms, previously described in the STRUCTURE analysis. This result partially explains the assignment of some cultivated accessions to the wild compartment, as suggested by the PCoA analysis. Indeed the first two coordinates accounted for, respectively, the 9.14% and the 4.74% of the total variation, and clearly separated the individuals according to geographical areas (ITP, NEA and MEA).

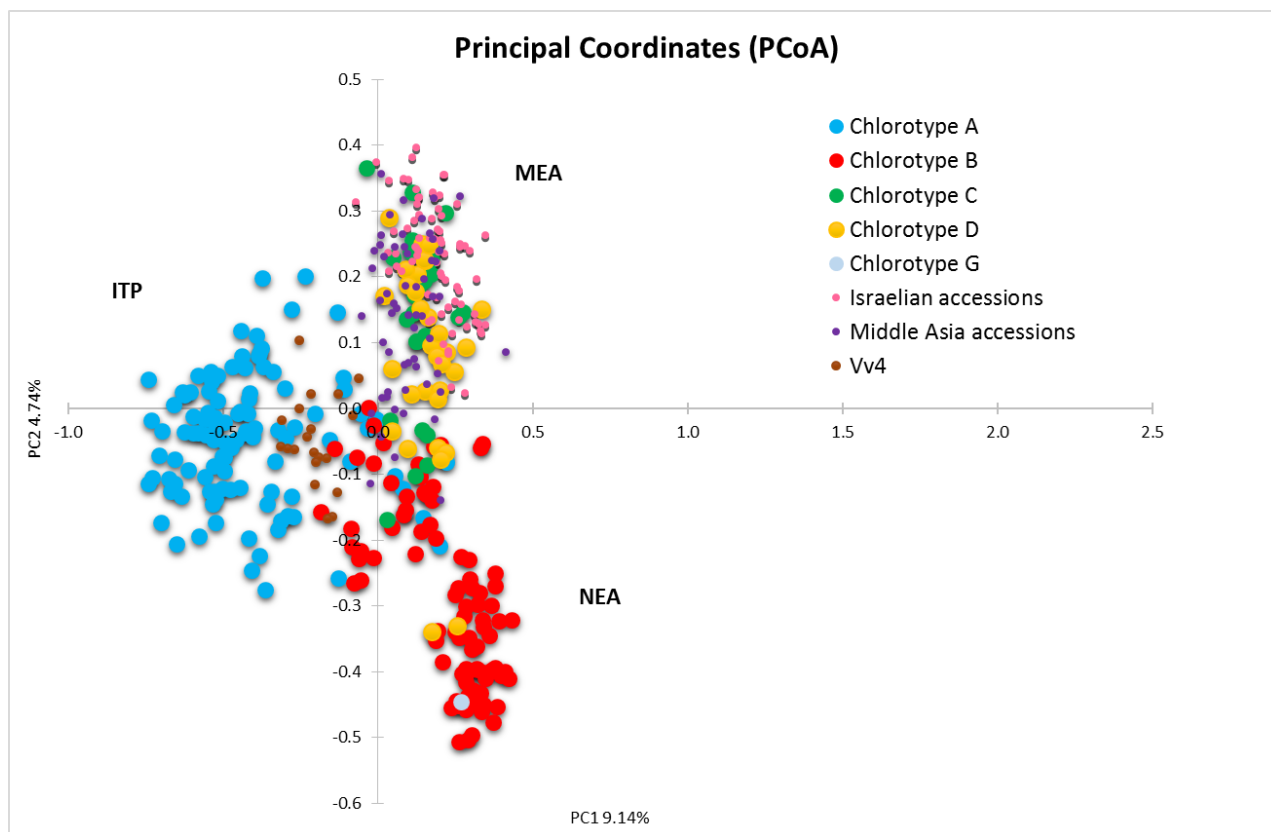


Figure 8 Scatterplot from a PCoA. Representation of two main principal coordinate axes for chloroplast SSR markers.

Maternal lineages detection of Georgian accessions based on chloroplast analysis

A preliminary analysis was carried out using a noncoding plastid *trnC-petN* marker [94] which allowed to detect a 54 nt deletion in numerous cultivars. Given the high number of regions shared between grapevine chloroplast and mitochondrion genomes, the marker used for this study was selected only from predicted unique plastome regions. According to Lózsa et al., 2015 [94], the presence and absence of a newly discovered 54 nt deletion suggested two maternal lineages: deletion (D) and non-deletion (ND). Seven already published chloroplast genomes (Table 2) have been analyzed and whole genome aligned in order to construct an UPGMA phylogenetic tree (Figure 9). This analysis allowed to compare *Vitis vinifera* genotypes (subsp. *caucasica*) with Asian and American *Vitis* species (*V. amurensis* and *V. aestivalis*), using *M. rotundifolia* as outgroup.

Table 2 List of grapevine accessions which chloroplast genome has been published. All the information are available in EMBL-EBI database.

Cultivar	Accession N°	Species	Sequence length
Maxxa	DQ424856	<i>Vitis vinifera</i> cultivar Maxxa	160,928
Rkatsiteli	AB856289	<i>Vitis vinifera</i> subsp. <i>caucasica</i>	160,927
Meskhuri Mtsvane	AB856291	<i>Vitis vinifera</i> subsp. <i>caucasica</i>	160,906
Saperavi	AB856290	<i>Vitis vinifera</i> subsp. <i>caucasica</i>	160,927
<i>Vitis amurensis</i>	KX499471	<i>Vitis amurensis</i>	160,953
Norton	KT997470	<i>Vitis aestivalis</i>	160,913
<i>Vitis rotundifolia</i>	KF976463	<i>Vitis rotundifolia</i>	160,891

The phylogenetic tree described a really interesting differentiation among the two main *Vitis* subgenera, *Muscadinia* and *Vitis*. The analysis revealed that *M. rotundifolia* (ND) was drastically separated from other *Vitis* accessions, whereas several other variants, discovered through the alignment, allowed to separate the

American *V. aestivalis* (ND) from the Asian *V. amurensis* (ND). Within the Asian accessions we found a diversification among *V. vinifera* genotypes. In particular we found a strict association of reference *V. vinifera* Maxxa with *V. amurensis*, also described by the absence of deletion in *trnC-petN* region (ND). On the contrary, different haplotype was detected in caucasian *V. vinifera* Rkatsiteli, Saperavi and M. Mtsvane which were characterized by a deletion in the noncoding region (D). These results were well described in Lózsa et al., 2015 [94] where they suggested that the more ancient cultivars such as Pinot Noir, Riesling, Afus ali and Tsolikouri, belonged to a single haplotype group (ND) in which the deletion was absent, assuming the presence of different maternal lineages.

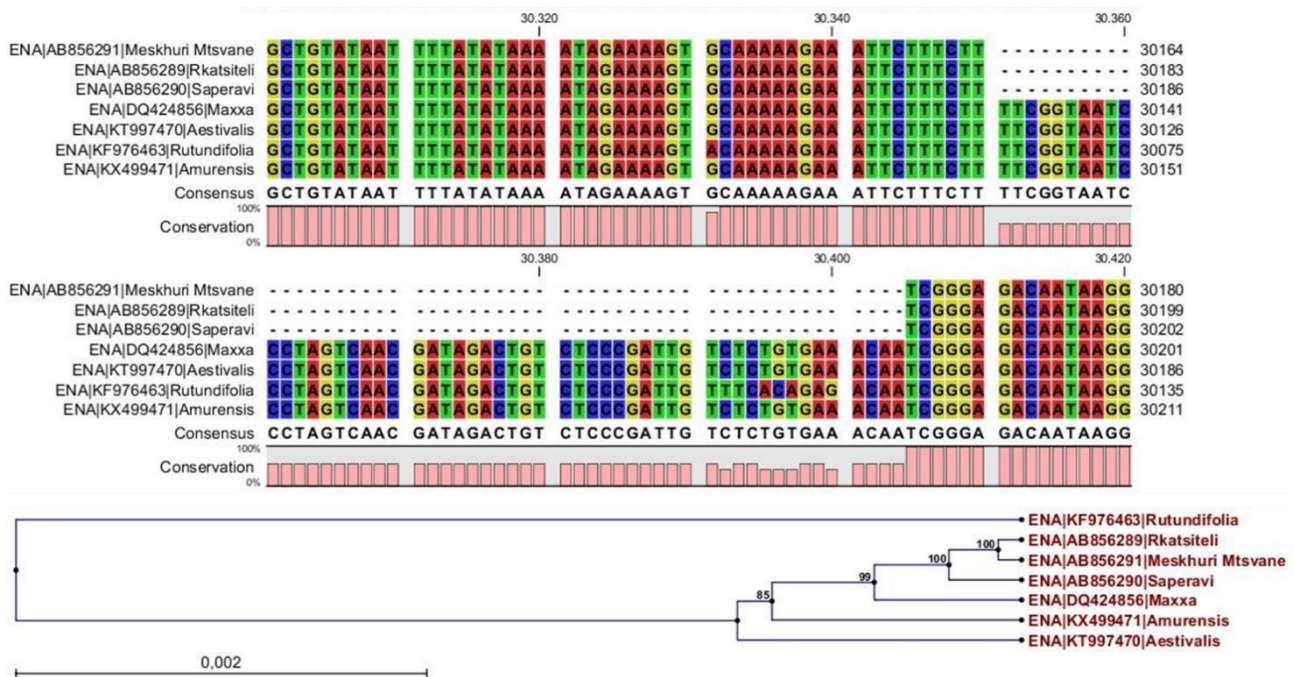


Figure 9 **CLC output**. Here is represented the alignment of chloroplast genome of seven grapevine accessions where is clearly highlighted the indel in the range of *trnC-petN* region. Following an UPGMA phylogenetic tree described the relationships among studied genotypes on the base of chloroplast variations.

In this regard, we compared our results with the data of the above cited work, which comprised genotypes of the same origin, in order to better understand the possible relationships between Georgian and European accessions.

To better explain the overlapping between wild and cultivated forms, we tested separately ITP and NEA accessions. In agreement with the previous research works we detected two main haplotypes, distinguished by the presence (ND) or the absence (D) of 54 nt deletion in the *trnC-petN* region. Our results recorded only a few cultivated NEA samples without the deletion (ND). Those individuals fell within the wild Georgian group, which clustered closer to European *syvestris* population in the above phylogenetic analysis. This subdivision within the Georgian germplasm collection seems to reflect their geographical origin, in particular from Eastern accessions to Western accessions (Figure 10).

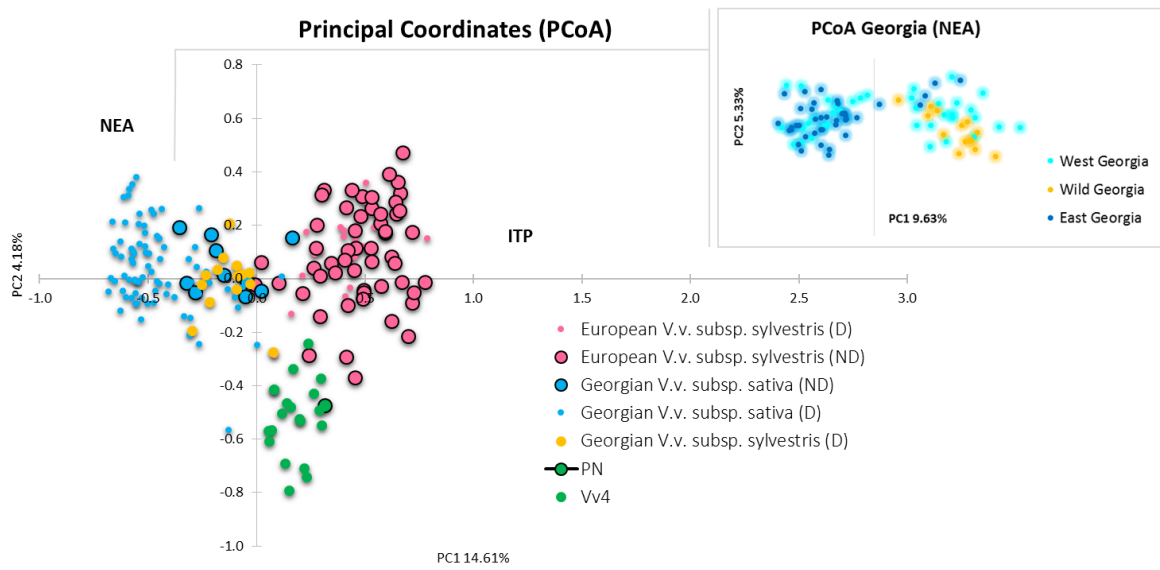


Figure 10 PcoA analysis based on 21 SSRs which defined a geographical barrier. Representation of principal coordinates which marked down the separation between Eastern and Western Georgia. As plotted, the Western Georgia was characterized by a mixture of wild and cultivated accessions in which were present both D and ND haplotypes. Meanwhile, the Eastern part was composed by only cultivated accessions with D haplotype.

Discussion

Caucasian germplasm assessment

Over the last few years Eurasian *Vitis vinifera* varieties have become of great interest, especially after the identification of the powdery mildew resistance gene *Ren1*, discovered first in Kishmish vatkana accession and further in many other cultivars of Central Asia. These records suggested the presence of interesting and unexploited genetic traits in *V. vinifera* germplasm worthy to be unraveled. To date, researchers have paid a specific attention on European *Vitis* varieties, and no evidences of resistance to downy mildew have been found. In this study we exploited available genetic information to investigate a germplasm population composed by 25 Caucasian cultivated *V. vinifera* accessions, which were characterized by a tolerance to downy mildew disease. Our study based on the use of several markers associated to the major published resistance loci confirmed the absence of possible introgression of already known resistance traits to Downy mildew. Moreover, the phylogenetic analysis based on 21 SSRs, placed this investigated germplasm collection within the Georgian population, except for a few accessions which showed a high similarity with individuals of the proles *pontica* and *orientalis*.

Georgian germplasm structure and conservation

Once verified the membership of the Caucasian germplasm collection to the Georgian ones, we focused our attention on the whole Georgian population. The results of the genetic diversity analysis, underlined a high level of genetic variation, which marked out this germplasm collection, as a genetic reservoir. Hierarchical clustering approach of the Central Asia germplasm, defined a clear separation between the individuals from Georgia, Israel and Middle Asia. In particular, the accessions from Georgia and Israel drew a well-defined structure, reflecting the historical records related to the domestication process. According to the long list of private alleles of the Georgian and Israelian accessions, we could not suppose common ancient genetic roots, since these populations appeared really isolated one from each other. Undoubtedly, considering the historical reports about the Holy Land and its genetic features, Israel regions represented a reserve of great interest [110], but the analysis of the most likely number of clusters (K) obtained from population structure indicated that the best possible division of the Central Asia germplasm was into 2 groups, one containing Georgian population and one containing all the others. These results suggested that, despite the cultural exchanges documented [113], [114], Georgia region identified a branch apart with apparently no admixture with other countries from Central Asia.

Another interesting aspects was described by the PCoA analysis, which revealed a genetic differentiation within the Georgian population as if to reflect the geographical barrier constituted by Likhi Mountains connecting Major and Minor Caucasus, thus running in a north to south direction across Georgia and dividing the territory into two mayor parts. Indeed, two separated groups of accessions were drawn, one more distant including cultivars putatively originated in the eastern regions of Georgia (Kartli, Kakheti) and another more similar to wild accessions, deriving from the western part of the country (Abkhazeti, Adjara, Samegrelo, Racha-Lechkhumi, Guria). Moreover we identified several accessions from Imereti region closely related to the wild Georgian accessions, and characterized from a high rate of inbreeding. Both analysis of population structure and population differentiation statistic (F index) computed across the investigated Georgian collection indicated that the overall level of genetic differentiation between cultivated and wild grapes was moderate. Indeed we could be able to detect a separation among sativa and sylvestris accessions by using K=5 in STRUCTURE analysis. This low level of genetic differentiation suggests the existence of genetic exchange between cultivated and wild individuals, supporting the hypothesis that the introgression from local wild sylvestris has played an important role during grapevine domestication.

Karatas et al., 2014 [115] contributed to clarify the relationships between wild and cultivated grape accessions from southeastern Turkey, which is an area of particular significance in grapevine domestication history. According to their analysis based on plastid markers, chlorotype A and B were completely absent in Turkish germplasm, while chlorotype C and D were the most frequent. Comparable results could be discussed in our research work. Our germplasm from Georgia was mainly defined by the putatively ancestral chlorotype B, which has a special importance to better understand grapevine domestication process, according to [115]. Moreover, in agreement with the cited work, we also detected chlorotypes C and D in MEA.

Archeological and historical evidences suggest that grape domestication took place in the Near East as well as several studies have also proposed the existence of secondary domestication events along the Mediterranean basin [116].

Another possible scenario suggested by the analysis with plastid markers could explain the presence of chlorotype A in NEA and revisited the well-documented historical knowledge that described Georgia as strategically located on the crossroad from Europe to Asia, between the Black and Caspian seas on the main trading roads, from the second century BC to the seventeenth century AD [117]. In agreement to our results, the European *sylvestris* were characterized from a mixture of D and ND haplotypes, which were probably inherited during the domestication process in the cultivated forms Vv4 such as Pinot Noir. Differently, the wild Georgian population lacked of ND haplotypes, which were unexpectedly found in a group of Georgian cultivated accessions characterized by a high homozygosity, strictly related to the wild population. In light of these remarks, regardless of the limited number of wild Georgian accessions tested, we can conclude that these cultivars characterized by a high homozygosity and the ND haplotype, could represent an ancestral form of domesticated grapevines. According to Lózsá et al., 2015 [94], ND haplotype delineated the more ancient cultivars from which have been originated all the modern varieties. In addition, the presence of ND haplotype only in some NEA *sativa* and ITP accessions, suggest that after a first domestication event occurred in the western Georgia, commercial exchanges allowed to introduce these ancestral grapevines in western Europe which is characterized by a strong genetic variability as described in Marrano et al., 2017 [118].

Supplementary data

Table S1 List of RPV loci associated markers tested on 25 Caucasian accessions and relative sizes. Sizes linked to resistant traits are in bold.

Id	RPV1			RUN1				RPV3				RPV12				RPV10				
	VVIm11	VVIm11	VMC1g3.2	VMC1g3.2	VMC8g9	VMC8g9	VMC4f3.1	VMC4f3.1	UDV737	UDV737	VMC7f2	VMC7f2	UDV370	UDV370	UDV350	UDV350	GF09_46	GF09_46	GF09_47	GF09_47
<i>M. rutundifolia</i>	270	292	118	136	156	162	186	188	-	-	-	-	-	-	-	-	-	-	-	-
<i>V. amurensis</i>	-	-	-	-	-	-	-	-	-	-	-	-	194	198	308	308	410	420	294	296
<i>V. rupestris</i>	-	-	-	-	-	-	-	-	280	296	200	210	-	-	-	-	-	-	-	-
Caucasus01	270	270	124	130	172	174	172	174	-	-	202	202	196	198	-	-	416	416	294	294
Caucasus02	252	252	124	136	168	174	172	182	-	-	200	204	-	-	-	-	416	416	292	292
Caucasus03	278	284	124	136	164	174	166	180	-	-	200	204	192	194	300	300	-	-	292	296
Caucasus04	270	292	130	138	162	172	174	178	286	292	202	204	194	196	300	306	418	418	294	294
Caucasus05	260	270	124	136	172	174	172	188	-	-	200	200	190	196	-	-	-	-	288	292
Caucasus06	260	284	124	136	162	164	178	180	-	-	202	204	190	196	306	306	418	420	294	294
Caucasus07	270	280	124	136	164	174	180	186	-	-	200	204	196	198	-	-	418	418	290	294
Caucasus08	260	270	124	136	172	174	172	188	-	-	200	200	190	196	306	306	420	420	294	294
Caucasus09	270	280	124	130	168	172	174	182	-	-	202	204	190	192	-	-	410	420	-	-
Caucasus10	270	278	130	130	164	172	174	188	-	-	202	204	188	194	-	-	420	420	294	294
Caucasus11	270	284	126	130	162	168	172	182	296	296	200	200	190	190	306	308	418	418	294	294
Caucasus12	278	284	124	136	164	174	166	180	294	296	200	204	192	196	300	300	420	420	294	294
Caucasus13	280	284	124	130	162	168	172	182	292	296	200	204	190	196	298	298	418	420	294	294
Caucasus14	270	270	124	124	164	166	178	182	292	294	204	204	196	198	298	298	418	420	294	294
Caucasus15	270	270	120	124	162	180	178	206	292	296	200	200	190	192	308	322	406	406	288	292
Caucasus16	278	284	124	128	162	174	180	208	-	-	202	204	190	192	300	300	402	402	290	294
Caucasus17	278	278	124	130	180	180	180	206	290	296	200	200	196	198	300	300	408	408	290	294
Caucasus18	260	278	124	130	164	168	178	182	286	294	200	204	190	196	-	-	408	420	290	294
Caucasus19	270	282	128	136	174	174	166	178	284	284	200	204	190	198	-	-	410	420	294	294
Caucasus20	270	278	136	136	168	174	166	186	296	296	200	200	192	198	300	322	418	418	294	294
Caucasus21	260	278	116	130	-	-	174	174	-	-	200	204	190	192	300	300	416	416	292	296
Caucasus22	252	252	124	130	162	174	172	178	-	-	200	204	-	-	-	-	-	-	-	-
Caucasus23	254	254	128	128	168	174	172	178	-	-	196	200	-	-	-	-	-	-	288	292
Caucasus24	260	284	124	124	164	174	206	208	292	292	200	206	196	198	306	306	389	402	291	294
Caucasus25	270	270	128	136	174	174	186	186	294	294	206	206	188	196	306	308	402	418	290	294

Table S2 List of REN1 loci associated markers tested on 25 Caucasian accessions and relative sizes. Sizes linked to resistant traits are in bold.

Id	UDV124	UDV124	UDV124	SC8-0071-014	SC8-0071-014	SC8-0071-014	SC47-18	SC47-18	VMC9h4	VMC9h4	VMC4e10	VMC4e10	VMC4e10	VMC4e10	UDV20	UDV20	UDV20	UDV20
<i>V. vinifera</i> <i>Kishmish v.</i>	214	218	-	142	176	-	226	248	276	282	254	258	298	-	124	134	144	158
Caucasus01	184	196	-	162	206	-	216	248	-	-	250	254	288	298	144	158	-	-
Caucasus02	197	204	-	160	206	-	216	248	250	250	250	254	298	-	144	158	-	-
Caucasus03	194	196	-	174	206	-	216	216	274	274	250	274	296	-	144	158	-	-
Caucasus04	-	-	-	-	-	-	-	-	-	-	-	-	-	-	-	-	-	-
Caucasus05	184	232	-	160	162	-	230	248	260	276	236	254	282	298	134	146	-	-
Caucasus06	186	194	-	144	158	198	214	236	-	-	262	270	276	316	144	156	-	-
Caucasus07	194	196	-	174	204	206	216	216	274	274	250	258	276	296	144	158	-	-
Caucasus08	-	-	-	-	-	-	-	-	-	-	-	-	-	-	-	-	-	-
Caucasus09	186	200	-	202	202	-	200	236	298	298	250	276	322	-	144	144	-	-
Caucasus10	186	232	-	158	172	-	214	214	274	292	250	270	296	316	144	156	-	-
Caucasus11	188	214	232	160	174	-	216	240	-	-	250	296	-	-	144	158	-	-
Caucasus12	-	-	-	-	-	-	-	-	-	-	-	-	-	-	-	-	-	-
Caucasus13	-	-	-	-	-	-	-	-	-	-	-	-	-	-	-	-	-	-
Caucasus14	186	232	-	174	200	-	216	236	-	-	250	276	296	-	144	158	-	-
Caucasus15	-	-	-	-	-	-	-	-	-	-	-	-	-	-	-	-	-	-
Caucasus16	186	204	-	162	172	-	216	240	284	284	262	262	-	-	132	150	-	-
Caucasus17	204	204	-	142	172	-	240	240	284	310	262	286	308	334	124	134	144	146
Caucasus18	186	194	-	140	166	172	206	216	274	274	250	258	296	-	124	144	158	-
Caucasus19			-			-	214	216	274	274	250	270	296	-	144	158	-	-
Caucasus20	194	232	-	146	172	-	216	216	274	274	250	296	-	-	144	158	-	-
Caucasus21	186	190	214			-	236	240	-	-	262	276	-	-	144	156	-	-
Caucasus22	190	200	-	160	168	-	-	-	276	278	254	256	298	-	134	144	150	162
Caucasus23	-	-	-	-	-	-	-	-	-	-	-	-	-	-	-	-	-	-
Caucasus24	-	-	-	-	-	-	-	-	-	-	-	-	-	-	-	-	-	-
Caucasus25	186	204	-	200	202	-	236	236	292	298	270	276	316	322	144	158	-	-

Table S3 Proportion of membership of each pre-defined population in each of the 5 clusters. Inferred ancestry of individuals at K=5, Q>0.8. Georgian cultivars which were assigned to wild Georgian populations are highlighted. *Vitis vinifera* subsp. *sylvestris* are in bold.

Origin	K=5, Q>0.8	Armenia/Azerbaijan	Middle Asia	Israele	Georgia subsp. <i>sylvestris</i>	Georgia subsp. <i>sativa</i>
Middle Asia	1001	0.01	0.979	0.005	0.003	0.003
Middle Asia	1002	0.014	0.958	0.004	0.012	0.012
Middle Asia	1005	0.016	0.898	0.016	0.011	0.06
Middle Asia	1006	0.076	0.863	0.05	0.005	0.007
Middle Asia	1007	0.008	0.96	0.021	0.006	0.004
Middle Asia	1008	0.007	0.906	0.049	0.031	0.008
Middle Asia	1010	0.002	0.952	0.008	0.031	0.006
Middle Asia	1011	0.004	0.98	0.006	0.002	0.007
Middle Asia	1012	0.003	0.981	0.004	0.003	0.009
Middle Asia	1013	0.006	0.987	0.004	0.003	0.001
Middle Asia	1014	0.003	0.989	0.003	0.002	0.002
Middle Asia	1015	0.005	0.976	0.005	0.009	0.006
Middle Asia	1016	0.023	0.953	0.007	0.011	0.005
Middle Asia	1018	0.004	0.943	0.01	0.019	0.024
Middle Asia	1019	0.007	0.953	0.015	0.011	0.014
Middle Asia	1021	0.011	0.939	0.025	0.022	0.003
Middle Asia	1022	0.003	0.931	0.039	0.013	0.014
Middle Asia	1023	0.004	0.947	0.038	0.002	0.008
Middle Asia	1024	0.007	0.982	0.007	0.002	0.002
Middle Asia	1025	0.005	0.952	0.025	0.013	0.005
Middle Asia	1026	0.007	0.982	0.003	0.005	0.003
Middle Asia	1027	0.004	0.87	0.115	0.006	0.006
Middle Asia	1028	0.008	0.964	0.005	0.019	0.004
Middle Asia	1029	0.011	0.966	0.004	0.014	0.005
Middle Asia	1030	0.005	0.975	0.002	0.006	0.012
Middle Asia	1031	0.21	0.773	0.005	0.009	0.003
Middle Asia	1032	0.005	0.988	0.003	0.002	0.002
Middle Asia	1033	0.008	0.985	0.004	0.002	0.002
Middle Asia	1034	0.01	0.982	0.003	0.003	0.002
Middle Asia	1037	0.006	0.966	0.007	0.018	0.003
Middle Asia	1038	0.005	0.985	0.002	0.005	0.003
Middle Asia	1039	0.021	0.941	0.012	0.016	0.011
Middle Asia	1043	0.096	0.894	0.003	0.003	0.003
Middle Asia	1044	0.139	0.83	0.012	0.015	0.004
Middle Asia	1045	0.021	0.836	0.1	0.032	0.011
Middle Asia	1046	0.003	0.989	0.003	0.002	0.004
Middle Asia	1047	0.004	0.952	0.004	0.012	0.028
Middle Asia	1048	0.005	0.984	0.004	0.003	0.003
Middle Asia	1049	0.037	0.955	0.004	0.002	0.002
Middle Asia	1051	0.011	0.975	0.003	0.008	0.004
Middle Asia	1056	0.006	0.987	0.003	0.002	0.002

Origin	K=5, Q>0.8	Armenia/Azerbaijan	Middle Asia	Israele	Georgia subsp. <i>sylvestris</i>	Georgia subsp. <i>sativa</i>
Middle Asia	1057	0.003	0.976	0.002	0.017	0.002
Middle Asia	1059	0.003	0.986	0.002	0.004	0.004
Middle Asia	1061	0.006	0.984	0.003	0.003	0.004
Middle Asia	1062	0.018	0.941	0.013	0.011	0.018
Middle Asia	1063	0.011	0.978	0.005	0.003	0.002
Middle Asia	1064	0.007	0.965	0.018	0.005	0.005
Middle Asia	1065	0.002	0.977	0.002	0.016	0.003
Middle Asia	1068	0.057	0.919	0.012	0.008	0.004
Middle Asia	1069	0.016	0.939	0.033	0.009	0.003
Middle Asia	1070	0.005	0.981	0.009	0.003	0.002
Middle Asia	1071	0.027	0.965	0.004	0.002	0.002
Middle Asia	1072	0.002	0.989	0.004	0.002	0.004
Middle Asia	1073	0.129	0.863	0.003	0.002	0.002
Middle Asia	1074	0.006	0.988	0.002	0.002	0.002
Middle Asia	1075	0.003	0.991	0.002	0.002	0.001
Middle Asia	1157	0.005	0.985	0.002	0.004	0.004
Middle Asia	1159	0.007	0.981	0.003	0.004	0.005
Middle Asia	1076	0.003	0.985	0.006	0.002	0.004
Middle Asia	1077	0.008	0.96	0.026	0.003	0.003
Middle Asia	1079	0.002	0.987	0.003	0.002	0.005
Middle Asia	1080	0.002	0.966	0.003	0.015	0.014
Middle Asia	1082	0.002	0.989	0.002	0.003	0.004
Middle Asia	1086	0.008	0.935	0.004	0.006	0.047
Middle Asia	1087	0.003	0.988	0.004	0.002	0.003
Middle Asia	1088	0.007	0.918	0.015	0.023	0.038
Middle Asia	1089	0.003	0.979	0.003	0.006	0.01
Middle Asia	1091	0.003	0.979	0.007	0.003	0.009
Middle Asia	1092	0.003	0.989	0.004	0.002	0.003
Middle Asia	1095	0.005	0.976	0.006	0.003	0.009
Middle Asia	1096	0.004	0.985	0.006	0.002	0.003
Iran	IRZA13	0.007	0.979	0.004	0.003	0.008
Iran	IRZA12	0.01	0.83	0.115	0.014	0.031
Iran	IRZA04	0.004	0.98	0.004	0.003	0.009
Iran	IRZA06	0.009	0.902	0.007	0.011	0.07
Iran	IRZA08	0.007	0.843	0.02	0.012	0.119
Iran	IRZA11	0.008	0.979	0.005	0.003	0.005
Georgia	1097	0.003	0.004	0.004	0.002	0.988
Georgia	1098	0.002	0.002	0.003	0.002	0.992
Georgia	1099	0.003	0.003	0.004	0.006	0.984
Georgia	1100	0.002	0.003	0.003	0.003	0.99
Georgia	1101	0.028	0.038	0.011	0.003	0.92
Georgia	1102	0.002	0.002	0.002	0.003	0.99
Georgia	1103	0.003	0.002	0.002	0.002	0.99

Origin	K=5, Q>0.8	Armenia/Azerbaijan	Middle Asia	Israele	Georgia subsp. <i>sylvestris</i>	Georgia subsp. <i>sativa</i>
Georgia	1104	0.003	0.043	0.008	0.043	0.903
Georgia	1105	0.003	0.003	0.002	0.002	0.99
Georgia	1108	0.02	0.007	0.002	0.004	0.967
Georgia	1109	0.001	0.002	0.002	0.002	0.992
Georgia	1113	0.002	0.008	0.002	0.038	0.949
Georgia	1115	0.002	0.004	0.002	0.002	0.99
Georgia	1116	0.002	0.002	0.002	0.002	0.992
Georgia	1119	0.001	0.002	0.002	0.002	0.993
Georgia	1122	0.005	0.04	0.004	0.007	0.944
Georgia	1124	0.004	0.003	0.002	0.003	0.989
Georgia	1129	0.003	0.006	0.004	0.004	0.983
Georgia	1130	0.005	0.003	0.005	0.887	0.099
Georgia	1131	0.007	0.006	0.016	0.013	0.958
Georgia	1135	0.013	0.069	0.004	0.008	0.907
Georgia	1136	0.004	0.032	0.027	0.004	0.933
Georgia	1137	0.002	0.002	0.002	0.002	0.993
Georgia	1138	0.012	0.007	0.016	0.024	0.941
Georgia	1141	0.004	0.03	0.054	0.007	0.905
Georgia	1145	0.01	0.011	0.003	0.005	0.972
Georgia	1146	0.008	0.005	0.007	0.003	0.977
Georgia	1147	0.006	0.007	0.004	0.002	0.98
Georgia	1149	0.004	0.098	0.058	0.009	0.831
Georgia	1151	0.002	0.004	0.003	0.986	0.005
Georgia	1153	0.003	0.012	0.003	0.98	0.003
Georgia	1155	0.004	0.143	0.004	0.005	0.844
Georgia	1156	0.031	0.01	0.004	0.929	0.025
Georgia	12G11B	0.004	0.004	0.012	0.963	0.016
Georgia	12G12-1	0.004	0.023	0.013	0.944	0.016
Georgia	12G12-2	0.002	0.002	0.002	0.99	0.003
Georgia	12G13-1	0.007	0.007	0.003	0.977	0.006
Georgia	12G13-2	0.005	0.003	0.002	0.007	0.983
Georgia	12G13-3	0.003	0.004	0.007	0.962	0.025
Georgia	12G15-I	0.002	0.003	0.002	0.012	0.982
Georgia	12G17D	0.021	0.055	0.009	0.83	0.085
Georgia	12G19B	0.006	0.003	0.003	0.005	0.983
Georgia	12G19D	0.037	0.01	0.014	0.058	0.88
Georgia	12G20B	0.002	0.002	0.002	0.002	0.991
Georgia	12G21A	0.003	0.003	0.002	0.005	0.987
Georgia	12G21-B	0.017	0.009	0.007	0.952	0.015
Georgia	12G21D	0.005	0.008	0.004	0.065	0.918
Georgia	12G21-E	0.003	0.002	0.002	0.005	0.987
Georgia	12G23-1	0.003	0.009	0.012	0.955	0.02
Georgia	12G23-2	0.003	0.012	0.002	0.006	0.977

Origin	K=5, Q>0.8	Armenia/Azerbaijan	Middle Asia	Israele	Georgia subsp. <i>sylvestris</i>	Georgia subsp. <i>sativa</i>
Georgia	12G26-1	0.005	0.006	0.005	0.981	0.002
Georgia	12G26-2	0.044	0.044	0.01	0.87	0.032
Georgia	12G27-1	0.002	0.002	0.006	0.005	0.985
Georgia	12G27-2	0.007	0.004	0.009	0.956	0.025
Georgia	12G28-1	0.006	0.009	0.045	0.052	0.888
Georgia	12G29-1	0.003	0.011	0.005	0.032	0.949
Georgia	12G3	0.12	0.078	0.006	0.787	0.009
Georgia	12G30-1	0.009	0.004	0.003	0.981	0.003
Georgia	12G31-1	0.004	0.013	0.004	0.021	0.958
Georgia	12G31-2	0.002	0.002	0.002	0.988	0.006
Georgia	12G32-1	0.004	0.009	0.003	0.948	0.036
Georgia	12G32-4	0.003	0.022	0.002	0.018	0.955
Georgia	12G33-1	0.003	0.007	0.006	0.004	0.98
Georgia	12G33-2	0.002	0.004	0.004	0.859	0.131
Georgia	12G35-1	0.002	0.003	0.002	0.003	0.99
Georgia	12G36-1	0.004	0.007	0.007	0.061	0.922
Georgia	12G39-1	0.002	0.002	0.003	0.002	0.991
Georgia	12G4-1	0.005	0.004	0.002	0.006	0.983
Georgia	12G4-2	0.001	0.002	0.002	0.003	0.992
Georgia	12G4-3	0.003	0.019	0.003	0.046	0.929
Georgia	12G5-1	0.013	0.046	0.013	0.018	0.91
Georgia	12G5-2	0.004	0.048	0.017	0.906	0.026
Georgia	12G5-3	0.002	0.002	0.003	0.05	0.944
Georgia	12G6-2	0.003	0.002	0.002	0.005	0.987
Georgia	12G7-1	0.004	0.004	0.004	0.006	0.983
Georgia	12G8-1	0.001	0.002	0.002	0.002	0.993
Georgia	12G8-2	0.002	0.002	0.003	0.989	0.003
Georgia	12G9-1	0.002	0.004	0.002	0.985	0.007
Georgia	12G9-2	0.002	0.003	0.002	0.989	0.004
Georgia	12G9-3	0.003	0.004	0.004	0.904	0.085
Georgia	G2_2011	0.002	0.002	0.002	0.004	0.991
Georgia	12G44-1	0.003	0.016	0.012	0.952	0.017
Georgia	12G45-1	0.003	0.002	0.002	0.99	0.003
Georgia	12G47-1	0.002	0.002	0.002	0.99	0.004
Georgia	12G47-2	0.002	0.003	0.002	0.989	0.005
Georgia	GEO_21	0.004	0.002	0.004	0.973	0.017
Georgia	12G48-1	0.002	0.002	0.002	0.99	0.004
Georgia	12G48-2	0.004	0.002	0.002	0.99	0.002
Georgia	L22	0.003	0.007	0.003	0.982	0.005
Georgia	M22	0.004	0.057	0.043	0.89	0.005
Georgia	EST1-14B	0.011	0.004	0.004	0.056	0.925
Georgia	EST1-17A	0.003	0.004	0.003	0.006	0.984
Georgia	EST11f	0.002	0.003	0.004	0.003	0.988

Origin	K=5, Q>0.8	Armenia/Azerbaijan	Middle Asia	Israele	Georgia subsp. <i>sylvestris</i>	Georgia subsp. <i>sativa</i>
Georgia	EST1-7B	0.004	0.003	0.007	0.005	0.982
Georgia	EST2-17A	0.017	0.009	0.011	0.017	0.946
Georgia	EST2-8A	0.003	0.005	0.002	0.003	0.988
Georgia	g19	0.001	0.001	0.002	0.002	0.993
Georgia	g34	0.004	0.006	0.003	0.025	0.962
Georgia	EST.WF10	0.011	0.006	0.018	0.096	0.869
Georgia	EST.WF110/2	0.042	0.007	0.014	0.701	0.237
Georgia	EST.WFK52	0.004	0.003	0.003	0.987	0.004
Georgia	EST.WFK12	0.009	0.007	0.013	0.953	0.019
Georgia	EST.GEOW27	0.004	0.003	0.003	0.963	0.027
Georgia	EST.GEOW19	0.003	0.006	0.007	0.971	0.014
Israele	9002	0.012	0.004	0.976	0.004	0.004
Israele	9005	0.056	0.02	0.914	0.007	0.003
Israele	9006	0.01	0.008	0.977	0.003	0.002
Israele	9012	0.024	0.008	0.95	0.011	0.006
Israele	9019	0.042	0.01	0.935	0.011	0.003
Israele	9024	0.037	0.006	0.939	0.005	0.012
Israele	9026	0.005	0.01	0.96	0.022	0.003
Israele	9034	0.022	0.016	0.921	0.015	0.026
Israele	5	0.005	0.004	0.983	0.006	0.002
Israele	15	0.011	0.003	0.98	0.004	0.003
Israele	71	0.015	0.025	0.945	0.011	0.004
Israele	99	0.039	0.028	0.921	0.004	0.008
Israele	177	0.045	0.065	0.878	0.004	0.008
Israele	182	0.008	0.012	0.959	0.012	0.009
Israele	187	0.008	0.01	0.948	0.015	0.019
Israele	191	0.006	0.003	0.985	0.005	0.002
Israele	220	0.009	0.008	0.976	0.004	0.003
Israele	243	0.004	0.008	0.98	0.003	0.004
Israele	181	0.019	0.01	0.947	0.014	0.01
Israele	69	0.018	0.286	0.672	0.018	0.006
Israele	1	0.002	0.012	0.981	0.002	0.003
Israele	2	0.008	0.003	0.981	0.005	0.004
Israele	3	0.002	0.003	0.955	0.006	0.034
Israele	4	0.005	0.009	0.977	0.007	0.002
Israele	22	0.052	0.004	0.94	0.003	0.002
Israele	23	0.004	0.003	0.99	0.002	0.001
Israele	24	0.003	0.003	0.99	0.002	0.002
Israele	48	0.005	0.003	0.986	0.002	0.003
Israele	50	0.003	0.002	0.992	0.002	0.002
Israele	51	0.003	0.003	0.992	0.002	0.001
Israele	54	0.003	0.002	0.991	0.002	0.002
Israele	56	0.002	0.003	0.989	0.002	0.004

Origin	K=5, Q>0.8	Armenia/Azerbaijan	Middle Asia	Israele	Georgia subsp. <i>sylvestris</i>	Georgia subsp. <i>sativa</i>
Israele	59	0.002	0.002	0.99	0.004	0.001
Israele	128	0.003	0.003	0.989	0.002	0.002
Israele	142	0.005	0.004	0.985	0.003	0.002
Israele	145	0.097	0.013	0.864	0.02	0.005
Israele	146	0.005	0.012	0.9	0.01	0.073
Israele	147	0.003	0.011	0.923	0.005	0.058
Israele	148	0.004	0.004	0.979	0.008	0.005
Israele	149	0.004	0.008	0.975	0.008	0.005
Israele	150	0.005	0.005	0.971	0.008	0.012
Israele	151	0.012	0.012	0.966	0.004	0.005
Israele	152	0.017	0.003	0.97	0.003	0.006
Israele	153	0.018	0.009	0.958	0.007	0.008
Israele	156	0.034	0.017	0.931	0.007	0.011
Israele	157	0.01	0.009	0.975	0.003	0.003
Israele	158	0.086	0.009	0.887	0.003	0.015
Israele	159	0.003	0.005	0.911	0.005	0.076
Israele	160	0.003	0.004	0.984	0.004	0.004
Israele	162	0.003	0.005	0.988	0.002	0.002
Israele	164	0.003	0.038	0.942	0.014	0.003
Israele	175	0.002	0.003	0.984	0.006	0.004
Israele	184	0.003	0.018	0.97	0.003	0.006
Israele	192	0.003	0.005	0.984	0.003	0.005
Israele	193	0.006	0.007	0.972	0.007	0.009
Israele	196	0.007	0.003	0.986	0.002	0.002
Israele	197	0.002	0.003	0.986	0.005	0.003
Israele	221	0.002	0.004	0.987	0.003	0.004
Israele	222	0.002	0.002	0.993	0.002	0.002
Israele	224	0.003	0.004	0.989	0.002	0.002
Israele	225	0.009	0.006	0.977	0.003	0.005
Israele	226	0.005	0.002	0.988	0.003	0.002
Israele	227	0.006	0.006	0.983	0.003	0.002
Israele	234	0.006	0.004	0.953	0.035	0.002
Israele	236	0.111	0.063	0.819	0.004	0.004
Israele	237	0.003	0.003	0.989	0.002	0.003
Israele	238	0.008	0.024	0.955	0.005	0.008
Israele	258	0.001	0.002	0.992	0.002	0.002
Israele	259	0.002	0.004	0.989	0.002	0.002
Israele	260	0.002	0.004	0.988	0.003	0.003
Israele	261	0.002	0.002	0.992	0.002	0.002
Israele	262	0.003	0.004	0.988	0.003	0.002
Israele	263	0.003	0.007	0.981	0.005	0.004
Israele	265	0.002	0.003	0.99	0.003	0.002
Israele	266	0.002	0.002	0.991	0.003	0.002

Origin	K=5, Q>0.8	Armenia/Azerbaijan	Middle Asia	Israele	Georgia subsp. <i>sylvestris</i>	Georgia subsp. <i>sativa</i>
Israele	268	0.002	0.002	0.993	0.002	0.002
Israele	269	0.004	0.005	0.986	0.003	0.003
Israele	272	0.037	0.028	0.906	0.026	0.003
Israele	276	0.026	0.007	0.96	0.005	0.002
Armenia/Azerbaijan	12AZ12	0.713	0.016	0.238	0.03	0.002
Armenia/Azerbaijan	12AZ14	0.914	0.051	0.022	0.011	0.003
Armenia/Azerbaijan	12AZ15	0.986	0.004	0.003	0.004	0.002
Armenia/Azerbaijan	12AZ17	0.991	0.003	0.002	0.002	0.002
Armenia/Azerbaijan	12AZ18	0.974	0.014	0.003	0.006	0.003
Armenia/Azerbaijan	12AZ19	0.958	0.026	0.007	0.003	0.007
Armenia/Azerbaijan	12AZ21	0.99	0.003	0.002	0.003	0.002
Armenia/Azerbaijan	12AZ23	0.983	0.004	0.006	0.004	0.003
Armenia/Azerbaijan	12AZ25	0.931	0.014	0.017	0.033	0.005
Armenia/Azerbaijan	12AZ27	0.977	0.011	0.004	0.004	0.005
Armenia/Azerbaijan	12AZ28	0.981	0.008	0.005	0.003	0.003
Armenia/Azerbaijan	12AZ3	0.969	0.023	0.004	0.002	0.001
Armenia/Azerbaijan	12AZ30	0.983	0.007	0.002	0.003	0.005
Armenia/Azerbaijan	12AZ31	0.993	0.003	0.002	0.001	0.001
Armenia/Azerbaijan	12AZ32	0.971	0.006	0.016	0.004	0.003
Armenia/Azerbaijan	12AZ33	0.99	0.002	0.003	0.002	0.004
Armenia/Azerbaijan	12AZ37	0.988	0.003	0.004	0.003	0.003
Armenia/Azerbaijan	12AZ38	0.99	0.003	0.002	0.003	0.002
Armenia/Azerbaijan	12AZ42	0.989	0.003	0.004	0.002	0.002
Armenia/Azerbaijan	12AZ44	0.953	0.008	0.007	0.019	0.012
Armenia/Azerbaijan	12AZ45	0.684	0.003	0.003	0.307	0.003
Armenia/Azerbaijan	12AZ7	0.835	0.048	0.005	0.094	0.018
Armenia/Azerbaijan	12AZC	0.857	0.021	0.007	0.108	0.008
Armenia/Azerbaijan	12AZD	0.098	0.002	0.002	0.004	0.893
Armenia/Azerbaijan	AR-10	0.991	0.002	0.002	0.002	0.002
Armenia/Azerbaijan	AR-15	0.991	0.002	0.003	0.002	0.002
Armenia/Azerbaijan	AR-22	0.938	0.007	0.009	0.006	0.04
Armenia/Azerbaijan	AR-25	0.844	0.12	0.025	0.007	0.005
Armenia/Azerbaijan	AR-27	0.991	0.003	0.002	0.002	0.001
Armenia/Azerbaijan	AR-29	0.684	0.016	0.274	0.024	0.002
Armenia/Azerbaijan	AR-30	0.957	0.02	0.012	0.004	0.006
Armenia/Azerbaijan	AR-31	0.988	0.003	0.004	0.002	0.003
Armenia/Azerbaijan	AR-33	0.709	0.063	0.208	0.004	0.016
Armenia/Azerbaijan	AR-6	0.993	0.002	0.002	0.001	0.001
Armenia/Azerbaijan	AR-8	0.984	0.006	0.002	0.003	0.004

Chapter 3

GENETIC MAPPING AND QTL ANALYSIS IN MGALOBLSHVILI NOIR

Abstract

Grape downy mildew (DM), caused by the biotrophic peronosporomycete *Plasmopara viticola*, is a devastating fungal disease that affects most *Vitis vinifera* cultivars, resulting in severe epidemics under warm and humid conditions. We have previously identified and characterized a panel of 25 Caucasian accessions of *V. vinifera* which showed traits of low susceptibility to *P. viticola*. Experimental inoculation and disease assessment in field conditions were carried out in a multi-year activity in order to assess the degree of susceptibility of this germplasm collection and the disease incidence. Among these genotypes, 'Mgaloblishvili N.', a georgian accession, showed a constant tolerant behavior as reported in Toffolatti et al., 2016 [1]. Since our previous genotype analysis at known resistance loci didn't support introgression of the resistance trait from already characterized Asian and American accessions, in order to identify the eventual genetic basis of the Mgaloblishvili N. phenotype, a mapping population was obtained by selfing this variety. As segregation of the DM disease could be observed in the population after the first infection trial, a linkage map construction and a QTL mapping experiment, based on artificial inoculation with *P. viticola* performed under controlled conditions, were included in this research work. The genetic map was built essentially with SSR markers and enriched with RAD-derived SNPs chosen to fill in several gaps and it was used to perform a preliminary QTL analysis. QTLs for downy mildew resistance were detected on different chromosomes, although they were not repeated among seasons. Obtained results were studied separately for further in-depth analysis.

Background

The cultivation of *Vitis vinifera* originated in Georgia, in the south of Caucasus, before the introduction of New World diseases, and the ancient varieties have been vegetative propagated for centuries, still persisting today because of their distinguished wines. To date, the creation of hybridized forms marked the dawn of grapevine breeding for diseases such as powdery and downy mildew; before that, *V. vinifera* was susceptible to local diseases and indigenous grapes of Atlantic Coast were unsuitable for wine making. From the breeding point of view, it is highly desirable to combine as many resistance genes as possible in a new cultivar in order to make resistance as sustainable as possible [76], therefore finding sources of resistance in *V. vinifera* could be a great innovation, as it could really improve the breeding programs producing new varieties with the quality levels required for wine production. Recently, identification of powdery mildew resistance in accessions of *V. vinifera* [92] indicates that some genetic resistances may be present in the germplasm. Several works that have exploited available genetic information on the powdery mildew genetic resistance have already been published. For instance a research group has took advantage of genetic data on locus Ren1 to identify additional germplasm that shared a Ren1-like local haplotype, and then attempted to clarify the evolution of powdery mildew resistance and its domestication in cultivated *V. vinifera* subsp. *sativa*. Ten new powdery mildew resistant accessions were discovered that possess a Ren1-like local haplotype, which was earlier identified in 'Kishmish vatkana' and 'Dzhandzhal kara' (syn. 'Karadzhandal') from Central Asia [90]. These last new records, suggested the existence of intriguing and unexplored traits of resistance to pathogen in *V. vinifera* accessions, which brought to the attention the European grapevine. To date, only a few research works demonstrated the presence of resistant traits in *V. vinifera* species concerning powdery mildew disease, but no evidence of resistance for downy mildew were recorded. Nevertheless, different levels of susceptibility to *P. viticola*, the causal agent of grapevine downy mildew, were detected in some Georgian autochthonous varieties, and they were analyzed with artificial inoculations as reported in Bitsadze et al., 2015 [119], demonstrating the existence of potential genetic variation, probably due to the high genetic diversity which characterizes the center of grape domestication.

To date, several studies regarding the genome sequencing and the realization of genetic maps by using different molecular markers and high-throughput technologies have been published; this has allowed to undertake advanced research aimed at localization of genes of agronomic interest and identification of QTLs. In grape, the disease-related genes represent a significant part of the genome and such detailed knowledge of it will serve to accelerate the development of genetic strategies to counter crop loss due to dynamic and genetically diverse pathogens. Since microsatellite markers are robust markers that are readily shared among laboratories, the grape genetics community worked cooperatively to develop a large number of these markers in the *Vitis* Microsatellite Consortium (VMC) managed through AGROGENE, Moissy Cramayel, France. Across the years, the set of grape available markers were enriched with several other microsatellites increasing grapevine database.

At the same time, huge progress have been reached for high throughput SNP genotyping thanks to the introduction of array-based technologies. With the advent of next-generation sequencing (NGS), there are several of such approaches, which are capable of discovering, sequencing and genotyping thousands of SNPs per assay across almost any genome of interest in a single step, even in populations in which little or no genetic information is available. One of these approaches is the restriction-site associated DNA sequencing (RAD-seq) based which allows to develop robust markers population genetics analyses. Pfender et al., 2011 [120] successfully used RAD-seq to construct a high-density genetic map, employing the obtained data to detect QTL for resistance to stem rust in *Lolium perenne* and at a later time Wang et al., 2012 [121] implemented this approach on a grapevine population. Across the years, several modification were applied on the original RAD-seq protocol and one of the last records is reported in Marrano et al., 2017 [118], in which several cultivated and wild forms of *V. vinifera* have been analyzed, making available a tool for investigations of grapevine domestication.

Several grape linkage maps have previously been published, but most of the mapping populations were obtained from interspecific hybrids, often chosen because the parents are sources of disease resistance. To date, only a few genetic maps based on self-crosses of *V. vinifera* varieties have been developed [55], [56] and

moreover no records of genetic maps based on grapevine from Georgia, the cradle of domestication, accessions have been reported. Accordingly, the major objective of this study was to construct a framework genetic map for 'Mgaloblishvili N.', investigate the segregation of response to downy mildew inoculation and perform a preliminary QTL analysis in order to better understand the genetic bases of the tolerant phenotype observed in 'Mgaloblishvili N.'

Methods

Plant material and DNA extraction

The mapping population finally consisted of 156 individuals derived from a self-cross of 'Mgaloblishvili N.', which was recently identified as interesting Georgian genotype presenting a constant tolerant behavior to downy mildew infection. Given its tolerance phenotype to fungal infection, the choice of using a self-fertilized population was intended to avoid the loss of the trait of interest, allowing rather its segregation among the offspring. The starting plant material was composed by 133 seedlings and it has been enriched, in a second moment, by 23 individuals identified among the open pollinated genotypes using molecular markers.

DNA was isolated from young leaves following a modified [122] procedure. Freeze-dried tissue was grinded with MM 300 Mixer Mill system (Retsch., Germany) and the powder was scraped into 600 μ l of preheated (60°C) CTAB buffer (CTAB 3% (w/v)), 2 M NaCl, 0.2% (v/v) of 2-mercaptoethanol, 25 mM EDTA, 1 M Tris HCl (pH 8.0) and 1% (w/v) polyvinylpyrrolidone (PVP-40). Samples were incubated at 60°C for 35 m, then extracted with chloroform-isoamylalcol 24:1. DNA was precipitated with cold isopropanol added with RNase (20 ng/ml), recovered by centrifugation (14000 rpm, 10 m), washed with a solution of ethanol (76% v/v) containing 7.5 M of ammonium acetate, air dried and re-suspended in H₂O. Finally, isolated DNA was quantified by NanoDrop ND-8000 and diluted to approximately 4 ng/ μ l (Figure 1).



Figure 1 Mapping population of 'Mgaloblishvili N.'. The whole experimental population was preserved in the green house of Tavazzano-Lodi.

Simple Sequence Repeats (SSRs)

The primer pairs flanking microsatellite loci from marker sets VMC (Vitis Microsatellite Consortium), VVS [123], VVMD [124], VrZag [88], VChr [125], SCUv [126], UDV [52] and VVI [51], were initially screened for segregation using small panel composed by 6 offspring plus the parental line and the polymorphic ones were used to genotype the entire mapping population. All forward primers were 5'-end labeled with different fluorescent dyes (6-FAM, HEX and NED) and grouped for multiplex reactions. PCR amplifications were performed in 11.5 μ l reactions consisting of 4 ng template DNA, 0.2 μ M of each primer, 200 μ M of dNTPs, 1X gold PCR buffer (Perkin Elmer), 1.5 mM MgCl₂ solution and 0.5 unit Taq DNA polymerase (AmpliTaq, Gold™, Applied Biosystems, Foster City, CA).

Additional microsatellite markers were selected based on the available map position information reported in Fechter et al., 2014 [127] in order to increment the number of informative SSRs for the genetic map construction. These markers (GFs 01-19) were developed in Geilweilerhof Institute for Grapevine Breeding and genotyped with a modified EcoR1-tailed primer method [107]. All forward primers were designed with an EcoR1 FAM-labeled tail and combined with reverse primer were added in the reaction in a ratio 1:5, respectively, as already described in the section Methods of Chapter 2.

Amplification conditions were optimized for each primer pairs using various annealing temperatures and the touch-down protocol used provided for 10 m at 95°C, followed by 10 cycles (1 m 95°C, 1 m 59°C minus 0.5°C each cycle, 2 m 72°C), 25 cycles (1 m 95°C, 1 m 54°C, 2 m 72°C), and a final extension of 10 m at 72°C.

PCR products were analyzed by capillary electrophoresis (ABI 3130 Genetic Analyzer) and peaks were identified by size with GeneMapper v3.5 software after a denaturation treatment with a mixture of formamide and GeneScan™ -500 ROX® standard. Any ambiguous genotype was re-run, re-amplified or left as unknown (missing data).

Single Nucleotide Polymorphisms (SNPs)

In order to enrich the genetic map and to fill in several gaps, a few SNPs, discovered from a set of *V. vinifera* cultivars, as described in RAD-seq experiment [118], were chosen. Primers were designed using NCBI/Primer-BLAST (www.ncbi.nlm.nih.gov/tools/primer-blast/) to yield products 266-1002 bases long. Target sequence fragments have been amplified in the parental line in order to select the available allelic variations.

Sanger sequencing provides for several steps. A first PCR reaction (DNA [5ng/ul]), using designed primer pairs, allowed to amplify the region of interest and the amplicons were evaluated using agarose gel electrophoresis. In order to remove the excess PCR primers and dNTPs the products were purified through an enzymatic method involving Shrimp Alkaline Phosphatase (SAP) and Exonuclease I (EXO I) treatment before sequencing (Thermo Fisher Scientific). The products of Sanger sequencing were run on the 96-capillary 3730xl DNA analyzer (Applied Biosystems®) and finally analyzed by using STADEN package v2.0.0 (Illumina inc.:Infinium® Genotyping Data Analysis 2014)[128].

Once selected informative SNPs, genotyping of the entire mapping population was performed through multiplexed minisequencing ABI PRISM® SNaPshot™ method. This approach was optimized to be used both as a single and multiplex SNP assay by adding the primers for the minisequencing reactions with a variable length tail and the generated amplicons were purified with ExoSap according to the manufacturer's protocol. SNaPshot reaction was performed in a final volume of 10 ul that contained 1 ul of SNaPshot primers mix (0.4 uM each primer), 2 ul of SNaPshot Multiplex Ready Reaction, 1.5 ul H₂O and 6.5 ul of purified PCR product. Thermal amplification conditions consist of a denaturation of 96°C for 1 m followed by 25 cycles of 96°C for 10 s, 50°C for 5 s, and 60°C for 30 s. Final products (0.5 ul) were mixed with 9.25 ul of formamide and 0.25 ul of GeneScan™ -120 LIZ® size standard (Applied Biosystems), run in ABI PRISM 3130xl Genetic Analyzer (Applied Biosystems) and analyzed by GeneMapper v3.5 software.

Segregation and linkage genetic map construction

Genetic map was constructed using JoinMap® 4.1 [129] with Kosambi's mapping function [130], used to estimate map distances, linkage with a recombination threshold of 0.40 and a LOD threshold of 3. The outcross pollinated (CP) full-sib family was used as population type to analyze the S1 population derived from a heterozygous parent. All codominant markers were scored using the same segregation pattern <hkxhk>. SSR and SNP amplified fragments were encoded as "hh" and "kk" for homozygous genotypes for the different alleles and "kh" for the heterozygous ones whereas missing data were recorded in case of unclear or ambiguous peaks.

The goodness-of-fit between observed and expected Mendelian ratios (1:2:1) was analyzed for each marker locus using a χ^2 test with a significant threshold of $\alpha=0.05$ and markers showing a distorted segregation were included in the mapping computation unless they significantly affected the order of their neighbors. Grouping was based on linkage LOD (with LOD>3) using the regression method. Moreover different parameters were set up for the analysis such as goodness-of-fit jump threshold for removal loci=5.0, ripple=1 and the third round. Finally marker scores were checked for putative double recombination events using the genotype probabilities output from JoinMap® and in a number of cases, markers that caused high tension were omitted from the final map.

MapChart [131] was used to draw the genetic linkage maps.

Estimation of genome length and map coverage

The genome length estimation was determined by a method of moments estimator $G_e = N(N-1)X/K$ [132], where N is the number of markers, X is the maximum observed map distance between marker pairs above a threshold LOD Z, 3 in this work, and K is the number of locus pairs having LOD values at or above Z. The

observed genome map coverage was calculated as the ratio between observed and estimated genome length [133].

Phenotypic evaluation of downy mildew tolerance

Phenotypic evaluation was performed by the partner group at University of Milan. A total of 156 seedlings, maintained in pot in the greenhouse of Tavazzano (Lodi), was screened for downy mildew tolerance after inoculation with *P. viticola* collected from natural infected leaves in a vineyards located in Sirmione (Brescia) not exposed to any treatment against mildews. Disease evaluation was scored in 2013, 2014, twice in 2015 (May and July) and in 2016 through leaf disks assay. To assess the response to the pathogen, Pinot Noir and Bianca genotypes were used as reference susceptible and resistant varieties, respectively.

The experimental inoculation procedure was carried out in the screenhouses of Tavazzano (Lodi), at the beginning of grapevine growing seasons. Three leaves (3th-5th leaf starting from the shoot apex) were detached from each accession. Three leaf discs (15 mm diameter) were cut from each leaf with a cork borer and placed lower surface upward on a moistened filter paper placed in a Petri dish (6 cm diameter). Three plates containing three leaf discs were obtained for each grapevine genotype. The leaf discs were sprayed with 1 mL *P. viticola* sporangia suspension [$5 \cdot 10^4$ sporangia/ml] and incubated in growth chamber at 22 °C for 7- 10 days.

In addition, parental plants have been observed also in the field collection at FEM (both treated and not treated with fungicides) where they showed a good tolerance to the pathogen attack in natural conditions.

Data analysis

Each leaf disc was scored for the surface covered by sporulation at the stereo microscope (Leica Wild M10) by attributing the following classes: 0 = absence of sporulation; 1 = 0.1-2.5% of the surface covered by sporulation; 2 = 2.5-5%; 3 = 5-10%; 4 = 10-25%; 5 = 25-50%; 6 = 50-75%; and 7 = 75-100% of the leaf area covered by sporulation according to Toffolatti et al., 2012 [134].

The disease severity was estimated by the Percentage Index of Infections (I%) calculated from the formula of Townsend and Heuberger (1947)

$$I\%I = \frac{\sum(n \cdot v)}{(n^{\circ}class - 1) \cdot N} \cdot 100$$

where n is the number of leaf discs in each class, v the numerical value of each class and N represents the total number of leaf discs in the sample. The plants with I% lower than 25% were considered resistant.

The normality of trait distribution was evaluated by the Shapiro Wilk test. Year effect was tested with analysis of variance using R package and the phenotypic correlations between the years were determined using the parametric Pearson correlation coefficient.

QTL analysis

QTL analysis was performed on S1 genetic map using MapQTL®6 [135] and the phenotypic data from separate years. The analysis was based on different methods which included the nonparametric Kruskal-Wallis (KW) test, the Simple Interval Mapping (SIM) [136] and the Multiple Qtl Mapping (MQM). The genome-wide and LG-specific LOD (logarithm of the odd) thresholds at $\alpha = 0.05$ (5%) were calculated by at least 1,000 permutations.

Results

Analysis of SSR and SNP markers

A total of 467 microsatellite (SSR) were at first tested in a small panel of 6 randomly chosen progeny plants together with the parental line. Out of these, 191 were homozygous, 106 didn't amplify or gave unclear or multi-locus amplifications and only 170 were found informative and analyzed over the entire mapping population. Three of the polymorphic markers were further discarded since they displayed a deviated segregation 3 (hk):1 (hh or kk) resp. 1 (hh):2 (hk):1 (kk) ratio, showing only two out of the three haplotypes expected.

In addition to the microsatellite markers, several SNPs were chosen to fill in the gaps of the first frame map. Out of 137 RAD-derived SNPs discovered in a set of *V. vinifera*, 110 were homozygous whereas only 37 were heterozygous in the parental line and 14 primer pairs were designed *ad hoc* to test the entire population through SNaPshot™ approach. Among these, one primer pair was discarded from the analysis because of a distorted segregation 3:1.

Altogether, this analysis yielded 180 fully informative markers (supplementary table S1).

Genetic linkage map

Starting plant material was composed by 133 seedlings and in order to increase the size of studied population we screened additional open pollinated accessions with molecular markers to be able to identify the casual genotypes produced by self-crossing of 'Mgaloblishvili N.' Over 46 accessions, we found out 23 additional self-crossed seedlings to be added to the mapping population.

Using all the marker set together and 154 individuals of the offspring (2 of 156 were put by because of the huge amount of missing data), a total of 177 markers was aligned into 19 linkage groups, covering 1078.4 cM with an average distance between markers of 6.2 cM, and 3 gaps larger than 20 cM. Out of 180 fully informative markers, 3 of them were linked but unmapped due to weak linkages to other markers within the group. Chi-square analysis indicated segregation distortion (SD) for 58 markers (32.2%) of which many clustered on linkage groups LG05, LG10 and LG16. The obtained genetic map was aligned with the reference one (IGGP International Grapevine Genome Program; <http://www.vitaceae.org>) for numbering and marker order comparison. Only three hotspots for SD were apparently present on chr 5, on chr 8 and on chr 19, which showed an inversion confirmed by the physical positions reported in Genoscope annotations.

47.1% of SSRs and 25% of SNPs were heterozygous in the parental line, which means that around 41.6% of tested markers could be mapped. The estimated genome length was 3071.1 cM and the observed genome map coverage reached barely 35.1%. (Figure 2, Table 1)

Table 1 **Summarizing outline of 'Mgaloblishvili N.' map.** "Unpositioned" markers could be assigned but not placed on the maps because of insufficient linkage to the other loci or location conflicts.

	L22
N° of analyzed markers	180
N° of mapped markers	177
SSRs	128
SSRs GF (a)	36
SNPs (b)	13
N° of unpositioned markers	3
N° of linkage groups (LG)	19
Mean number of markers/LG	9
Total length (cM)	1078.4
Mean LG length (cM)	57
Average map distance between loci (cM)	6.2
N° of gaps between 20 and 30 cM	2
N° of gaps > 30 cM	1

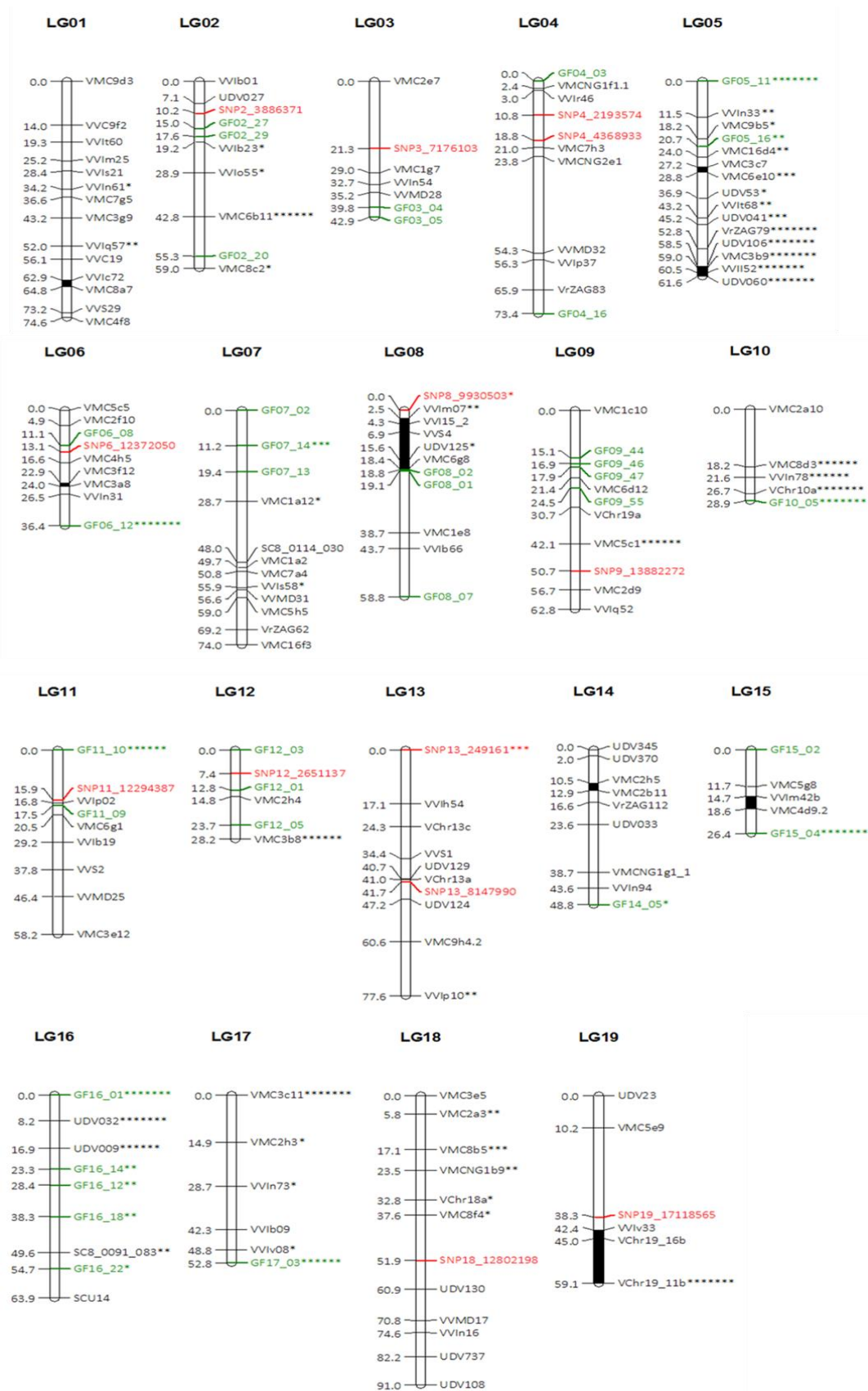


Figure 2 Linkage map of 'Mgaloblishvili N.'. Linkage groups were numbered according to Adam-Blondon et al., 2004 [53]. Distorted markers have an asterisk showing the level of distortion (* = $p \leq 0.1$; ** = $p \leq 0.05$; *** = $p \leq 0.01$; **** = $p \leq 0.005$; ***** = $p \leq 0.001$; *****) = $p \leq 0.0005$; *****) = $p \leq 0.0001$). SNP markers were colored in red and GF markers were colored in green. Black zones defined the inversions according to Genoscope annotations and hotspots for SD.

Phenotypic data distribution

The response to artificial inoculation with *P.viticola* was scored for different seasons at 10 days post-inoculation and phenotypic data distributions showed a continuous variation of the trait. According to results obtained from Shapiro-Wilk normality test, despite the p -value ≤ 0.05 , W (0.99) very close to 1, indicated that the distribution was close to normal (Figure 3).

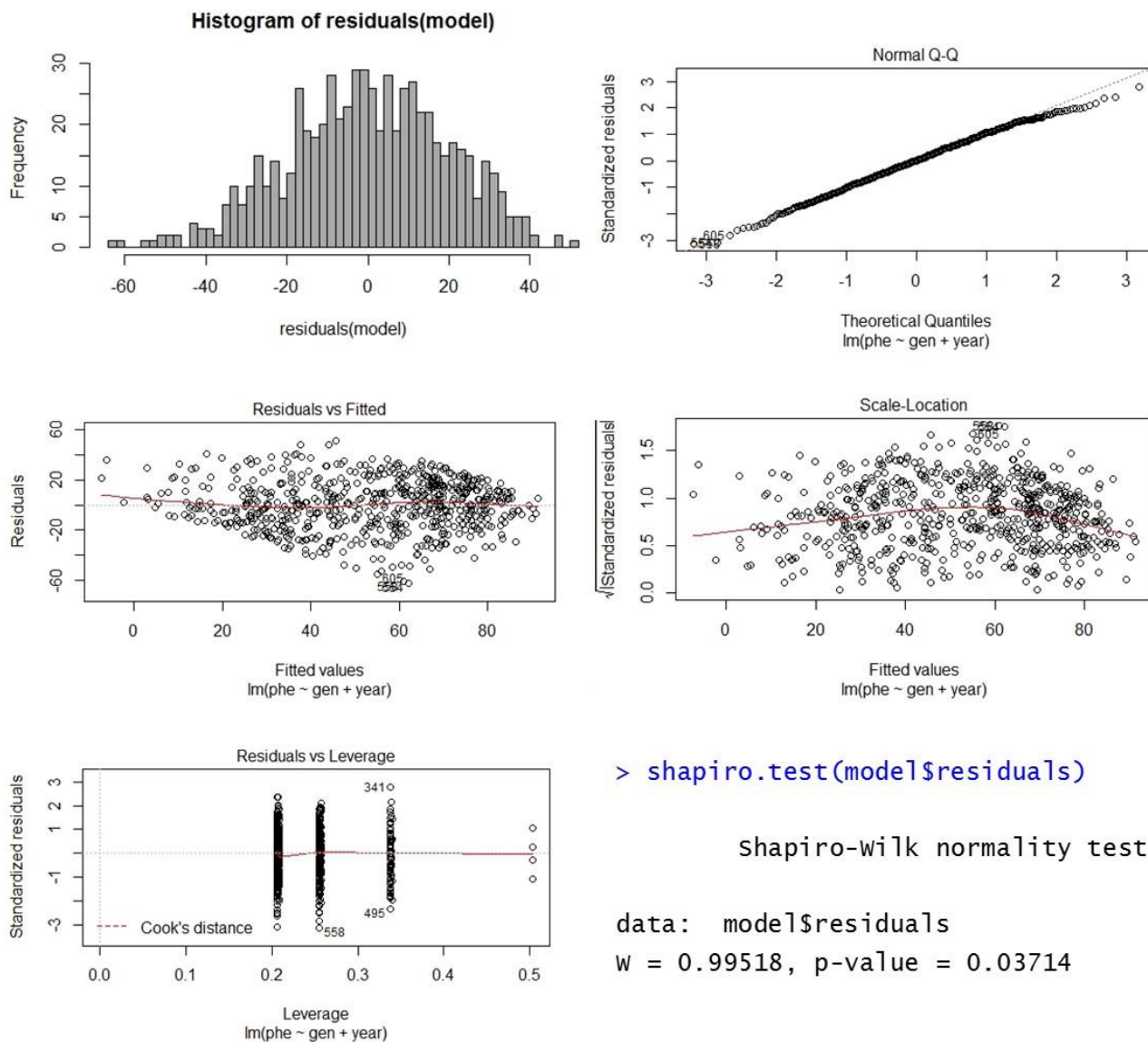


Figure 3 Statistical representation of residuals distribution among different years of phenotyping. i) Histogram of residuals ii) Normal QQ-plot of the theoretical percentiles of the normal distribution versus the observed sample percentiles iii) Residuals vs Fitted plot shows if residuals have a linear pattern iv) Scale location plot showed if residuals are spread equally along the ranges of predictors v) Residual vs Leverage plot helps to find eventual influential cases through Cook's distance

Parametric (Pearson) and non-parametric (Spearman) correlation analysis applied to the distribution of trait, among the different seasons evaluated, showed a significant correlation only once, whereas in other cases no correlations or discordant ones were calculated. As described in Table 2, Figure 4 a positive correlation between years 2014 and 2015 (July) were found and a significant but negative correlation were detected between years 2014 and 2015 (May).

Table 2 Values of Pearson and Spearman correlations among different years of phenotyping. Significance levels were marked out with asterisk (* = $p \leq 0.05$, ** = $p \leq 0.01$)

	2013	2014	May 2015	July 2015	2016
Pearson test 2013	1.00				
Spearman test 2013	1.00				
Pearson test 2014	0.17	1.00			
Spearman test 2014	0.12	1.00			
Pearson test May 2015	0.10	-0.27*	1.00		
Spearman test May 2015	0.10	-0.24**	1.00		
Pearson test July 2015	-0.01	0.22*	0.11	1.00	
Spearman test July 2015	-0.09	0.19*	0.1	1.00	
Pearson test 2016	-0.12	-0.09	-0.03	0.05	1.00
Spearman test 2016	-0.13	-0.02	-0.08	0.16	1.00

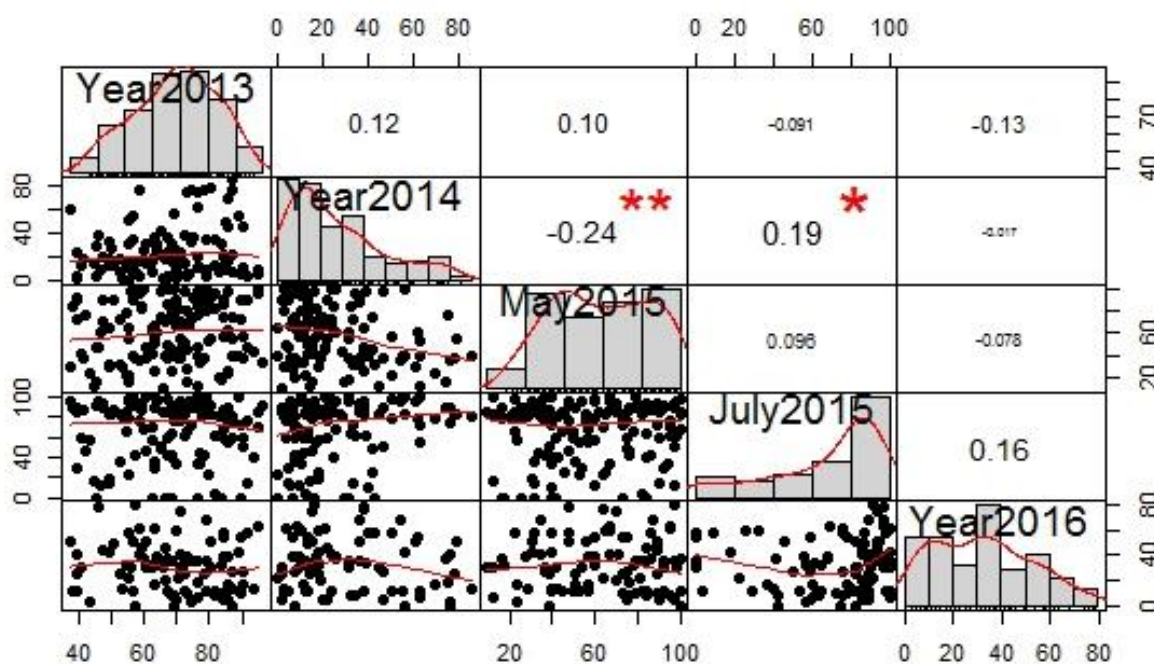


Figure 4 Correlation matrix. The distribution of each variable is shown on the diagonal. On the bottom of the diagonal: the bivariate scatter plots with a fitted line are displayed. On the top of the diagonal: the value of the correlation plus the significance level as stars (* = $p \leq 0.01$, ** = $p \leq 0.001$)

Analysis and mapping of phenotypic traits

Simple interval mapping (SIM) analysis identified several QTLs distributed in different LGs, but not always reproduced among the different years. After a first round of interval mapping (IM), markers with the highest LOD value were selected as cofactors for MQM mapping. Moreover, a permutation test was run in order to define the LOD threshold (Genome Wide and Chromosome specific) to obtain 95% confidence of detecting a putative QTL (Table 3).

A first QTL in LG01 was detected with the phenotypic data collected in 2014, the position of the peak (max LOD value at 9.82 cM) was closed to the VMC8a7 marker and explained 15.8% of total phenotypic variation. Moreover in the same year other two significant LOD peaks were found in LG11 and LG07 (max value at 40.736 cM and 59.565 cM) closed to markers GF11-09 and GF07-14, explaining 14.4% and 16.1% of total phenotypic variation, respectively.

A second significant QTL in LG05 was detected analyzing phenotypic data collected in 2016, the peak (max LOD value at 2.564 cM) was linked to the marker VMC3b9 and explained 17.2% of variance. The position of this QTL coincides with the already discovered *Rpv11* locus [137] [66].

QTL showing minor effects on the resistance phenotype, detected in different seasons (2013, May 2015 and July 2015), were located in LG13, LG10 and LG03 respectively as reported in Table 3 with the corresponding flanking markers and KW analysis. These minor QTLs spanned over large regions, without trace a regular trend so we couldn't be able to define a specific peak position. Nevertheless, they probably provided additive effects, contributing to the phenotypic trait.

Table 3 **Location, significance and effect of QTLs detected for downy mildew tolerance.** LG=Linkage group; QTL position=QTL position as estimated by the cM distance of the local LOD maximum; LOD peak SIM= LOD value at QTL position detected by Simple Interval Mapping; LOD peak MQM= LOD value at QTL position detected by Multiple Qtl Mapping; Interval 1-LOD= confidence interval of QTL position in cM; LOD threshold = chromosome wide LOD threshold; LOD threshold GW = genome wide LOD threshold; marker = marker nearest to the QTL position; %Var expl = proportion of the total phenotypic variance explained by the QTL; KW = Kruskal-Wallis significance level, given by the P value (* = $p \leq 0.1$; ** = $p \leq 0.05$; *** = $p \leq 0.01$; **** = $p \leq 0.005$; ***** = $p \leq 0.001$; ***** = $p \leq 0.0005$; ***** = $p \leq 0.0001$)

Year	LG	QTL position (cM)	LOD peak SIM	1-LOD interval (cM)	LOD peak MQM	LOD threshold $\alpha=0.05$	LOD threshold GW	Marker	% Var expl	KW
2013	13	77.551	2.99	33.297-77.551	2.79	2.3	3.6	VVlp10	9.60%	****
2014	1	9.82	4.47	0-19.516	5.55	2.2	3.7	VMC8a7	15.80%	*****
	7	59.565	3.45	55.565-67.781	4.23	2.3		GF07-14	16.10%	****
	11	40.736	4.05	31.976-47.335	3.94	2.1		GF11-09	14.40%	*****
	18	-	-	-	3.29	2.5		-	-	-
	9	-	-	-	2.3	2.3		-	-	-
May 2015	10	5	2.23	0-9	3.05	2	3.7	VMC2a10	9.40%	****
July 2015	3	36.243	2.75	33.693-38.243	-	2.2	3.7	VVMD28	8.90%	****
	10	28.871	2.04	-	-	2		GF10-05	6.70%	**
	18	33.782	-	29.505-34.782	2.54	2.4		Chr18a	7.80%	*
	19	-	-	12.183-21.183	2.08	2		-	7.80%	-
2016	5	2.564	3.95	0-10.754	4.41	2.3	3.7	VMC3b9	17.20%	*****
	7	0	-	0-9.858	3.3	2.5		VMC16f3	10.80%	**
	8	6.916	-	0-9.916	2.93	2.3		VVS4	9.80%	**

Integration of QTL regions

QTL regions appeared quite large, including several genes as described in supplementary table S2. In order to deepen the obtained results, regions of interest were integrated with additional markers which are described in supplementary table S1. The integration allowed to narrow down the region of interest, reducing the number of genes to examine in depth. As explained in Figure 5, the results are strongly supported by Kruskal Wallis analysis and the both SIM and MQM mapping approaches confirmed the detected QTL regions. Information on markers physical position were collected from French National Sequencing Center (Genoscope) Database, whereas GF markers positions were collected from European Vitis Database (www.eu-vitis.de) whose a process of quality checking is ongoing and the data could still contain some errors.

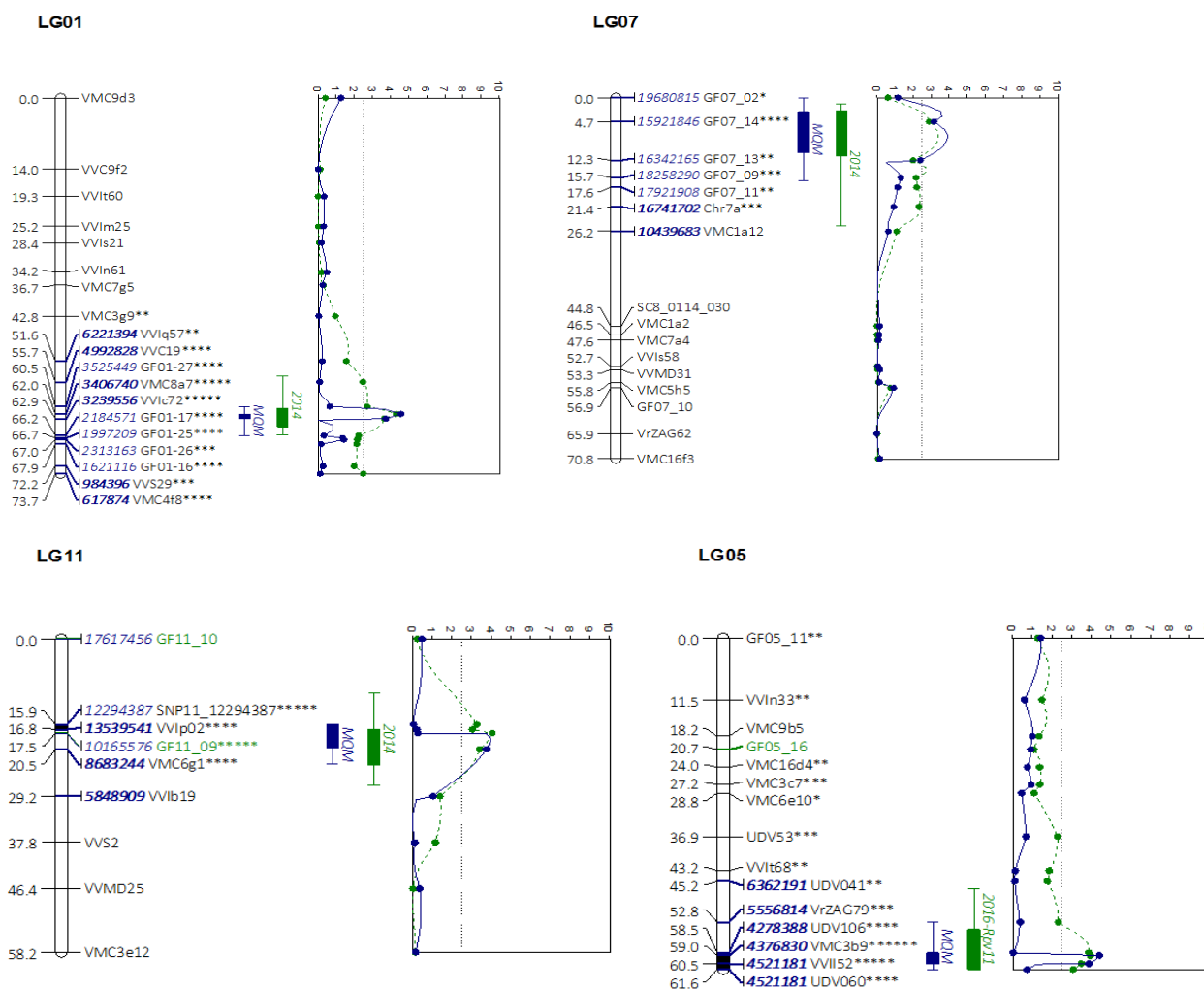


Figure 5 QTL plots. Quantitative trait loci for *Plasmopara viticola* tolerance identified on LGs 01, 07 and 11 in 2014 and on LG 05 in 2016, of the 'Mgaloblishvili N.' genetic map by Interval Mapping (green) and MQM (blue). Physical position of linked markers are in blue.

Discussion

A self-crossed population and the framework map for 'Mgaloblishvili N.'

Due to the lack of a strong resistance in 'Mgaloblishvili N.' cultivar, the choice of a mapping population obtained from selfing was preferred aiming to generate the segregation of response to downy mildew trait among individuals. Selfing or full-sib family selection increases the expression of genetic variance on total variance, and allows refinement of the plant population with suitable traits [138]. In a few cases, the development of S1 lines may broaden genetic variability for specific traits as a result of transgressive segregation, manifestation of recessive genes, and fixation of alleles [139]. On the other hand, transgressive (extreme) phenotypes can be negative in terms of fitness, inducing the inbreeding depression. The obtained framework map is considerably poor of marker loci, despite the huge amount of molecular markers screened, due to the unusual high homozygosity of the parental line (59.25 %). Similar results were described in Duchene et al., 2009 [140] which studied a progeny from a selfing of Muscat Ottonel to evaluate terpenol content. Muscat Ottonel showed a considerable homozygosity (56%), consequently it resulted more difficult to find segregating loci and to expect a good coverage of the genome, since some telomeric regions were not represented in that map [140]. Population size is an important issue in constructing a linkage map, because it is highly associated with the accuracy of detecting recombination events and in order to increase the size of the offspring we decided to screen several open pollinated accessions to find out casual genotypes produced by self-crossing of 'Mgaloblishvili N.'. This finally enabled to add further 23 individuals to the mapping population. The presence of few large gaps in the map (> 20 cM) could be caused by the type of crossing used; in the specific case, a self-fertilization could have produced a certain number of double crossing overs. Despite this, we were able to achieve all the 19 expected linkage groups on a framework map, which exhibited a high level of synteny and co-linearity compared with other published maps. A recent study about self-crosses reported as oral communication at SIGA annual congress [141], described the characterization of different progenies obtained by self-crossing of several varieties. Preliminary results of the cited work disclosed a balanced translocation in Rkastiteli variety, a Georgian cultivar. In our study, we detected inversions on chr 5 and chr 8, which could lead to think about an introgression from other species, but considering the analysis with markers associated to already known *Rpv* loci, reported in the Appendix, these inversions could be rather caused by mutations due to the type of crossing as explained in the cited work.

Segregation distortion

Segregation distortion is a ubiquitous phenomenon that is defined as a deviation of the observed genotypic frequency from representative Mendelian segregation ratios. Segregation distortion is always associated with a cluster of skewed markers within a chromosomal region, termed as segregation distortion region (SDR) [142]. The genotyping in the S1 'Mgaloblishvili N.' population indicated a high number of markers significantly deviating from the expected segregation ratio (1:2:1). The level of this segregation distortion is 32.2%, a value higher than previously observed in *V. vinifera* crosses (19-20%, Salmaso et al., 2008, 11.6%, Troggio et al., 2007, 7-11%, Doligez et al., 2006). This phenomenon is a common aspect of mapping population analysis, especially for recombinant inbred line and could be influenced by many factors which vary significantly with the species, crosses and mapping populations. There is a variety of mechanisms that could cause this event and in most systems act in genetic effects including pollen tube competition, pollen lethal, preferential fertilization, sterility and chromosome translocation and the first three types were defined as gametic selection. Among the markers used for the genotyping, we excluded four of them from the analysis since they showed a deviated segregation (3:1). The selfed population, obtained from an accession strongly homozygous, may have a higher segregation ratio distortion because of transgressive segregation. Nevertheless, as explained in Xu et al., 2008 and Zhang et al., 2010 [143], [144], sometimes, the distortion can result in a higher genetic variance than that of non-distortion, and therefore could benefit the detection of linked QTLs. In particular, as for segregation distortion, if the distorted marker is not closely linked with any QTL, it will not have significant impact on QTL mapping; otherwise, the impact of the distortion will depend on the degree of dominance of QTL, frequencies of the marker types, the linkage distance between the distorted marker and QTL, and the mapping population size.

QTL analysis

The skewing of segregation occurs when a molecular markers locus links to a distorter that could be related with a lethal effect or with a QTL. Observing the phenotypic data after the artificial inoculation, the unstable behavior of the offspring among the seasons is clearly pointed out and this could be explained by the loss of fitness due to the inbreeding depression together with the environmental factors that occurred among the years, such as the plentiful rains of 2014 and 2016 against the dry heat of 2015, which definitely influenced the aggressiveness of the pathogen.

To better discuss these results, we have had to reconsider the main feature of disease resistance. In terms of number of genes involved, there are two type of resistance. The first is called major-gene or single-gene resistance, in which plants usually have one or a few specific well-defined genes that confer a high level of resistance to a specific pathogen (e.g. Powdery mildew). The second type, called polygenic resistance (e.g. Downy mildew), involves several genes and is harder to define which genes are involved Polygenic resistance is usually effective against all races of a pathogen, contrary to the monogenic resistance which may confer high level of resistance to a specific race. Often quantitative traits don't give a plant as high a level of resistance as the monogenic one.

It may be considered that parental plants showed different level of disease during the various inoculation test therefore the segregation of the phenotype was finally called into question. The poor repeatability of response to downy mildew inoculation could suggest that several genetic factors with minor effects are involved, which could explain the absence of a strong QTL. In this study we also used the non-parametric Kruskal-Wallis method in order to confirm that QTLs detected with interval mapping were not artefacts due to large gaps, segregation distortion or abnormal distribution of traits, but despite this, the general reliability of our results was not supported by QTL stability over the years.

A glance of candidate genes

In grape, disease-related genes represent a significant part of the genome and are scattered all over the chromosomes with a large nucleotide binding site (NBS) gene family frequently organized in complex clusters. Since QTL analysis indicated regions of the genome which contribute to trait variation, the following step of our study was to narrow down there regions to the point where the effects can be ascribed to specific genes. Our results showed the presence of four QTLs, three detected in 2014 on chromosomes 1, 7 and 11 and one detected in 2016 on chromosome 5. QTL positions are quite rough because the associated confidence intervals cover regions of several megabases, containing various candidate genes (CGs) listed in supplementary table S2 and it is widely known that validation experiments are more or less complex according to the nature of the trait (mono- or poly- genic). Analyzing the range of different genes close related to the markers with max LOD peak, we were able to find arguable in silico predictions in LG01, LG07, LG11 and LG05 QTLs, employing different databases such as Gramene database (<http://www.gramene.org>) and Grape Genome Database hosted at CRIBI (<http://genomes.cribi.unipd.it/grape>). Interestingly, in all QTL ranges we were able to detect predicted genes involved in the basal immune system, leaf development and carbohydrate metabolism suggesting the activation of constitutive defenses referred to morphoanatomical characteristics such as trichomes we found density, cell wall composition, and constitutive compounds with antimicrobial activity production.

In LG01 QTL interval we found different in silico predictions of regulators which showed a synteny with Arabidopsis genomes. Interestingly, a relevant Ethylene Responsive Factor (ERF118 like protein VIT_201s0011g03470) has been predicted and acts in Arabidopsis as a transcriptional activator, binding the GCC-box pathogenesis-related promoter element and involved in the regulation of gene expression by stress factors and by components of stress signal transduction pathways. In the same range a Jagged (JAG) gene (VIT_201s0011g03600) was identified to be a member of the zinc finger family of plant transcription factors and encodes a protein with a single C2H2 zinc finger domain involved during leaf development. A third gene included in the region of interest was a R2R3-type MYB transcription factor (MYB62 VIT_201s0011g03730) which was induced, in Arabidopsis, in response to Pi deficiency and described in detail in Devaiah et al., 2009 [145].

A second significant LOD peak was found on chromosome 7. According to the used databases and comparing markers physical positions with the genetic ones, we were able to detect a large region of interest spanning over 1600000 bp. Two WRKY transcription factors, annotated as WRKY7 (VIT_207s0031g00080) and WRKY13 (VIT_207s0031g01840) and a probable WRKY transcription factor 51-like (VIT_207s0031g01710) were found in the QTL interval. WRKY genes are components of plant biotic stress regulatory networks and they have a complex response pattern. For example, the Arabidopsis thaliana WRKY7 gene is induced by pathogen infection and salicylic acid (SA) treatment and may therefore play a role in plant defense responses, in particular it seems to act as transcriptional repressor in plant cells by enhancing plant susceptibility to *Pseudomonas syringae* [146]. Moreover, WRKY7 has been shown to bind a Ca²⁺-dependent calmodulin [147], suggesting an additional mechanism of regulation of the WRKY protein. On the contrary, *Oryza sativa* WRKY13 plays a vital role in the cross talk between abiotic and biotic stress signaling pathways by suppressing abiotic stress resistance and activating disease resistance, however the regulation mechanisms are still partially unknown [148]. Finally, according to Gao et al., 2011 [149] also WRKY51 protein plays a role as positive regulator of SA-mediated signaling but as negative regulator of JA ones. In addition other two genes, VIT_207s0031g00705 and VIT_207s0031g00710 encoding for RRTF1 ethylene-responsive transcription factor and ethylene-responsive transcription factor ERF109-like respectively, strictly related one to each other, were found in the middle of the QTL region. In detail, Redox Responsive Transcription Factor 1 (RRTF1) plays a crucial role in reactive oxygen species (ROS) production and is involved in age-dependent and systemic stress signaling [150]. Instead, ERF109 gene is involved in a number of biological processes, in particular is required for promotion of vascular cell division during both primary and secondary growth [151] and it has a dual effect under both programmed cell death and salt stress [152], retarding the PCD and improving salt tolerance in plants.

Focusing on LG11 QTL range, the most considerable gene we were able to find in correspondence to the peak, was Tetraspanin TET8 gene (VIT_211s0037g01130), a senescence associated protein which is partially described in Wang et al., 2015 [153], investigated in Arabidopsis and presumably characterized by a promoter regions containing defense and pathogen response elements. The cited research work suggested a function for TET8 in the defense response, describing an up-regulation upon pathogen treatment and all the putative regulatory elements involved.

Screening our results, we focused the attention on the strict QTL region detected in 2016, which coincided with an already discovered resistance locus, known as *Rpv11*. The associated marker in our study was VMC3b9 which is co-located with VVMD27 confirming the correspondence to *Rpv11* locus found in the susceptible 'Chardonnay' ([66] and in Regent hybrid [70,137]. In correspondence to the linked marker, we found the VIT_205s0020g02760 gene, which encodes for a signal peptidase complex subunit 3b (SPCS3) but the specific role is still unknown. According to Salmaso et al., 2008 [60], this locus was close related to a gene encoding a Ca²⁺-binding protein associated with the hypersensitive reaction.

Taking these considerations into account, we can assert that the presence, in the interval of confidence of detected QTLs, of interesting genes, mostly related to defense responses, could describe the tolerant phenotype of 'Mgaloblishvili N'. However, the lack of repeatability suggests a low stability of these QTLs, presumably due to differences in other factors among the years. This question of stability often arises with complex traits resulting from different processes affected by environmental factors. Once the S1 individuals will be grown in the field additional evaluation may provide more stable results for the QTL analysis based on phenotypes of adult plants. Another way to take into account this variability is to further investigate the processes and decipher the component traits that mainly cause the variability. Physiological analysis could provide arguments for or against the role of the candidate genes (CGs), usually by measuring CG expression at the mRNA level (by quantitative RT-PCR) but it could be not sufficient evidence to validate a CG. If the CG is a member of a multigene family (e.g. stilbenes, MYBs, ERFs, WRKYs), expression analysis only provide an estimation of the collective expression of all members of the family unless specific probes of the gene of interest are designed carefully.

Supplementary data

Table S1 Marker list.

Marker	LG	Marker Type	Reverse (NCBI)	Forward (NCBI)	Reference
VMC16d4	5	SSR	GGTTAGGATGCATATAGAAGAAG	TAGAATACACAGGCCATATACAA	[54]
VMC16f3	7	SSR	ATATTAATGTTGCTCCTCCAC	CCAATAATGCAACACATCTT	[54]
VMC1a12	7	SSR	TTCTGTTTTGCCTATCTATCC	ATGTAATTACCGGTCATGAGTT	[154]
VMC1a2	7	SSR	AACATAAATGGCCACCAGGG	TAAAATGTAGGGCGGCCACC	[54]
VMC1c10	9	SSR	ACAAGCCTCCGCCACTCTC	CACAGCTGTCCAAGTCCCA	[154]
VMC1e8	8	SSR	GATCATAGCTTCAACGGCTTTT	CAGCGAGCTCTTGATTTATTGT	[154]
VMC1g7	3	SSR	AGCCCATAAAGGCCTTAAAAAC	GGGTCCACATAGGTAGGAGATT	[154]
VMC2a10	10	SSR	AAGAATTCACCGCCAATATC	GAAGACCCATGAAGTTGACCTG	[54]
VMC2a3	18	SSR	CTTGTGTAGAAGCTTACAGGT	ATTGAAACTCCGGAAGCTTAGG	[155]
VMC2b11	14	SSR	CCCCTCACCTGTTACCAA	AAGAAGGTGACACCAGCGGA	[54]
VMC2d9	9	SSR	TCAACCCTCGTCTTAGTC	TGAATTCGAATTGGGTCT	[54]
VMC2e7	3	SSR	ACTCTCAAGTTAAGCTCTTCCT	TCTTATTGAGTAAAGCAACAG	[54]
VMC2f10	6	SSR	ATCAGAGCTCCTCTTTCCTCC	AGATTCTCTGATGGTGTGGG	[54]
VMC2f12	8	SSR	TTCCAGAACACAGGCCACATAC	GGATTGGGCTCAGAAATAGGCT	[54]
VMC2h3	17	SSR	GACATCATGTATAAGATGAAGGCA	AACCCGTTAGAAGGAAAAGAAA	[54]
VMC2h4	12	SSR	TCTCTGGAACATCCAATCAAC	ACCAGGTGTGCCTATAAGAATC	[155]
VMC2h5	14	SSR	CATAACATGGGGTATGATGAAAA	TCATAACCTGCGTCTACTGCTT	[54]
VMC3a8	6	SSR	AAATGAAGCTGGAAAAGATAGAAA	ACCATGAGATCAAATTGGAACA	[54]
VMC3b8	12	SSR	CTCGTGTCTTCTGGGAACTC	CCGCTTCTCTTTGGCTTGTA	[54]
VMC3b9	5	SSR	ACCAGATCTGAATACATCCGTAAG	ATTCTCAATCTCCCTGCTCCT	[54]
VMC3c11	17	SSR	CAAAGCGTTTAGCCAAAACCTCA	GATGGATGCAACTCGAAAAAGA	[2]
VMC3c7	5	SSR	AATATTCAGAAAATTTGTGTC	AATTTGGCTAAGAAAAGGA	[54]
VMC3d7	10	SSR	TATTTTCAGTGACCACTCTTAC	GCACCATCTGCCATTATGATT	[54]
VMC3e12	11	SSR	TGTGGCAAGCATTGTCTATTCC	ATCAAAGGCCTAGGATTTACC	[54]
VMC3E5	18	SSR	CCAGGAGACTTGTCTTGTATT	GATTTGTCTTTACAAGGCGTTC	[156]
VMC3f12	6	SSR	ATGAAGCTGGAAAAGAATAGAA	GCTTTGAATGAACACTGTTATG	[54]
VMC3g9	1	SSR	CAAGCCACTAGTAGTCATCCCTT	GATCCTTTTTGGGAATCTCA	[54]
VMC4d9.2	15	SSR	GTTCAAATGTCATGGCCCGTAG	CTCAATGCCAATGGCTTCTTC	[157]
VMC4f8	1	SSR	CTGCCAGTATACTGATTCTCTC	CATTTTCATAGGGTTTTACAGC	[157]
VMC4h5	6	SSR	CAAGTGGAAAGCAATCTAGGAA	GATTTGTGACACTTGTGTAGCG	[54]
VMC5c1	9	SSR	AGATCTTCCACCAATGACTT	TTCCCTTATGGGTTAGGTTTC	[56]
VMC5c5	6	SSR	CCCAGCTCCTTAGCTCCTCAC	GGAAAGCAAAGCAGACCACAAC	[56]
VMC5e9	19	SSR	TCACAGCTTTCTCATTACCCTT	ATCCAGAGCCATAACAGATTCA	[54]
VMC5g8	15	SSR	CATCATTGCTTCCAAAAGTCTC	CATGCACATCTGTCTCACTCT	[54]
VMC5h5	7	SSR	ATGGCCTCCCTACAAAAGAAAC	TACTTGCCCAATGGGTAATGAC	[56]
VMC6b11	2	SSR	TTGCTTACCATCAAAAAGAAA	TGATTATGGCAATAATCACACC	[158]
VMC6d12	9	SSR	TCCTGCCGGCGATAACCAAGCTATG	ACCTGGCCGACTCCTTGTATGC	[158]
VMC6e10	5	SSR	CATTTGTGGGTAGTTGTGAGGA	CTAGGTGTGCCAAGAGATCAGA	[158]
VMC6g1	11	SSR	TCTGTCAATTGCTGTCCCTTCA	TGCATAGTCTGTAGGCCATTG	[54]

Marker	LG	Marker Type	Reverse (NCBI)	Forward (NCBI)	Reference
VMC6g8	8	SSR	CCCCTCATCTCTTCTATCTAA	GAGTGTCACTCTCAAATAAGGA	[158]
VMC7a4	7	SSR	AAACTCCAAAGCATCTGATTCT	TAAGGTGGATTAGTTTTGGGTC	[54]
VMC7g5	1	SSR	TTTCAGGGTTGTTGTCCTTCTG	CCCACCTTCATCTCACAGATTCA	[159]
VMC7h3	4	SSR	ACTAGAAAAATGCACAATCTCCC	TCAGATATTGAAGAACCACCA	[159]
VMC8a7	1	SSR	GTGGGAGCACTGTTGCTTTAG	GCAGCAACTCTTACACACCG	[54]
VMC8b5	18	SSR	GCCTTGATCTTCTTCTAAT	AAAGGAGACATCTGCATCAT	[53]
VMC8c2	2	SSR	TGAAGACATCTACGTAGGTGAA	AAGGAATTTGGATACTGAAGGT	[53]
VMC8d3	10	SSR	ATAGAGTCCTGCAAAATCCAAGA	TGGCAAGACACAATAAACAGA	[53]
VMC8f4	18	SSR	GAAGTTAGCGCAGATGAAAGAT	GCGTAAAGCATATTCAAGCATT	[2]
VMC9b5	5	SSR	CTGCCGTTTGGGTAAGATGCT	ATGCCCGAGAAGAGTCGAGAA	[54]
VMC9d3	1	SSR	TGCAAAGACTGTGAGATGAGGG	GATTTGAAAGTCGAAAGCCAGG	[54]
VMC9h4.2	13	SSR	CACATCATTATTGATGAGGCT	GCAGTTGATGCAAAACAACAGT	[54]
VMCNG1b9	18	SSR	AACCTGCATTCTCCCTTTG	TCATTCATGACATATGCCTGCC	
VMCNG1f1.1	4	SSR	GACTATATAAACCTCTCCCAA	GAGTACTGTACTTCTTCAGCCA	[56]
VMCNG1g1_1	14	SSR	TTTTCTCAATTCAGAGGTAC	ATGTTACATTTCCACCCTTT	
VMCNG2e1	4	SSR	TATGGAGGGAGACCGTTGTTTC	TTTGTGCTTCACTGTTGTTTC	
VVC19	1	SSR	GCGGCTGTTAAGGCTTT	TCAGAATCAGTCTCTTTAATCCTTT	[160]
VMC9f2	1	SSR	CAACCTGTTGATGAAAGGGAAA	AAACATGATCTGATGCAGGTGA	[54]
VVib01	2	SSR	TGGTGAGTGCAATGATAGTAGA	TGACCCTCGACCTTAAATCTT	
VVib09	17	SSR	CCTAAGAGCCATTCAAGATTAA	ATGTTTTGATTCTTAGGTGAC	
VVib19	11	SSR	GCATAAGGGCATTGTTGTAAT	TGGATGTTCTAAACCTTAAGT	
VVib23	2	SSR	TTTGTATTTGGGCATTTGCAG	GGTCACGTAGATATTGAAGTTG	
VVib66	8	SSR	TTGTATTGTGTCCTCTTCTCA	CCACTAGTGGTCAGAAAAGAAG	
VVic72	1	SSR	GGACAAGGAGTTAGATATGAAC	GTATTGTGTAAGCATTGTGTGG	
VVih54	13	SSR	CAAACCGTTTTACACCAGCAG	CCGCACTTGTGTTGAATTCAG	
VVII52	5	SSR	CTTGATCTTTAGTTGCAGTCTG	AGATTTAGAGACGAAAAAGGGT	
VVIm07	8	SSR	TTATTACATGGATAGGCACTCA	TGGTGTCAACATTCCTTACAAG	
VVIm25	1	SSR	GAGAGTGATGTGGGATTTGTTA	TGTTTTAACAGAAGCCTACACG	
VVIm42b	15	SSR	ACACAAATATGCATACACACGC	CCCTCAAGACCTTAAAATTGT	
VVIn16	18	SSR	AAGGGAGTGTGACTGATATTTT	ACCTCTATAAGATCCTAACCTG	
VVIn31	6	SSR	GGATAGAATCACATTTGTAGCG	GTTGAATAGTGTCCATGTTGTG	
VVIn33	5	SSR	ATTTTGATCCACCTAACTCTG	TGCCAAAGCAAGTATCAACATG	
VVIn54	3	SSR	TCTTTATGAAGGTATTGAGCTG	CCATAAATCCAACACAACACTT	
VVIn61	1	SSR	ATGAGTACCTTCAAAATGACA	ATAATAGATGACGCCAAAGCAA	
VVIn73	17	SSR	AATACATAAGGTGAAGATGCCT	TACTTCACCTAACAATACAGCT	
VVIn78	10	SSR	ACTGAGTATGGTGAATTTGAT	TAAAGGACCATCTCAATGTTT	
VVIn94	14	SSR	TCTTTAGTAGTGCTTCAACTCG	CTGATCTCAGTGCATATGTTGA	
VVio55	2	SSR	GATCAAATGCATATGCTAACCG	CCGTATTGGACAAAAATTAACC	
VVIp02	11	SSR	TCGAGTTGAAAGAAAATTGCCA	CATTAAGTTAAGGCAACCACA	
VVIp10	13	SSR	TGCCTTGACATTGTTTTATCC	GAAACTGGGCTGTTATTGTTGA	
VVIp37	4	SSR	GTATGTTTCAATGCTCCTAAGC	AGGACCAAGTGAAGGCTTATA	
VViq52	9	SSR	ACAGGAAAGTGTCAATGGTTA	TAAAAGGATGGTATGACAGA	

Marker	LG	Marker Type	Reverse (NCBI)	Forward (NCBI)
VViq57	1	SSR	TATGCCCTGTACTATCTATGA	TGAACCTCTATCTTCCATGTAG
VVir46	4	SSR	TGAAATCGACTGCAGCATCTTG	ATTTAATCCAGTGGTGGTAGC
VVis21	1	SSR	CCAAGGATGGTGAATGGAATT	CCACATGGTCTTACTCAACTAA
VVis58	7	SSR	ATATTCTACTACTTCTCCGG	GATTTTCAATTTTGGTCTGGC
VVIt60	1	SSR	TATTATGCCTATCCAGTTTCGA	AACTTGATTGAACAAAGGCCTA
VVIt68	5	SSR	GGGTTGTTTCGTGTATTGTATG	GTGAATGAACAAAGTGGGAAAG
VVlv08	17	SSR	AGAAAAGAAAGTCCAGGTATGA	AAATTAACAATGGGCAAAGCTC
VVlv15_2	8	SSR	GGGGGCAAAAATGTGTGATTAT	AAACCATAGTTCATCCAAAACC
VVlv33	19	SSR	TGGGTGTTCTTGCTACTATAAT	AAAGAAAACGAGTTTGAAGGC
VVMD17	18	SSR	CACACATATCATACCACACGG	TGACTCGCCAAAATCTGACG
VVMD25	11	SSR	TTGGATTTGAAATTTATTGAGGGG	TTCCGTTAAAGCAAAAAGAAAAGG
VVMD28	3	SSR	TCATCAATTTTCGTATCTCTATTTGCTG	AACAATTCATGAAAAGAGAGAGAGA
VVMD31	13	SSR	CTTCTCAATGATATCTAAAACCATG	ACAATTGAAAACCGCGTGGAG
VVMD32	4	SSR	GGAAAGATGGGATGACTCGC	TATGATTTTTTGGGGGGTGGAG
VVS1	13	SSR	CTTCTCAATGATATCTAAAACCATG	ACAATTGAAAACCGCGTGGAG
VVS2	11	SSR	AAATTCAAAATTCTAATCAACTGG	CAGCCCGTAAATGTATCCATC
VVS29	1	SSR	TGCAAAGCAAATAAAGCTTCCA	CCCCAAGGCTCTGAAAACAAT
VVS4	8	SSR	CCCACCTTGCCCTTAGATGTTA	CCATCAGTGATAAAACCTAATGCC
VrZAG112	14	SSR	TGGCTCCATACTGCTTCACGTAGGC	CGTTTTAAAGCCAGCTGAATCTGGG
VrZAG62	7	SSR	CCATGTCTCTCCTCAGCTTCTCAGC	GGTGAAATGGGCACCGAACACACGC
VrZAG79	5	SSR	TGCCCCATTTTCAAATCCCTTCC	AGATTGTGGAGGAGGGAACAAACCG
VrZAG83	4	SSR	ACGCAACGGCTAGTAAATACAACGG	GGCGGAGGCGGTAGATGAGAGGGCG
SC8_0091_083	16	SSR	TGGCTTTTGACCTACTTGGGA	CAGTGTGGATAGAGGCAGGA
SC8_0114_030	7	SSR	AACCAACAAAACAAAACCTCGT	ATAGGAAAAGCCAATCAAGAAAA
SCU14	16	SSR	TGTTATATGATCCTCCCTCCTC	CTGCACTTGAATACGAGCAGGTC
UDV009	16	SSR	GGGTTAATCCTCCATTTTCC	CTCTCTAGTAAATCCATAACAATGGTG
UDV023	19	SSR	GAATCCGCACCTGAAGCATT	AATTTGGGAAAACAACTATACATACA
UDV027	2	SSR	CACGAAGTGCTTTTCTCCTC	TGGCAACACCCACAGAAATG
UDV032	16	SSR	CATGGCATGTGCTTTGTTAT	CATGCGTATGTGTTAGAGAGCA
UDV033	14	SSR	TCTGCATAAGGGGTGATTAAGA	TTGTCCGTTTTAGCTCAATG
UDV041	5	SSR	TGGGATCTCTTTCCACATCA	AAGATCCCTCCACCCAAAAA
UDV053	5	SSR	GGGAGAAAAAGGCATGGATA	GTTGGTGGCTTTCTTTTTGC
UDV060	5	SSR	TGGGGTAAAACCTGGGTGTTT	CCTGCCACACCACAATACAA
UDV106	5	SSR	CCATGATGGGGAAGAGAAA	CCCAGAAAAAGGGGTATGC
UDV108	18	SSR	CCTTTTTATATGTGGTGGAGCA	TGTAGGGTTCCAAAGTTCAGG
UDV124	13	SSR	AGTGCATTTGTCAAAGTCGTG	GCATCTTCTTCTCCCAACC
UDV125	8	SSR	TTCAGCTATGCACCGAGGTA	GGCACTCTAGATGATTTGTCC
UDV129	13	SSR	TTTCTAGATGCTGACTTCTCAAGTG	AAGCTAAGGTCTTATGGCATCTG
UDV130	18	SSR	TGTATGCTTATTTGATGTAAGGGAAA	TCCATATAGCGAAACAAAAATAACC
UDV345	14	SSR	CCATTTGAGAGGAGGGATCA	TTGTCCAATATTAGCTCCTACGG
UDV370	14	SSR	CAGAAAGCCCTGATCTCCTG	TGGTTGAGCACAGTCTTGG
UDV737	18	SSR	TCCTGCAGCTGTTGACGATA	TTTGCATGCGATACCTGAAG

Marker	LG	Marker Type	Reverse (NCBI)	Forward (NCBI)	EcoR1 tail
VChr10a	10	SSR	TTTGTTCGGAAGTACTCTTCTTCA	AAATGTTTAGTAGCCTCATTGTTT	
VChr13a	13	SSR	TCGTCTATATGCGACCTTGG	TGGCAGAGCAAATGAATCAA	
VChr13c	13	SSR	AACACCGTTAGGCATACTCCA	GACTGCGTACGAATTTAGACCCAAGGGCAAGTACT	GACTGCGTACGAATTC
VChr18a	18	SSR	CATCCAAACATCAGCTGAG	TTCCACCCGGTAAATATGA	
VChr19_11b	19	SSR	GGTATCAAAGAAGACCGTGTG	GACTGCGTACGAATTTCTTAGTGCTACTCCACATGCACC	GACTGCGTACGAATTC
VChr19_16b	19	SSR	TGGGTGGAGTTTGAATTTGAAC	GACTGCGTACGAATTTCTGCTCTCATATCCAACAACCTTATG	GACTGCGTACGAATTC
VChr19a	19	SSR	CGAGGATACCAACAAGAATGAA	TGGATTACCATTGCTCTCA	
VChr7a	7	SSR	ATTAGGGCACTGCCTCTTCC	TCCGTGTCACAAAGAACATGA	
GF01_16	1	SSR	GCTGTTCCCTTGGACAACTCAT	GACTGCGTACGAATTTCTCAGGCTATGCAGGATGGAA	GACTGCGTACGAATTC
GF01_17	1	SSR	CCCATTCCCTTGTCTATTCTTCAG	GACTGCGTACGAATTTCTAAGATTGTGGTGGGCAAGATT	GACTGCGTACGAATTC
GF01_25	1	SSR	CGGGAAAAATGGAAGAACTAGA	GACTGCGTACGAATTTCTAACTGCACCTCTCTGGAATCA	GACTGCGTACGAATTC
GF01_26	1	SSR	AATGTATGGACCCAACTTCACC	GACTGCGTACGAATTTCTGTGTGCAGGAGTAAATCACGAG	GACTGCGTACGAATTC
GF01_27	1	SSR	TTTTCAGTCCCTCCAATTCAC	GACTGCGTACGAATTTCTACGTTCAGGTAGTGAGCTTGT	GACTGCGTACGAATTC
GF02_20	2	SSR	GTGGGATGATGACAAACCTCTT	GACTGCGTACGAATTTCTACGATATGTTCCCAAGACAC	GACTGCGTACGAATTC
GF02_27	2	SSR	AAGTTCCAGGGGCTCTATC	GACTGCGTACGAATTTCTGCAGGTGAGAATGAAAATCC	GACTGCGTACGAATTC
GF02_29	2	SSR	GTGAGAAAATGGAGAGAGTGGG	GACTGCGTACGAATTTCTCAAAGAAAGGAGAAAGGAGCA	GACTGCGTACGAATTC
GF03_04	3	SSR	CAATGGGTGGGACATCAA	GACTGCGTACGAATTTCTAATGAGTTGTGGATGCGTG	GACTGCGTACGAATTC
GF03_05	3	SSR	AAGGTGCCAAACCACATAAATC	GACTGCGTACGAATTTCTGCAATAAGCTCCCCTACTT	GACTGCGTACGAATTC
GF04_03	4	SSR	GTAACTAACCAAGCAGCCACC	GACTGCGTACGAATTTCTCAAATATCCAAGAGGCTTCA	GACTGCGTACGAATTC
GF04_16	4	SSR	GAATGCTAGAAGAGAGATTGTTGAG	GACTGCGTACGAATTTCTCGGTGGGTGTATAGGTTTTGTA	GACTGCGTACGAATTC
GF05_11	5	SSR	CCGTGACCACCTTCTTCTAC	GACTGCGTACGAATTTCTGTAACACATGCCGGAACAATA	GACTGCGTACGAATTC
GF05_16	5	SSR	ACCACCCAGTTTGTATCTCC	GACTGCGTACGAATTTCTGAGAAAGGGCTAGGGTTATGA	GACTGCGTACGAATTC
GF06_08	6	SSR	AAGATTTTGTAAAGCAGCAGCG	GACTGCGTACGAATTTCTGGGACGACACTTTGATTTAGCA	GACTGCGTACGAATTC
GF06_12	6	SSR	CATTTACACAACCCACAAAAC	GACTGCGTACGAATTTCTCTCTGCTTAATTGGGCTTA	GACTGCGTACGAATTC
GF07_02	7	SSR	TTTTTTTTCTGGAGGGTCTTG	GACTGCGTACGAATTTCTCAGCATCAAATCAAAGTCCAC	GACTGCGTACGAATTC
GF07_09	7	SSR	TGTTAGGAGATCAATGTGGACAAG	GACTGCGTACGAATTTCTCAGATTAGGCTGTTGGT	GACTGCGTACGAATTC
GF07_10	7	SSR	GGTCTCTCACACATTCTGCCT	GACTGCGTACGAATTTCTCACTGTCTTCTCCATTTGCTG	GACTGCGTACGAATTC
GF07_11	7	SSR	CCAAGGAAGTGAAGTGCAAACT	GACTGCGTACGAATTTCTAAGCCATCTTCCAAGGTTTTG	GACTGCGTACGAATTC
GF07_13	7	SSR	ACTCACTCTCCACAGTCCCA	GACTGCGTACGAATTTCTAAGGGTTTTGGCTTCACTTC	GACTGCGTACGAATTC
GF07_14	7	SSR	GAAGTTCCCTTGTTCACATC	GACTGCGTACGAATTTCTCTTGTATGGAGATGGTTTTCA	GACTGCGTACGAATTC
GF08_01	8	SSR	TGTGACCATAAACAAGCAGTCA	GACTGCGTACGAATTTCTGTAACCAGGAAAAATGGCTTC	GACTGCGTACGAATTC
GF08_02	8	SSR	CGATTCTCTCACTCCCTCATCT	GACTGCGTACGAATTTCTAGTAGTGTTGTTTTGTGGGGAC	GACTGCGTACGAATTC
GF08_07	8	SSR	TTGGCCTCTCTACACCTTTTC	GACTGCGTACGAATTTCTCGATGAGTGATACTGCTCAAGA	GACTGCGTACGAATTC
GF09_44	9	SSR	GCTAATGGAGGGTAGTGCTCAA	CATCGTTCTTCTTACTCGCT	
GF09_46	9	SSR	ATCCACGTTTGTAGCCTTTTGT	GAGAGATTTGAGGGATTGTTGG	
GF09_47	9	SSR	CTGTTGTAAGGGCTCCCAATTA	CCACATTCTCTGCACATAAA	
GF09_55	9	SSR	CAGGTTCAAGTTAGCAGGTGAT	ACTCTGTGATTTTAGGGACGA	
GF10_05	10	SSR	AAGGAGGTGGTTACTTGTCCA	GACTGCGTACGAATTTCTATCTAGTGGTCTGCTTGTGA	GACTGCGTACGAATTC
GF11_09	11	SSR	GAATAAGCGAGGCACAGGAG	GACTGCGTACGAATTTCTGACTTGTGAGCACATCCAT	GACTGCGTACGAATTC
GF11_10	11	SSR	TGGTTGTTCTTTTGGCAAGG	GACTGCGTACGAATTTCTTGGTATGGCCAGTAAAGTACC	GACTGCGTACGAATTC
GF12_01	12	SSR	TAGAAACAAGAGGATGGTTGCC	GACTGCGTACGAATTTCTGAGATTTTCAAGTCCGTTCACT	GACTGCGTACGAATTC
GF12_03	12	SSR	GTTTCAATTTACTACCGACGC	GACTGCGTACGAATTTCTATGTTATATGGCTTTCATGGC	GACTGCGTACGAATTC

Marker	LG	Marker Type	Reverse (NCBI)	Forward (NCBI)	EcoR1 tail
GF12_05	12	SSR	CAAACACTCTCAGCCCCAAATG	GACTGCGTACGAATCTAGAAGCAAATGACAAGATGGGA	GACTGCGTACGAATTCT
GF14_05	14	SSR	AGAAAGCAAACGGATCTTCATC	GACTGCGTACGAATCTTGAATTATCTTGGAGGTGGAGG	GACTGCGTACGAATTCT
GF15_02	15	SSR	TGCCTTTGGAGATATGATTGC	GACTGCGTACGAATCTTATCCCAGCGGATATGGTCT	GACTGCGTACGAATTCT
GF15_04	15	SSR	TGATCTTTCCCATTTCTCTCT	GACTGCGTACGAATCTGATGAGGCACAGAAGTTGAAAC	GACTGCGTACGAATTCT
GF16_01	16	SSR	GTTTGGATAAGGGCAAAAAGACA	GACTGCGTACGAATCTCTCTGAGGTGTTGATCCTTC	GACTGCGTACGAATTCT
GF16_12	16	SSR	ATTGTAATTTGCTCACGATCCC	GACTGCGTACGAATCTACAGAGAGGAGGAGACACAAGC	GACTGCGTACGAATTCT
GF16_14	16	SSR	CATTTCCAAAGTTGTAGCCCTC	GACTGCGTACGAATCTCTCTTTCATGGATTGTCGGAT	GACTGCGTACGAATTCT
GF16_18	16	SSR	TATGCTTATGTGGATTGATGGG	GACTGCGTACGAATCTGAGAAACAGAGAGAATTGCACCT	GACTGCGTACGAATTCT
GF16_22	16	SSR	CCAGTGAGTCGAAGAAGAAAGG	GACTGCGTACGAATCTTACCAAATACCCCAAACCTCG	GACTGCGTACGAATTCT
GF17_03	17	SSR	GCTCCAAATACCACCTCTGTTC	GACTGCGTACGAATCTCTTCCATTTACCCAAGATCCAC	GACTGCGTACGAATTCT
Chr2_3886371	2	SNP	ATTTATCGGCCCGCTGTTTG	GATGGCAACAGGACATCCGAAAC	
Chr3_7176103	3	SNP	TGTTCCATCCACCATAGTGTGCCA	TTGCAGGTCCTTTCCACCAC	
Chr4_2193574	4	SNP	TGTTGTGAGACTGCCTGCATT	TTTCTCGGGTTTTGGTCGGT	
Chr4_4368933	4	SNP	ATAAGCTGATCCGCAGCCAAT	CCACTGTCACCTCATGGCTTGCTTA	
Chr6_12372050	6	SNP	TCATGCCTTGCTTTTAGGGCATAA	TTATAGGGCCACGACGGGTA	
Chr8_9930503	8	SNP	GCGACAATTCAGCACCAAGT	AGCTTGCGTTTGACCTACAT	
Chr9_13882272	9	SNP	GACGACATGACTCCTAGCTACC	ATACACCCGACGCAATCCAG	
Chr11_12294387	11	SNP	TGATCGTATAAGCGCAGTCAA	GTCATGGATCGTACCCCGTC	
Chr12_2651137	12	SNP	TTAATGCGCTGTGCTGGAGT	AATGGCGAACCTTGATGC	
Chr13_249161	13	SNP	CCACTCCTACGACTACCCAAC	CTACAGCGTGGTAGGAGCAC	
Chr13_8147990	13	SNP	CCATGTCAACCCCCACTCA	AGCAAACAATAGGTAGTCAACTCTT	
Chr18_12802198	18	SNP	CCCTATTGAGTGAGCTCGCAG	CCTCATGGTCTCCGTTTCCA	
Chr19_17118565	19	SNP	AGACCACAGAAGTGGAGCAT	TTCTAAGGTGGCTACCGTGC	
					Segregation
VVlv61	12	SSR	GGTTGGAGTTTTGGATTAATGG	ACAACCAACTGTAATTTCCCTA	3:1
GF02_21	2	SSR	CCAATAGGTTGAGGTGACAGGT	TTGAAGTGGGTAGGAACCCTTA	3:1
GF15_06	15	SSR	TGAAGGTCTCATACCCAAGA	GGTTAGGTTTTCTTATGGCTTTC	3:1

Table S2 List of Candidate genes included in QTL ranges.

Chr	Gene Id	Position-Start	Position-End	Name	Function
1	VIT_201s0011g03410	3083936	3093070	RAD23C	dna repair protein rad23-3 uv excision repair protein
1	VIT_201s0011g03450	3127695	3132325	XYL1	alpha-xylosidase precursor
1	VIT_201s0011g03470	3142869	3144296	VIT_201s0011g03470	ethylene-responsive transcription factor erf118
1	VIT_201s0011g03480	3147199	3149521	VIT_201s0011g03480	cinnamoyl- reductase
1	VIT_201s0011g03500	3174924	3179566	HMT-1	homocysteine s-methyltransferase 1
1	VIT_201s0011g03510	3179738	3185931	VIT_201s0011g03510	uncharacterized protein loc100242187 isoform 1
1	VIT_201s0011g03520	3190297	3193411	VIT_201s0011g03520	zinc finger protein constans-like 16
1	VIT_201s0011g03530	3204575	3205775	LBD41	lob domain-containing protein 41
1	VIT_201s0011g03560	3223281	3227712	VIT_201s0011g03560	fiber protein fb34
1	VIT_201s0011g03590	3246546	3249752	RPL15	hypothetical protein plastid ribosomal protein cl15
1	VIT_201s0011g03600	3252820	3255824	JAG	hypothetical protein
1	VIT_201s0011g03610	3265384	3270534	VIT_201s0011g03610	ist1 homolog
1	VIT_201s0011g03620	3270835	3278161	VIT_201s0011g03620	monoglyceride lipase
1	VIT_201s0011g03630	3281798	3283951	VIT_201s0011g03630	pentatricopeptide repeat-containing protein
1	VIT_201s0011g03640	3309093	3310130	IPT1	adenylate isopentenyltransferase
1	VIT_201s0011g03670	3329551	3333174	ENDO	nuclease s1
1	VIT_201s0011g03700	3341247	3358054	VIT_201s0011g03700	thioesterase-like protein
1	VIT_201s0011g03720	3368571	3370294	VIT_201s0011g03720	dna binding
1	VIT_201s0011g03730	3374934	3376616	MYB62	myb transcription factor
1	VIT_201s0011g03740	3380001	3395799	OVA9	glutaminyl-trna synthetase
1	VIT_201s0011g03750	3396142	3401075	DIN9	mannose-6-phosphate isomerase
1	VIT_201s0011g03790	3429615	3441498	ARG1	hypothetical protein
1	VIT_201s0011g03820	3450634	3473703	BTS	zinc finger zinc finger protein
1	VIT_201s0011g03830	3485637	3513238	VIT_201s0011g03830	beta-lactamase-like protein
1	VIT_201s0011g03860	3522624	3526069	VIT_201s0011g03860	probable leucine-rich repeat receptor-like protein kinase at1g68400-like
1	VIT_201s0011g03870	3530914	3547783	STE1	delta -sterol-c5 -desaturase
1	VIT_201s0011g03890	3548907	3552245	VIT_201s0011g03890	probable receptor-like protein kinase at1g67000-like
1	VIT_201s0011g03910	3564739	3570289	VIT_201s0011g03910	protein phosphatase 2c 15
1	VIT_201s0011g03920	3578051	3585576	NDT2	hypothetical protein
7	VIT_207s0031g00020	16284151	16291841	PEN2	phosphatidylinositol- -trisphosphate 3-phosphatase phosphatidylinositol- -trisphosphate 3-phosphatase and dual-specificity protein phosphatase
7	VIT_207s0031g00030	16291986	16295752	ATRER1A	protein rer1a-like
7	VIT_207s0031g00050	16300215	16303313	CP1	cysteine proteinase
7	VIT_207s0031g00060	16305457	16313032	IRX14-L	probable beta- -xylosyltransferase irx14h-like
7	VIT_207s0031g00080	16322146	16325192	WRKY7	wrky transcription factor

Chr	Gene Id	Position-Start	Position-End	Name	Function
7	VIT_207s0031g00090	16327674	16331470	VIT_207s0031g00090	trna-dihydrouridine synthase 1-like
7	VIT_207s0031g00100	16332009	16337077	VIT_207s0031g00100	2-oxoglutarate-fe -dependent oxygenase domain-containing protein
7	VIT_207s0031g00110	16337941	16339123	VIT_207s0031g00110	duf579 protein
7	VIT_207s0031g00120	16342012	16345722	VIT_207s0031g00120	probable inactive receptor kinase at5g67200-like
7	VIT_207s0031g00130	16346440	16362558	FRA1	kinesin-like protein
7	VIT_207s0031g00160	16377781	16385352	SCE1	ubiquitin-conjugating enzyme e2 i
7	VIT_207s0031g00180	16393823	16401210	VIT_207s0031g00180	rna recognition motif-containing protein
7	VIT_207s0031g00190	16404262	16405010	DEAR3	ap2 erf domain-containing transcription factor
7	VIT_207s0031g00200	16403734	16412174	LEJ2	hypothetical protein
7	VIT_207s0031g00210	16419354	16426743	PAB4	polyadenylate-binding protein 2-like
7	VIT_207s0031g00220	16436291	16441439	AP2	transcription factor apetala2
7	VIT_207s0031g00230	16447464	16459520	VIT_207s0031g00230	e3 ubiquitin-protein ligase march6
7	VIT_207s0031g00240	16459785	16470038	VIT_207s0031g00240	sec-c motif-containing protein otu-like cysteine protease family protein
7	VIT_207s0031g00250	16473725	16480589	VIT_207s0031g00250	filament-like plant protein 7-like
7	VIT_207s0031g00265	16492156	16493481	VIT_207s0031g00265	uncharacterized acetyltransferase at3g50280-like
7	VIT_207s0031g00270	16497684	16499285	VIT_207s0031g00270	uncharacterized acetyltransferase at3g50280
7	VIT_207s0031g00290	16527989	16528519	VIT_207s0031g00290	low quality protein: uncharacterized acetyltransferase at3g50280-like
7	VIT_207s0031g00320	16560116	16572925	CLF	polycomb protein ez1 set domain protein
7	VIT_207s0031g00330	16573066	16579178	VIT_207s0031g00330	pi-plc x domain-containing protein at5g67130-like
7	VIT_207s0031g00350	16584122	16586040	CCoAOMT1	caffeoyl- o-methyltransferase
7	VIT_207s0031g00355	16589850	16590740	ZFP1	hypothetical protein
7	VIT_207s0031g00370	16601231	16602190	VIT_207s0031g00370	zinc finger protein
7	VIT_207s0031g00390	16615612	16618016	VIT_207s0031g00390	zinc finger protein
7	VIT_207s0031g00420	16641499	16644428	VIT_207s0031g00420	ap2 erf domain-containing transcription factor
7	VIT_207s0031g00440	16651426	16652337	VIT_207s0031g00440	ring finger protein
7	VIT_207s0031g00450	16661056	16668170	SPT	transcription factor spatula
7	VIT_207s0031g00460	16671213	16682251	NAPRT1	nicotinate phosphoribosyltransferase-like
7	VIT_207s0031g00470	16682264	16697746	ICU2	dna polymerase alpha catalytic subunit
7	VIT_207s0031g00480	16701290	16704781	VIT_207s0031g00480	probable serine threonine-protein kinase at1g01540-like
7	VIT_207s0031g00490	16706169	16710850	VIT_207s0031g00490	pi-plc x domain-containing protein at5g67130-like
7	VIT_207s0031g00500	16714870	16717234	VIT_207s0031g00500	subtilisin-like protease
7	VIT_207s0031g00530	16722078	16724988	MAPKKK21	protein kinase-like protein
7	VIT_207s0031g00540	16732792	16733452	RALFL34	pinus taeda anonymous locus umn_2818_01 genomic sequence
7	VIT_207s0031g00570	16762703	16769227	VIT_207s0031g00570	hypothetical protein
7	VIT_207s0031g00600	16779953	16789867	VIT_207s0031g00600	rna recognition motif-containing protein
7	VIT_207s0031g00620	16795707	16804559	ABA1	zeaxanthin epoxidase
7	VIT_207s0031g00640	16814007	16820827	VIT_207s0031g00640	splicing arginine serine-rich 16
7	VIT_207s0031g00670	16842156	16845526	HSF4	heat shock transcription factor hsf4

Chr	Gene Id	Position-Start	Position-End	Name	Function
7	VIT_207s0031g00680	16847884	16851987	ACD2	red chlorophyll catabolite reductase
7	VIT_207s0031g00690	16852540	16859877	CYP707A4	cytochrome p450
7	VIT_207s0031g00700	16861134	16865866	CEN2	caltractin probable calcium-binding protein cml20-like
7	VIT_207s0031g00705	16873484	16874098	RRTF1	ethylene-responsive transcription factor
7	VIT_207s0031g00710	16884671	16885274	VIT_207s0031g00710	ethylene-responsive transcription factor erf109-like
7	VIT_207s0031g00740	16903658	16910483	VIT_207s0031g00740	atp-dependent rna helicase eif4a uncharacterized protein
7	VIT_207s0031g00750	16911064	16912860	ZF14	multidrug resistance
7	VIT_207s0031g00800	16937917	16940719	ICK5 VIT_207s0031g00800	cyclin dependent kinase inhibitor cyclin-dependent kinase inhibitor 1-like
7	VIT_207s0031g00820	16954012	16965191	MAP1D	methionine aminopeptidase
7	VIT_207s0031g00830	16967047	16973204	PLP1	pentatricopeptide repeat-containing protein at5g39350-like
7	VIT_207s0031g00850	16983828	17004882	PLP1 PLP4	patatin group a-3-like
7	VIT_207s0031g00870	17010043	17012309	PLP4	patatin group a-3-like
7	VIT_207s0031g00880	17025677	17030666	VIT_207s0031g00880	hypothetical protein nodulation protein h-like
7	VIT_207s0031g00920	17118167	17121680	MIPS2	myo-inositol-1-phosphate synthase
7	VIT_207s0031g00935	17128135	17129591	J20	chaperone protein dnaj
7	VIT_207s0031g00940	17132297	17137173	SULTR2;1	sulfate bicarbonate oxalate exchanger and transporter sat-1
7	VIT_207s0031g00970	17141445	17147615	AAT	bifunctional aspartate aminotransferase and glutamate aspartate-prephenate aminotransferase-like
7	VIT_207s0031g00980	17147616	17153536	AAT	aspartate aminotransferase
7	VIT_207s0031g00990	17157012	17159503	VIT_207s0031g00990	trafficking protein particle complex subunit 12-like
7	VIT_207s0031g01010	17178395	17181000	VIT_207s0031g01010	l-ascorbate oxidase
7	VIT_207s0031g01020	17182187	17183419	VIT_207s0031g01020	trafficking protein particle complex subunit 12-like
7	VIT_207s0031g01040	17191409	17193934	VIT_207s0031g01040	l-ascorbate oxidase
7	VIT_207s0031g01050	17201766	17204233	VIT_207s0031g01050	l-ascorbate oxidase
7	VIT_207s0031g01070	17207679	17213443	VIT_207s0031g01070	l-ascorbate oxidase
7	VIT_207s0031g01110	17231237	17231536	VIT_207s0031g01110	microtubule-associated protein spiral2-like
7	VIT_207s0031g01120	17242787	17247545	VIT_207s0031g01120	l-ascorbate oxidase
7	VIT_207s0031g01130	17247705	17250988	VIT_207s0031g01130	l-ascorbate oxidase
7	VIT_207s0031g01140	17253879	17256958	AGL104	mads-box family protein
7	VIT_207s0031g01150	17258744	17262219	FKBP16-2	fkbp-type peptidyl-prolyl cis-trans isomerase 4
7	VIT_207s0031g01170	17268568	17274871	VIT_207s0031g01170	aspartic proteinase-like protein 1-like
7	VIT_207s0031g01180	17275590	17288152	VIT_207s0031g01180	u-box domain-containing protein
7	VIT_207s0031g01200	17301599	17310364	VIT_207s0031g01200	probable ribosome biogenesis protein c16orf42 homolog rna polymerase i inhibitor protein
7	VIT_207s0031g01210	17311219	17317410	VIT_207s0031g01210	apoptotic chromatin condensation inducer in the nucleus
7	VIT_207s0031g01230	17320551	17323276	VIT_207s0031g01230	60s ribosomal protein l30
7	VIT_207s0031g01240	17324327	17330470	VIT_207s0031g01240	enth vhs family protein
7	VIT_207s0031g01250	17330690	17335040	VIT_207s0031g01250	short-chain dehydrogenase reductase family protein
7	VIT_207s0031g01270	17354201	17354899	RHA2A	hypothetical protein

Chr	Gene Id	Position-Start	Position-End	Name	Function
7	VIT_207s0031g01280	17366924	17376378	VIT_207s0031g01280	ring fyve phd zinc finger-containing protein
7	VIT_207s0031g01290	17383381	17392418	VIT_207s0031g01290	rna recognition motif-containing protein
7	VIT_207s0031g01320	17404970	17410595	TGA1	transcription factor tga1
7	VIT_207s0031g01330	17411549	17416381	AGT2	alanine--glyoxylate aminotransferase 2 homolog mitochondrial-like
7	VIT_207s0031g01340	17419917	17423981	VIT_207s0031g01340	pentatricopeptide repeat-containing protein
7	VIT_207s0031g01350	17424818	17437432	VIT_207s0031g01350	uncharacterized protein
7	VIT_207s0031g01360	17437626	17441311	EMB2453	pentatricopeptide repeat-containing protein
7	VIT_207s0031g01370	17453387	17454868	TT7	cytochrome p450
7	VIT_207s0031g01380	17459733	17461911	FAH1	cytochrome p450
7	VIT_207s0031g01390	17462624	17464829	CYP71B10	cytochrome p450
7	VIT_207s0031g01400	17472581	17475171	VIT_207s0031g01400	pentatricopeptide repeat-containing protein
7	VIT_207s0031g01410	17481726	17491508	SERK2	somatic embryogenesis receptor-like kinase
7	VIT_207s0031g01420	17492149	17517419	ATH13	uncharacterized protein sll1770-like
7	VIT_207s0031g01440	17531580	17539919	VIT_207s0031g01440	inactive receptor kinase
7	VIT_207s0031g01460	17548513	17549512	NF-YB3	heading date 5
7	VIT_207s0031g01480	17557907	17566200	VIT_207s0031g01480	atp gtp binding protein
7	VIT_207s0031g01490	17576144	17593660	RKP	ubiquitination-promoting complex protein 1
7	VIT_207s0031g01530	17627159	17630127	SEP2	stress enhanced protein 2
7	VIT_207s0031g01540	17631519	17644754	DPE1	4-alpha- chloroplastic amyloplastic-like
7	VIT_207s0031g01570	17663976	17665760	CYP78A7	cytochrome p450
7	VIT_207s0031g01580	17680388	7684205	SKIP6	f-box kelch-repeat protein skip6-like
7	VIT_207s0031g01600	17686749	17692495	SK1	shikimate kinase
7	VIT_207s0031g01605	17697925	17701696	VIT_207s0031g01605	pentatricopeptide repeat-containing protein
7	VIT_207s0031g01610	17704312	17706001	VIT_207s0031g01610	programmed cell death protein 2-like
7	VIT_207s0031g01620	17713513	17725756	VIT_207s0031g01620	developmentally-regulated gtp-binding protein 1
7	VIT_207s0031g01630	17729834	17733182	VIT_207s0031g01630	uncharacterized protein
7	VIT_207s0031g01640	17739395	17745600	GCN5	abc transporter family protein
7	VIT_207s0031g01650	17746843	17752646	VIT_207s0031g01650	programmed cell death protein 2-like
7	VIT_207s0031g01660	17757615	17760864	CYP96A10	cytochrome p450
7	VIT_207s0031g01670	17764334	17769272	CYP96A10	cytochrome p450
7	VIT_207s0031g01680	17778943	17780654	CYP96A10	cytochrome p450
7	VIT_207s0031g01700	17787029	17793311	LIP1	ras-related small gtp-binding family protein
7	VIT_207s0031g01710	17794258	17797278	WRKY51	probable wrky transcription factor 51-like wrky transcription factor
7	VIT_207s0031g01720	17810461	17812804	RABG3A	ras-related protein rab7
7	VIT_207s0031g01730	17816006	17819548	CPISCA	iron-sulfur assembly protein
7	VIT_207s0031g01740	17820573	17829782	MGP1	atp synthase
7	VIT_207s0031g01770	17855309	17858491	VIT_207s0031g01770	violaxanthin de-epoxidase-related protein
7	VIT_207s0031g01780	17858727	17867458	VIT_207s0031g01780	trnahis guanylyltransferase
7	VIT_207s0031g01790	17868467	17870838	VIT_207s0031g01790	glucan endo- -beta-glucosidase 8-like

Chr	Gene Id	Position-Start	Position-End	Name	Function
7	VIT_207s0031g01835	17943086	17946754	VIT_207s0031g01835	zinc finger protein
7	VIT_207s0031g01840	17958196	17961094	WRKY13	wrky transcription factor
7	VIT_207s0031g01850	17969313	17973374	BR11	brassinosteroid receptor
7	VIT_207s0031g01860	17985180	17995980	VIT_207s0031g01860	udp-galactose transporter 2-like
7	VIT_207s0031g01880	18007399	18013045	UBP27	ubiquitin carboxyl-terminal hydrolase 27 ubiquitin carboxyl-terminal hydrolase 27-like
7	VIT_207s0031g01900	18026962	18035798	EME1B	essential meiotic endonuclease 1a
7	VIT_207s0031g01920	18036230	18041933	VIT_207s0031g01920	probable serine threonine-protein kinase at1g54610-like
7	VIT_207s0031g01930	18043587	18049211	VIT_207s0031g01930	tsl-kinase interacting protein 1-like
7	VIT_207s0031g01960	18080029	18092969	VIT_207s0031g01960	zinc finger
11	VIT_211s0037g01040	9959488	10010312	VIT_211s0037g01040	cytosolic purine 5- pinus taeda anonymous locus cl3495contig1_03 genomic sequence
11	VIT_211s0037g01060	10047384	10048388	VIT_211s0037g01060	metal-dependent phosphohydrolase
11	VIT_211s0037g01100	10114438	10129523	VIT_211s0037g01100	phosphatidylinositol class b
11	VIT_211s0037g01120	10153642	10166151	COX6B	cytochrome c oxidase subunit 6b-1
11	VIT_211s0037g01130	10202586	10206209	TET8	senescence-associated protein
11	VIT_211s0037g01160	10240816	10247373	VIT_211s0037g01160	auxin-induced protein 5ng4
11	VIT_211s0037g01170	10251662	10254098	VIT_211s0037g01170	photosystem i p700 apoprotein a1
11	VIT_211s0037g01210	10399326	10406081	CER3	protein wax2-like
11	VIT_211s0037g01230	10495438	10496944	VIT_211s0037g01230	sequence-specific dna binding transcription factor
11	VIT_211s0037g01240	10540716	10543934	VIT_211s0037g01240	hypothetical protein ice binding uncharacterized protein
11	VIT_211s0037g01250	10560029	10560561	VIT_211s0037g01250	phosphatidylinositol class b
11	VIT_211s0037g01265	10570680	10571857	VRN1	b3 domain-containing protein
11	VIT_211s0037g01270	10578008	10579203	VIT_211s0037g01270	probable disease resistance protein at5g63020-like
11	VIT_211s0037g01280	10597758	10613990	VIT_211s0037g01280	hypothetical protein
11	VIT_211s0037g01324	10714125	10721442	VIT_211s0037g01324	serine threonine protein phosphatase 6 regulatory ankyrin repeat subunit a
11	VIT_211s0037g01326	10744451	10744825	ATL4	e3 ubiquitin-protein ligase atl4-like
11	VIT_211s0037g01340	10783401	10783538	VIT_211s0037g01340	nadh-plastoquinone oxidoreductase subunit 4
11	VIT_211s0037g01345	10783951	10785220	VRN1	b3 domain-containing protein
11	VIT_211s0037g01360	10817326	10818265	VIT_211s0037g01360	nadh dehydrogenase subunit 4
11	VIT_211s0037g01365	10865702	10866963	VRN1	b3 domain-containing protein
11	VIT_211s0037g01390	10913971	10915386	ACX3	acyl-coenzyme a oxidase peroxisomal
11	VIT_211s0037g01400	10944676	10946544	VIT_211s0037g01400	ring-h2 finger protein atl13
11	VIT_211s0037g01410	10996082	11005078	XBAT32	ankyrin repeat-rich protein
11	VIT_211s0037g01420	11039349	11039934	CPK13	calcium-dependent protein kinase
11	VIT_211s0037g01430	11039935	11040218	CPK13	calcium-dependent protein kinase 13
11	VIT_211s0078g00105	12101816	12102999	VIT_211s0078g00105	u-box domain-containing protein 43-like
11	VIT_211s0078g00150	12207450	12208406	VIT_211s0078g00150	protein executor chloroplastic-like
11	VIT_211s0078g00165	12226663	12227561	VIT_211s0078g00165	pentatricopeptide repeat-containing protein mitochondrial-like
11	VIT_211s0078g00180	12261386	12263844	VIT_211s0078g00180	hypothetical protein

Chr	Gene Id	Position-Start	Position-End	Name	Function
11	VIT_211s0078g00250	12442329	12449446	PECT1	ethanolamine-phosphate cytidyltransferase
11	VIT_211s0078g00280	12488958	12490994	VIT_211s0078g00280	wall-associated receptor kinase 2-like
11	VIT_211s0078g00290	12503269	12505262	C4H	trans-cinnamate 4-monooxygenase
11	VIT_211s0078g00300	12505656	12507147	HEN2	hua enhancer 2
11	VIT_211s0078g00310	12508645	12542426	ISA1	isoamylase
11	VIT_211s0078g00380	12589424	12600796	ISA1	isoamylase
11	VIT_211s0078g00420	12680093	12696262	GalAK	galactokinase
11	VIT_211s0078g00430	12731400	12742654	GalAK	galactokinase ghmp kinase family protein
11	VIT_211s0078g00440	12768854	12788364	DOT2	u4 tri-snrp-associated protein
11	VIT_211s0078g00450	12822043	12823840	VIT_211s0078g00450	probable alpha-mannosidase i mns5-like
11	VIT_211s0078g00460	12837031	12838915	PUM5	pumilio 6 protein
11	VIT_211s0078g00480	12860337	12861907	MYB93	hypothetical protein
11	VIT_211s0078g00490	12865608	12866147	NIP4;1	mip nip subfamily
11	VIT_211s0065g00020	13072765	13073801	CID7	pentatricopeptide repeat-containing
11	VIT_211s0065g00030	13087576	13101552	CAS1	lupeol synthase
11	VIT_211s0065g00040	13104932	13108116	CYP716A1	cytochrome p450
11	VIT_211s0065g00060	13136591	13136817	VIT_211s0065g00060	atp binding
11	VIT_211s0065g00076	13267009	13270058	VIT_211s0065g00076	hypothetical protein VITISV_001876 [Vitis vinifera]
11	VIT_211s0065g00080	13283207	13284258	CHR8	dna repair and recombination protein
11	VIT_211s0065g00120	13328665	13328900	CA2	carbonic anhydrase
11	VIT_211s0065g00130	13427386	13430454	CYP716A1	cytochrome p450
11	VIT_211s0065g00140	13477602	13485770	VIT_211s0065g00140	serine thronine protein
11	VIT_211s0065g00150	13509591	13529415	SS4	soluble starch synthase iv-1
11	VIT_211s0065g00160	13546322	13555053	ECT5	hypothetical protein uncharacterized protein
5	VIT_205s0020g02710	4446556	4451040	DSPTP1	dual specificity protein phosphatase 1
5	VIT_205s0020g02720	4453502	4455917	VIT_205s0020g02720	basic 7s globulin 2 precursor small
5	VIT_205s0020g02730	4456371	4457690	VIT_205s0020g02730	basic 7s globulin 2 precursor small
5	VIT_205s0020g02740	4462134	4463569	NIP7;1	mip nip subfamily
5	VIT_205s0020g02760	4471944	4478093	VIT_205s0020g02760	signal peptidase complex subunit 3b
5	VIT_205s0020g02770	4483940	4487917	AILP1	aluminum induced protein with ygl and lldr motifs aluminum-induced protein
5	VIT_205s0020g02790	4490987	4495658	NF-YC9	nuclear transcription factor y subunit c-9
5	VIT_205s0020g02800	4495689	4502807	VIT_205s0020g02800	pfkb-like carbohydrate kinase family protein
5	VIT_205s0020g02810	4509982	4514468	TBL11	uncharacterized protein
5	VIT_205s0020g02820	4515511	4529146	ECR1	nedd8-activating enzyme e1 catalytic subunit
5	VIT_205s0020g02840	4535578	4539184	VIT_205s0020g02840	rossmann-fold nad -binding domain-containing protein short-chain dehydrogenase reductase family protein
5	VIT_205s0020g02850	4539926	4546777	PRXIF	type iif peroxiredoxin
5	VIT_205s0020g02860	4549590	4553901	RHF1A	e3 ubiquitin-protein ligase rhf1a

Chr	Gene Id	Position-Start	Position-End	Name	Function
5	VIT_205s0020g02870	4554200	4560076	VIT_205s0020g02870	dead-box atp-dependent rna helicase 58 dead-box atp-dependent rna helicase chloroplastic-like
5	VIT_205s0020g02880	4559039	4563814	APL1	adp-glucose pyrophosphorylase large subunit
5	VIT_205s0020g02890	4600767	4604280	VIT_205s0020g02890	glycoprotein membrane precursor gpi-anchored protein
5	VIT_205s0020g02900	4607220	4617288	PNC1	peroxisomal membrane protein
5	VIT_205s0020g02910	4619125	4633396	NP3	mitogen activated protein kinase kinase kinase mitogen-activated protein kinase kinase kinase
5	VIT_205s0020g02930	4651037	4670494	VIT_205s0020g02930	rna polymerase iii subunit rpc82 family protein
5	VIT_205s0020g02940	4673443	4694685	KAPP	protein phosphatase 2c 70
5	VIT_205s0020g02950	4695286	4703436	VIT_205s0020g02950	hypothetical protein
5	VIT_205s0020g02960	4705744	4730333	ATCHR12	chromatin remodeling complex subunit
5	VIT_205s0020g02970	4728395	4730152	RANGAP2	ran gtpase activating protein 2
5	VIT_205s0020g03000	4744289	4745805	VIT_205s0020g03000	2-hydroxyisoflavanone dehydratase
5	VIT_205s0020g03020	4747460	4764728	ARIA	arm repeat protein interacting with abf2-like
5	VIT_205s0020g03030	4768424	4774376	VIT_205s0020g03030	hypothetical protein serine-threonine protein plant-
5	VIT_205s0020g03060	4794345	4798018	CYCT1;4	cyclin t1
5	VIT_205s0020g03070	4800109	4802663	VIT_205s0020g03070	cyclin family protein

Chapter 4

GENE EXPRESSION ASSAYS

Abstract

Crop wild relatives have shifted into the center of the attention of plant breeding and evolutionary biology, because they represent valuable genetic resources for breeding. Recent studies revealed that some wild grapevine genotypes are more tolerant than the cultivated grapevines against several grapevine diseases, including downy mildew (*Plasmopara viticola*) and powdery mildew (*Erysiphe necator*), despite *V. vinifera* subsp. *sylvestris* lacks in history of coevolution with these pathogens and it should not harbor any ETI-like defense against these diseases. The fact that genotypes of *V. vinifera* subsp. *sylvestris* can withstand these diseases might mean that they command a more efficient basal immunity (PTI) and could have potential as new breeding resources to be exploited for sustainable viticulture in the future. According to the phylogenetic analysis described in the previous chapters, the *V. vinifera* germplasm collection of Caucasus was characterized by a high genetic diversity and resulted rather different from the main European cultivars. Moreover, a few accessions were characterized by unusual ancestral features and by low susceptibility to downy mildew (DM) and among them 'Mgaloblishvili N' cultivar was mainly studied because of its constant tolerant behavior, by reducing the disease severity and the pathogen sporulation (Toffolatti et al., 2016) [1]. To integrate the obtained QTL results and to assess the genetic and physiological traits of this accession, we analyzed different genes on the parental line together with other two genotypes from the S1 offspring with different level of tolerance to DM. In the current study we first evaluated the phenotypic variation among the genotypes, identifying the most tolerant one and then we studied the differences in gene expressions by qRT-PCR assay. Candidate genes detected in the QTL region, four of which related to WRKY, MYB and ERF transcription factors (TFs), referred to the Ethylene dependent signaling pathway and were involved in basal immunity and secondary metabolite pathways. It was further observed that main differences among the three different accessions were detected by differential accumulation of the transcripts referred to chalcone- and stilbene-related genes, which are mainly involved during the defense response in ancestral lineages, as reported in literature.

Background

According to archeological evidence [161], the domestication of *Vitis. vinifera* subsp. *sylvestris* and its conversion into the efficient high yield and quality plant *V. vinifera* subsp. *sativa* have been traced in Caucasus and the grape growing region expanded over the centuries to the European continent. However, in the 19th century, the invasion of Phylloxera parasites devastated European vineyards and to control this pest the susceptible scions of cultivated grapes were grafted on resistant rootstocks derived from North America wild *Vitis* species, interrupting the complicated reproductive cycle of Phylloxera. Unfortunately, this process of grafting also contribute to introducing new fungal diseases to Europe one of which is known as Downy mildew. In contrast to the American *Vitis* species, that have co-evolved with the pathogen and developed a resistance against it, the European cultivars were susceptible. Since then, a long and intensive resistance breeding process recently assisted by molecular marker and biotechnology resources, have been started to introduce the genetic resistant traits into *V. vinifera*, trying to maintain its good quality. Only in the latest years, a major attention was focused on *V. vinifera* both in the wild and cultivated forms, because they could play an important role in the protection of native biodiversity and they could also serve as valuable sources of alleles and traits for ongoing plant breeding and crop improvement efforts.

Here we focus on Downy mildew caused by the oomycete *Plasmopara viticola*. The interaction between *Vitis* and *P. viticola* follows three distinct modes which describe respectively, a strong resistance in American *Vitis* where the pathogen is arrested early in its development, a moderate tolerance to the disease typical of Asian and putative European wild accessions and a high susceptibility detected in the cultivated *V. vinifera* genotypes. . The defense responses adopted by plants to resist to pathogen attack consist of both constitutive mechanisms, such as physical barriers, and inducible mechanisms involving the production of reactive oxygen species (ROS), programmed cell death (PCD) events, the synthesis of pathogenesis-related proteins (PR) and the localized accumulation of phytoalexins.

The immediate defense response of an infected part, typical of Asian and a few European *V.v.* subsp. *sylvestris* consists in a local reaction by producing secondary metabolites, where in the extreme case cells surrounding the infection site initiate a hypersensitive response reaction triggered by the formation of reactive oxygen species to avoid further spread of the infection. Plant stilbenes, together with flavonoids, belong to the plant polyketide class, which represents a major group of phenylpropanoids (PP) which are involved in constitutive and inducible defenses. The biosynthetic pathway leading to the production of stilbenes is a side branch of the general PP pathway and can be considered as an extension of the flavonoid pathway. All higher plants are able to accumulate compounds like p-coumaroyl-CoA and cinnamoyl- CoA through the action of ubiquitous enzymes such as PAL, C4H, and 4CL. These compounds represent substrates for both chalcone synthases (CHSs), fundamental enzymes leading to the biosynthesis of the flavonoids and for stilbene synthases (STSs), the key enzymes responsible for the biosynthesis of resveratrol and its derivatives. In the last years a growing number of TFs responsible for the regulation of flavonol, lignin or anthocyanins biosynthesis have been isolated including the R2R3-MYBs, a sub-group of the MYB TFs super family, and the basic helix-loop-helix (bHLH) transcription factors [39] and more recently also TFs involved in the regulation of the stilbene biosynthetic pathway have been identified [162].

In the previous chapters we described a set of Caucasian accessions in which genetic diversity, inbreeding extent and possible hybridization with wild grapevines were investigated through structural and phylogenetic analysis and among them we identified the Georgian cultivar 'Mgaloblishvili N.', characterized by several traits related to wild accession of *V. vinifera* and by a moderate tolerance to downy mildew infection. Since the information obtained from a preliminary QTL analysis were affected by an unstable behavior of the variety following DM inoculation in different years, we integrated our results by studying the earlier induction of defense responses linked with basal immunity and secondary metabolite pathways in the parental line and a few S1 offspring.

Methods

Micropropagation

Plant materials and explants preparation: for the purpose of *in vitro* plant propagation the explants were collected from the parental line 'Mgaloblishvili N.' (L22) and two different genotypes of the mapping population S1 (ID-85, ID-139), showing different levels of tolerance to DM, with a contrast behavior during the previous seasons. The two seedlings and the parental line were grown in the greenhouse at 25°C. Internode segments, each carrying on a small piece of stem tissue, were used to provide a single shoot and were treated with a sodium hypochlorite 20% solution for 20 m and subsequently rinsed with H₂O for 5 m. The sterilized explants were used as experimental materials.

Culture media and conditions: the Woody Plant Medium (WPM) (supplementary table S1, [163]) supplemented with vitamins [164] and sucrose (supplementary table S2) was prepared in jars and adjusted to pH 5.85 with NaOH 1M before being solidified with 4.3 g/l phytigel, then autoclaved at 121°C for 20 m. The transfer of the explants in the media was performed inside specific hood, sterilizing the tools used for dissection in order to avoid microbial contaminants. All cultures were kept in growth chamber at 25°C under 16-hours photoperiod under cool white florescent tubes. Subcultures for multiplication stage were done after about 4 weeks.

Acclimatization: the rooted shoots (neofomed plantlets) were maintained in their media for 3 months, to enhance the efficiency of roots. Once ready for the acclimatization, they were thoroughly washed to remove any medium residual, potted into peats covered by plastic supports (25°C and 80% relative humidity) and transferred to the greenhouse of Julius Kuhn Institute of Geilweilerhof, Siebeldingen (Germany). After 20 days, the plastic supports were removed off for further growth.

Controlled growth: after a month, all the propagated plants were transferred in a climate chamber, under 16 hours photoperiod, at 25°C, ~65 Klx and 60% relative humidity so that their physiological state approached a similar level.

P. viticola inoculum preparation and evaluation of severity with leaf discs infection test

Leaf disc tests were used to determine disease severity after inoculation with *P. viticola*. For standardizing the physiological stage, 3 leaves from 4 different biological replicates of each accession were used to excise four leaf discs per leaf (3 inoculated with sporangia suspension and 1 with H₂O) with an 18 mm diameter cork-borer. The leaf discs were placed upside-down in a Petri dish, previously sterilized under UV ray, containing 1% water agar. Each disc was artificially inoculated with 40 ul of a *P. viticola* sporangia suspension ($2 \cdot 10^4$ sporangia/ml) quantified into Neubauer counting chamber by using the Trypan blue exclusion test of cell viability [165]. Sporangia had been carefully recovered by brushing freeze-dried leaves of non-sprayed field-grown plants showing a good sporulation after incubation overnight in a wet chamber.

The infected discs were incubated overnight in the dark at 25°C and 70% Relative Humidity (HR) and then kept under climate chamber conditions (25°C and 99% RH) during the inoculation time course and constantly controlled with stereomicroscope. Moreover, the quantification of sporulation was performed by using the open source software ImageJ as described in Peressotti et al., 2011 [166].

Experimental design of qRT-PCR assay

A sporangial suspension of *P. viticola* was prepared in sterile water and set up with approx. $2 \cdot 10^4$ sporangia/ml, as determined by counting in a Neubauer improved counting chamber as previously described. For the inoculation experiment the already described accessions together with two plants of Riesling (positive control) were used. In particular, we employed 3 biological replicates of each genotype for every condition/timepoint. The inoculation was done on the whole plant by sprays of the prepared sporangial suspension until all leaves were fully covered on the abaxial surface and in order to prevent the desiccation, the plants were overlaid with a plastic foil. After 24 h of darkness the plastic foil was removed and a normal day/night cycle (16 hours day and 8 hours night) was adjusted. Sampling of leaves material was done in liquid nitrogen, at different time points (0 hpi, 8 hpi, 24 hpi, 48 hpi) after inoculation.

RNA extraction and cDNA synthesis

Collected leaves were used for the RNA extraction and the sample preparation provided a small piece of a young leaf and a spade point of PVPP (Polyvinylpolypyrrolidone) to inactivate phenolics in the sample combined in a reaction tube. The samples were grinded and homogenized with a mortar and pestle in the liquid nitrogen. Total RNA was isolated employing the Spectrum™ Plant Total RNA Kit (Sigma-Aldrich®, St. Louis, Missouri, USA) according to the manufacturer's instructions. Residual genomic DNA was digested with RNase-Free DNase I (Qiagen). RNA concentration of the samples was fluorometrically determined with the microplate reader CLARIOstar (BMG Labtech GmbH, Ortenberg, Germany). For the fluorometric examination of the RNA the Quanti-iT™ Ribogreen® RNA Reagent (Life Technologies GmbH, Carlsbad, California, USA) was used according to the instructions given by the supplier, while the RNA integrity was verified by agarose gel electrophoresis.

Complementary DNA (cDNA) was synthesized using the High Capacity cDNA Reverse Transcription Kit (Applied Biosystems™, Foster City, California, USA). For each 50 ul reverse transcription reaction mixture 25 ul of RNA (10 ng/ul) was used and RT reaction was carried according to the following protocol: 10 m at 25°C, 120 m at 37°C and 5 m at 85°C.

Candidate gene approach

Candidate genes are generally the genes with known biological function directly or indirectly regulating the developmental processes of the investigated trait, which could be confirmed by evaluating the effects of the causative gene variants in an association analysis. In this specific case, chromosomal regions affecting genetic variation of the investigated trait were detected in rather wide confidence intervals, so it proved hard to ultimate pinpoint identification of a positional candidate gene to validate. The critical point was represented by the requirement of information coming from the existing well-known physiological, biochemical or functional knowledge such as hormonal regulation or biochemical metabolism pathways, which were retrieved by using Gramene database (<http://www.gramene.org>), Grape Genome Database hosted at CRIBI (<http://genomes.cribi.unipd.it/grape>) and through comparative studies. In light of this, we selected different genes (supplementary table S3), chosen from literature and from our QTL results aiming to evaluate a possible biological response involved in DM infection. Based on a combination of criteria including significance of the QTL, gene information on relevance for pathogen defence and the predicted functional effects of identified regions, we propose here a subset of CGs of highest priority for further evaluation in functional studies. We analyzed the expression of genes related to stress tolerance, encoding for a variety of transcription factors that contain typical DNA binding motifs such as WRKY, MYB, ERF/AP2 and Zinc fingers. We first tested VvWRKY33 TF described in Merz et al., 2015 [167] and the related PR10 and PR5; subsequently we tested VvWRKY57 involved in the crosstalk between JA and auxin signaling. Moreover, given the phylogenetic placement of 'Mgaloblishvili N.' cultivar next to the wild accessions, according to Vannozzi et al., 2012 and Holl et al., 2013 [162,168], we studied the expression of VvMYB14, VvMYB15, PAL, VvSTS29 (isoforms STS29, STS25 and STS27), VvSTS41 (isoforms STS41 and STS45) and VvMYBA which detected the isoforms Vv-MYBA1, Vv-MYBA2, and Vv-MYBA3. Then, we selected in the confidence interval of the QTL detected on chromosome 7, VvWRKY13 and VvWRKY7 both related to the hormone regulation. Finally we evaluated the expression of two candidate genes detected in the QTL region on chromosome 1, VIT_201s0011g03470 and VIT_201s0011g03730 encoding for an Ethylene Responsive Factor ERF118 like-protein and for R2R3-type MYB transcription factor MYB62, respectively.

As concerns the choice to avoid the analysis of other CGs like TET8 gene located on chr 11 which was interesting for its functional prediction, we preferred to focus our study on smaller and more detailed regions. Indeed, sometimes, it could be difficult narrow the research on specific genes especially when a preliminary QTL analysis is unable to predict an accurate gene location.

Gene expression by quantitative Real Time PCR (qRT-PCR) and statistical analyses

Fourteen genes were chosen to study the defense response of 'Mgaloblishvili N.' to downy mildew infection, using qRT-PCR. Specific primer pairs for selected genes were designed using Primer3Plus and Blast tool as shown in supplementary table S3 and 2 ul of the undiluted cDNA were then used for each amplification

reaction in a final volume of 20 μ l. RT-qPCR was performed in a ViiATM 7 Real-Time PCR System (Applied Biosystems, Foster City, CA, USA), using the Power SYBR Green PCR Master Mix. Reaction composition and conditions followed manufacturer's instructions. The cycling protocol consisted of 20 s at 50°C, 10 m at 95°C, then 40 cycles of 15 s at 95°C and 1 m at 60°C, followed by a last step of 15 s at 95°C, 1m at 60°C, 30 s at 95°C and 15 s at 60°C.

Specificity of the PCR was assessed by the presence of a single peak in the dissociation curve after the amplification and results were calculated as the average of three independent biological replicates for each genotype, repeated twice, using actin, GAPDH [169] [170] and ubiquitin [167] as housekeeping genes. Threshold cycles (Ct) were converted to relative expression (fold change) according to Hellemans et al., 2007 [171] using two reference genes and the untreated control (0 hpi) as calibrator sample.

ANOVA was used to assess the significance of the differences among and within groups/treatments at each sampling stage, and Tukey's HSD at $P \leq 0.05$ clarified which groups showed significant differences.

Results

Assessment of plant material

In vitro propagation method was chosen in order to produce a number of biological replicates of each plant genotype, grown in laboratory conditions, in a short space of time. Compared to the traditional propagation, this technique allowed us to grow healthy and uniform plants both from the parental line and the two S1 offspring. According to our propagated materials, there were lots of evidence that micropropagated plants grew faster and more vigorously, despite about 30% of starting material have been discarded owing to a few contamination. Micropropagation process was started in the climate chambers of Fondazione Edmund Mach and the first growth of plantlets in glass flasks simplified their subsequent transfer to the greenhouse of Julius Kuhn Institute of Geilweilerhof, Siebeldingen (Germany). The propagation process started on February 2016 and lasted about 7 months. In August all the plants were ready for the infection experiment (Figure 1).



Figure 1 **In vitro propagation process.** i) Explants preparation by using internode segments ii) 15 days growth iii) 30 days growth iv) Acclimatization in vivo plants (June 2016) v) In vivo growth (August 2016).

Leaf discs evaluation

Due to the poor repeatability of the offspring phenotype to DM infection among the years, we focused on three accessions (L22, ID-139, ID-85), by considering two main aspects: the severity of *P. viticola* inoculum and the expected response to infection of each single accessions. A leaf discs test was performed using a water suspension of 2×10^4 sporangia/ml first testing the cell viability by using Trypan blue exclusion test. The phenotypic evaluation was performed at 8 dpi, based on categorical ratings of sporulation density according to the OIV 452-1 descriptor. In order to score disease severity, the percentage of the leaf disc area exhibiting symptoms of sporulation was measured with ImageJ software. One way ANOVA test ($\alpha=0.05$) on sporulation ratings, calculated on biological replicates of the three different accessions, indicated statistical significance among the variances and the post-hoc Tukey HSD test figured out which groups in our samples differed (95% family-wise confidence level). Even though all the accessions showed a moderate level of infection, covering no more than half of leaf discs, Tukey's test indicated a significant reduced sporulation in genotype ID-85, whereas the parental line (L22) and ID-139 presented major infected area, not limited to the infection site. Moreover, we observed the leaf disc sporulation to the stereomicroscope at 8 dpi, and we ascertained in all genotypes the presence of fungal mycelium characterized, in some points, by the absence of sporangia. These preliminary observations may indicate a partial resistance to the pathogen which allows the growth of mycelium but in some cases decrease sporangia production. Based on the microscopy observations, we supposed that the growth of *P. viticola* could be delayed but not stopped (Figure 2).

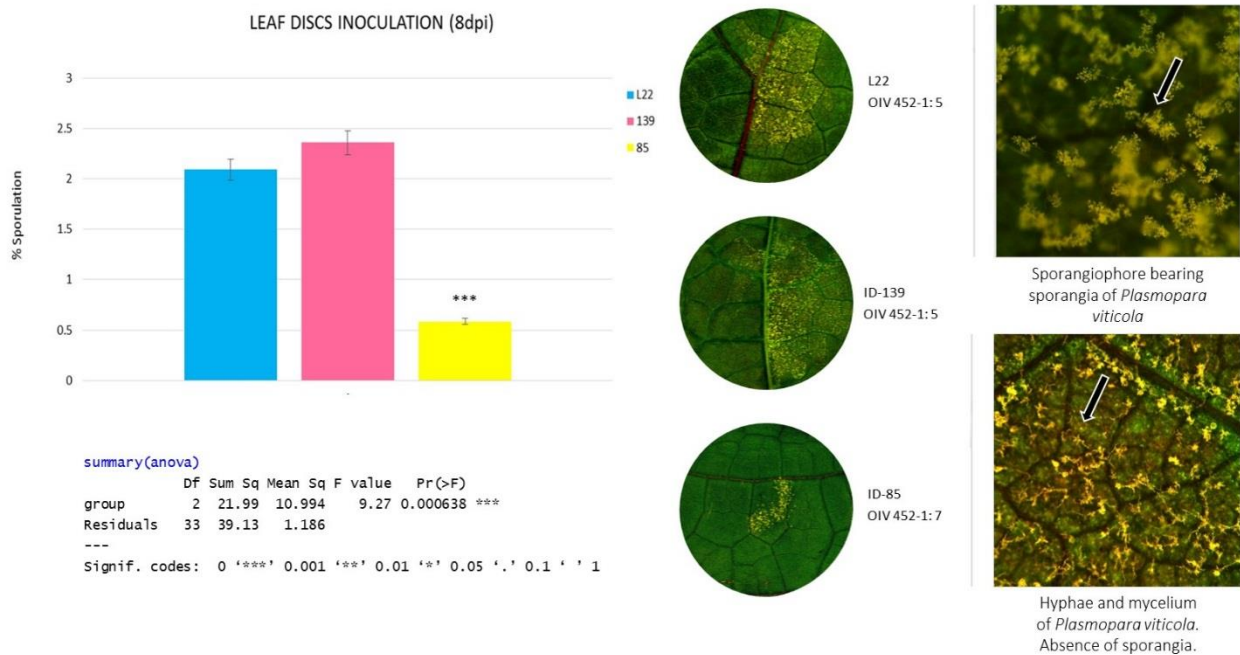


Figure 2 **Leaf discs inoculation.** i) Bar plot of sporulation (%) in L22, ID-139, ID-85 at 8 dpi and One-Way ANOVA test (***) = $p \leq 0$). ii) Sporulated leaf discs of L22, ID-139 and ID-85 at 8 dpi and focus on mycelium growth by stereomicroscope: complete sporulation and delay of sporangia production.

Phenotypic evaluation of whole plants

The studied plants were first infected with the pathogen as described in material and methods and maintained in a climate chamber for several days, during this period tissue samples were collected for subsequent RT PCR analysis. At 7 dpi humidity was increased to 90% in order to induce the sporulation. The rating of sporulation was calculated at 8 dpi employing the ratio among the number of infected leaves per single plant and the total number of leaves of the whole plant. The phenotypic observations allowed to detect an uncanny behavior among biological replicates, which exhibited a wide range of variation despite the controlled environment. According to the calculated ratings (% of sporulation), we didn't obtain any significant difference among accessions. Moreover we observed some infected leaves to the stereomicroscope to verify the successful and the degree of infection and we found that a few infected leaves presented necrotic spots probably due to the disease progression (Figure 3). However, we were able to detect, only in a few leaves of ID-85, some HR-like responses as shown in (Figure 4) which were absent in the susceptible genotype ID-139. The HR was generally recognized by the presence of brown, dead cells at the infection site and their number could vary from one to many. A visible brown lesion might develop if sufficient cells die.

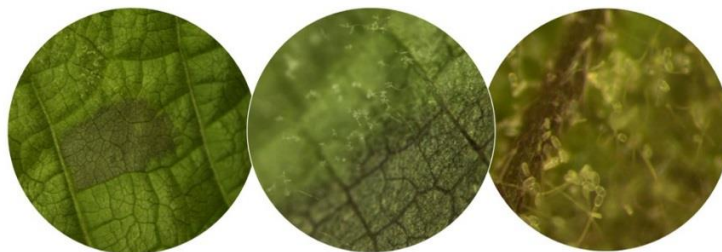


Figure 3 **Focus on leaf.** Representation of necrotic spot on leaf and relative blow-up.



Figure 4 **Focus on ID-85 leaf.** i) ID-85 untreated leaf at 5 dpi. ii) ID-85 treated leaf at 5 dpi. iii) Blow-up of HR-like response in ID-85 treated leaf at 5 hpi.

Comparison among gene expressions and validation of candidate genes detected in QTL regions

We analyzed the variations of candidate gene expressions among the chosen genotypes in order to better understand the eventual mechanisms of tolerance implicated in defense response and moreover in order to validate the reliability of QTL analysis. The choice of candidate genes was made on the basis of exceptional and unusual wild features of this cultivar. Expression of most of these genes was recently described in literature in experiments with *Vitis vinifera* species. Out of fourteen genes tested, about nine showed significant differences among and within groups through ANOVA test and further through post-hoc Tukey HSD test (supplementary table S4).

According to leaf discs experiment, ID-85 represented the accession which showed a reduced infection to *P. viticola*, whereas L22 and ID-139 maintained a higher level of infection (~40% of sporulation). Although high, the expression of PAL, VvSTS29, VvSTS41 genes encoding enzymes involved in stilbene synthesis, together with PR10 and VvWRKY57 genes didn't show significant differences among the three genotypes therefore they weren't considered in further study (data not shown). We must underline the wide variation within biological replicates, which didn't allow to obtain significant difference among genotypes despite the high expression of several genes related to immunity response. This variation mirrored the uncanny behavior detected in the visual phenotypic evaluation.

Recent findings suggested a VvWRKY33 transcription factor as an essential component in various stress-related signaling pathways by activating SAR and PR genes via binding to W-box cis-elements of corresponding promoters. As described in Merz et al., 2015 [167], ectopic expression of VvWRKY33 in grapevine improved resistance to biotrophic or necrotrophic pathogens, indicating an important role of VvWRKY33 for the defense reaction of grapevine against fungal pathogens; so we tested the expression of this gene on our three genotypes, in order to evaluate an eventual upregulation compared with the untreated control. Together with VvWRKY33 we tested also PR5 and PR10 in order to study their differential expressions among genotypes. PR10 didn't show any significant differential expression among genotypes, while VvWRKY33 presented an increase at 8 hpi in the more tolerant ID-85, reaching barely 1.9- fold. In addition a stronger but delayed induction of PR5 was detected in ID-85 at 24 hpi in the range of 2-fold. Despite the low degree of upregulation of these genes compared with the untreated control, this result is in agreement with the phenotypic evaluation of leaf discs infection in which accession ID-85 described the better defense response to the disease (Figure 5).

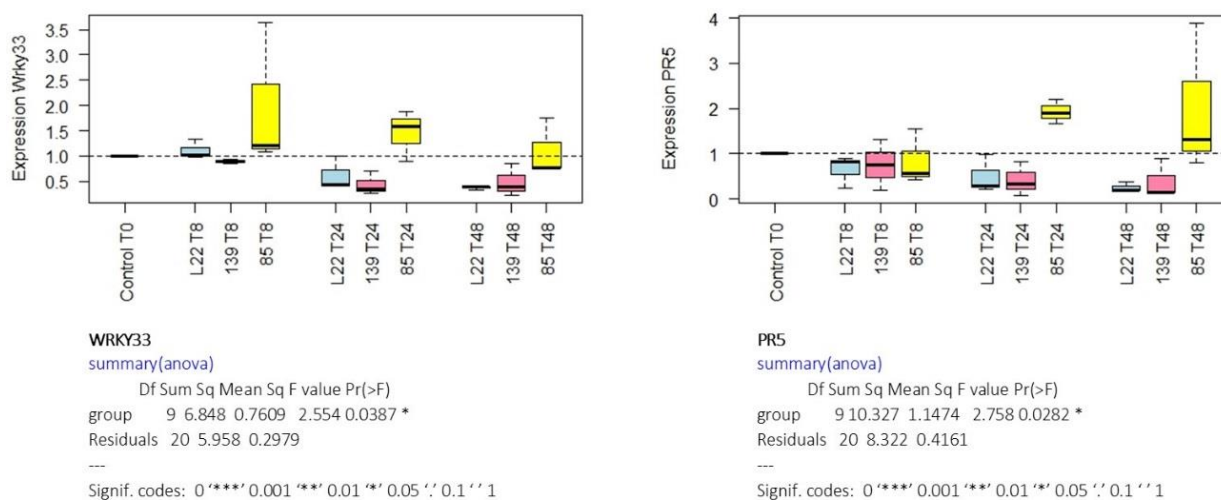


Figure 5 **Box plot of gene expressions.** Expression of VvWRKY33 and PR5 genes in L22, ID-139 and ID-85 at different time points and summary of ANOVA test (* = $p \leq 0.01$).

A few QTLs were detected in our previous analyses and despite the lack of repeatability among the years, we delved into the region of interest and we chose four genes of special features.

First we focused on chromosome 1 where the QTL analysis drew up the major peak (LOD 5.5). Genes included in the QTL region are listed in supplementary table S2, Chapter 3. Among them, we studied two genes VIT_201s0011g03470 and VIT_201s0011g03730, encoding for an Ethylene Responsive Factor ERF118 like-protein and for R2R3-type MYB transcription factor MYB62, respectively.

The ethylene signaling and response pathway includes ERFs, which belong to the transcription factor family APETALA2/ERF and it is well known that ERFs regulate molecular response to pathogen attack by binding to sequences containing AGCCGCC motifs (the GCC box), a cis-acting element. VIT_201s0011g03470 gene encoded for a putative uncharacterized protein, however the in silico prediction showed a domain like ERF confirmed by the comparative analysis performed on Gramene database through "Sinteny" tool, which matched this gene with the ERF 118 TF of *Arabidopsis thaliana*. In agreement to ANOVA test, which showed a high significance ($p \leq 0$), post-hoc Tukey HSD test showed a significant differential expression at 24 hpi of the parental line L22 (2.37- fold), respect to the untreated control and respect to the offspring. Meanwhile at 48 hpi the expression level of L22 maintained a constant behavior, the expression of ID-85 raised up to 2.20- fold, instead ID-139 accession showed a minimal but constant increase of expression across the different time points (Figure 6).

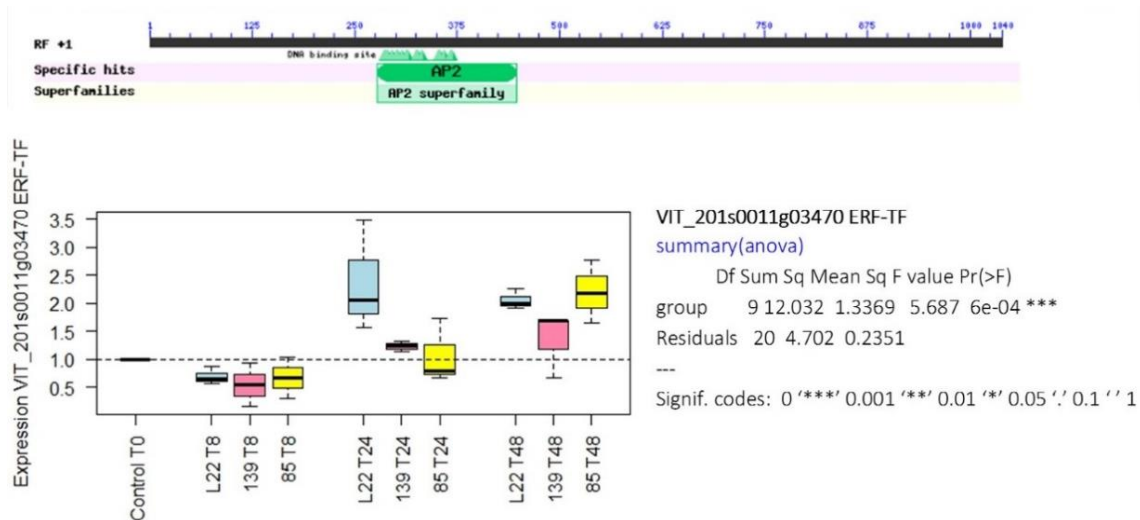


Figure 6 **VIT_201s0011g03470 gene**. i) Screenshot of conserved domain relative to the sequence of studied gene. DNA-binding domain found in transcription regulators in plants such as APETALA2 and EREBP (ethylene responsive element binding protein). In EREBPs the domain specifically binds to the 11bp GCC box of the ethylene response element (ERE), a promoter element essential for ethylene responsiveness. EREBPs and the C-repeat binding factor CBF1, which is involved in stress response, contain a single copy of the AP2 domain. APETALA2-like proteins, which play a role in plant development contain two copies. ii) Box plot of gene expression across different time point with relative ANOVA test (***) = $p \leq 0$.

VIT_201s0011g03730 gene encoded for R2R3-type MYB transcription factor MYB62, which was widely studied in Devaiah et al., 2009 [145]. According to this paper, in *Arabidopsis thaliana*, the overexpression of MYB62 resulted in altered root architecture, Pi uptake, and acid phosphatase activity, leading to decreased total Pi content in the shoots. The expression of several Pi starvation-induced (PSI) genes was suppressed in the MYB62 overexpressing plants and at the same time it has been reported that one of the characteristic responses of plants to phosphate starvation is the accumulation of anthocyanins. In light of these preliminary concepts, we analyzed expression of VvMYB62 gene in our accessions, at different time points. Our analyses showed a first downregulation of this gene in ID-85 at 8 hpi, followed by an overexpression (3.2- fold) at 24 hpi, and a slight decrease (2.77- fold) at 48 hpi. Meanwhile, in L22 and ID-139 it was downregulated across all time points. Overexpression of VvMYB62 in the most tolerant accession ID-85 led to assume a secondary increase of anthocyanins content induced by down mildew infection (Figure 7)

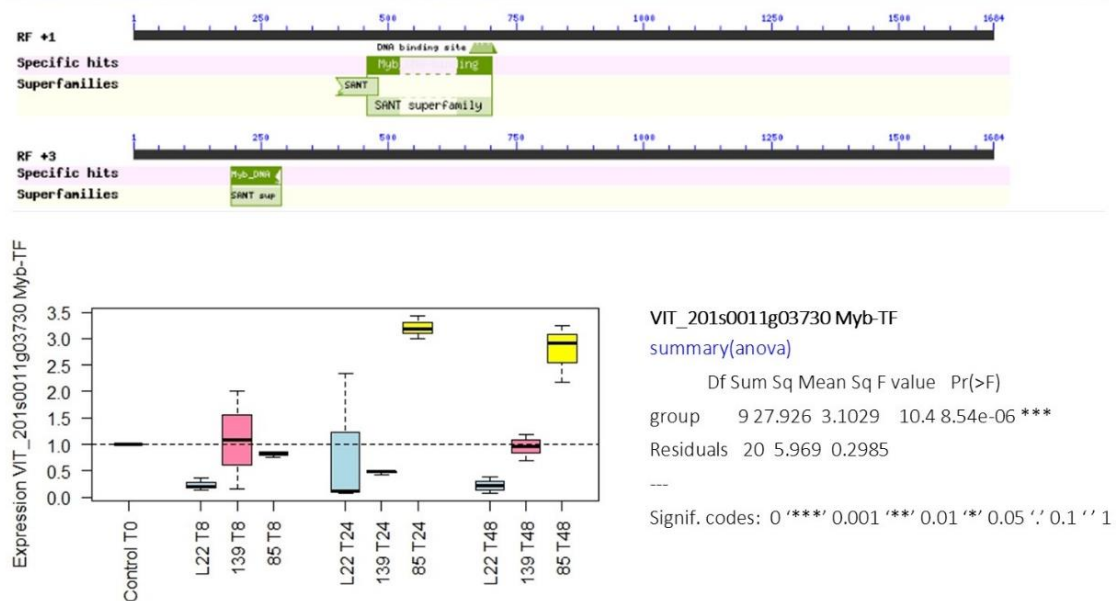


Figure 7 **VIT_201s0011g03730 gene**. i) Screenshot of conserved domain relative to the studied gene. Myb-like DNA-binding domain is a family which contains the DNA binding domains from Myb proteins, as well as the SANT domain family. SANT (Swi3, Ada2, N-Cor, and TFIIB) domain is a protein domain that allows many chromatin remodeling proteins to interact with histones. ii) Box plot of gene expression across different time point with relative ANOVA test (***) = $p \leq 0$.

A second major peak (LOD 4.23) on chromosome 7, obtained from our QTL analysis, was investigated because of the presence of two interesting WRKY TFs, VvWRKY13 and VvWRKY7. VvWRKY13 was described for the first time in Ma et al., 2015 [172], isolated from the grapevine cultivar 'Zuoyouhong' and broadly expressed in the root, stem, leaf, bud, flower and fruit with the highest expression levels detected in the stem and leaf. The cited research work revealed that the novel transcription factor VvWRKY13 was likely involved in ethylene biosynthesis by the regulation of ACS2 and ACS8 expression. According to our analysis, VvWRKY13 gene was significantly expressed (3.39- fold) in ID-139 respect to the parental line L22 (1.24- fold) at 8 hpi, meanwhile ID-85 showed a slight overexpression but not significant as confirmed by post-hoc Tukey HSD test (supplementary table S4).

On the other hand we tested a gene located in the same region of QTL, known as VvWRKY7 TF which is involved in calmodulin binding and accordingly, involved in the plant immune system. This gene didn't shown a high expression in none of the studied accessions, except for the tolerant ID-85 which barely gained a fold change of 1.22 at 48 hpi (Figure 8).

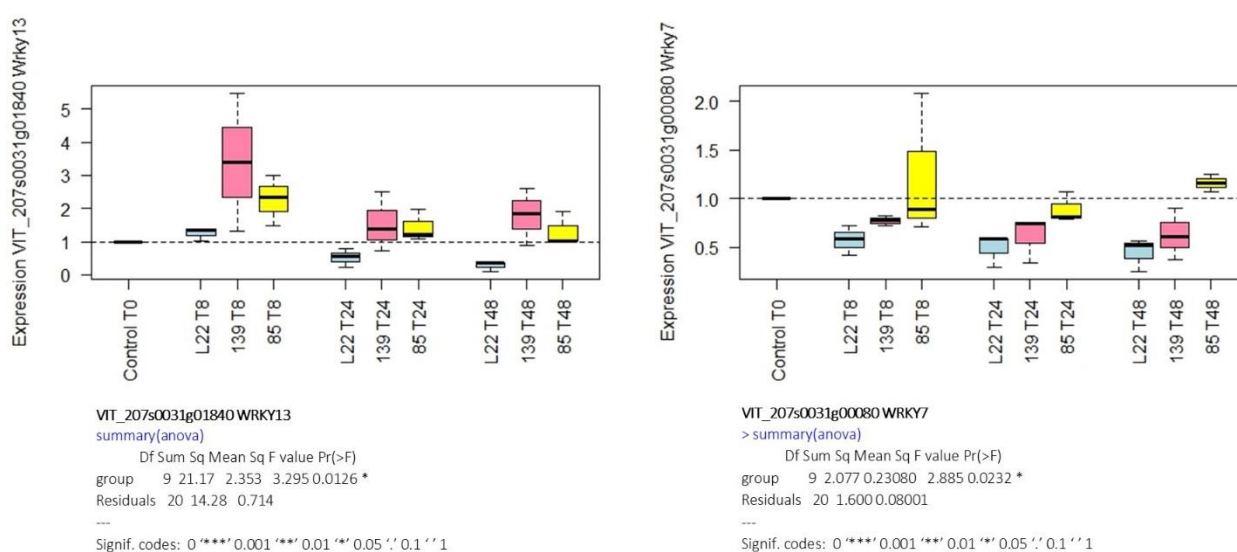


Figure 8 **VvWRKY13 and VvWRKY7 gene expression.** Box plot of gene expression of VvWRKY13 and VvWRKY7 TFs at different hpi. WRKY proteins are a group of transcription factors with highly conserved WRKY domain (WRKYGQK), which specifically interacts with W-box ((T)(T)TGAC(C/T)) in the promoter and activates the expression of the corresponding genes.

Ancestral features of 'Mgaloblishvili N.'

To validate the wild features of 'Mgaloblishvili N.', detected through the phylogenetic analysis, the transcription factors VvMYB14 and VvMYB15 were tested as main regulators of stilbene biosynthesis in ancestral lineages of *Vitis vinifera* [24]. Moreover VvMYBA gene, involved in anthocyanin synthesis, was tested according to Holl et al., 2013 [168], being part of chalcone synthases alternative pathway, which compete with the stilbene synthases' one (Figure 9). Focusing the attention on the expression of VvMYB14 and VvMYB15 genes, we could confirmed results obtained from leaf discs experiment, more precisely the expression of VvMYB14 and VvMYB15 resulted higher in ID-85, being the most tolerant genotype. In detail, exposure of ID-85 accession leaves to *Plasmopara viticola* increased the transcription of VvMYB14 and VvMYB15 by 4-fold and 5- fold, respectively, within 8 hpi of treatment compared with untreated control. On the contrary, VvMYB14 expression was increased only by 1-fold at 8 hpi in the less tolerant accession ID-139, meanwhile similarly to ID-85, VvMYB15 presented an earlier overexpression which reached 6- fold. In the parental line, neither of the two genes was induced. As it concerns VvMYBA gene, responsible for variation in anthocyanin content in the berries of cultivated grapevine, resulted differently upregulated at 8 hpi in ID-139 (3- fold) compared to its downregulation in L-85 (0-fold), reflecting the competition for precursors between STS and

CHS [173]. Indeed both CHS and STS use p-coumaroyl-CoA and malonyl-CoA as substrates and synthesize the same linear tetraketide intermediate and their biosynthetic pathways compete one against to each other, leading to the production of flavonoids and stilbenes, respectively. As already described previously for VvMYB62 gene, a later upregulation of VvMYBA related to anthocyanins biosynthesis was induced at 24 hpi in ID-85. Expression of STS genes confers significant resistance against fungal infection and the upregulation of VvMYB14 and VvMYB15 in accession ID-85 confirmed its tolerant phenotype. On the contrary, the downregulation of VvMYB14 together with the overexpression of VvMYBA gene in accession ID-139 suggested a lower induction of disease defenses of this genotype.

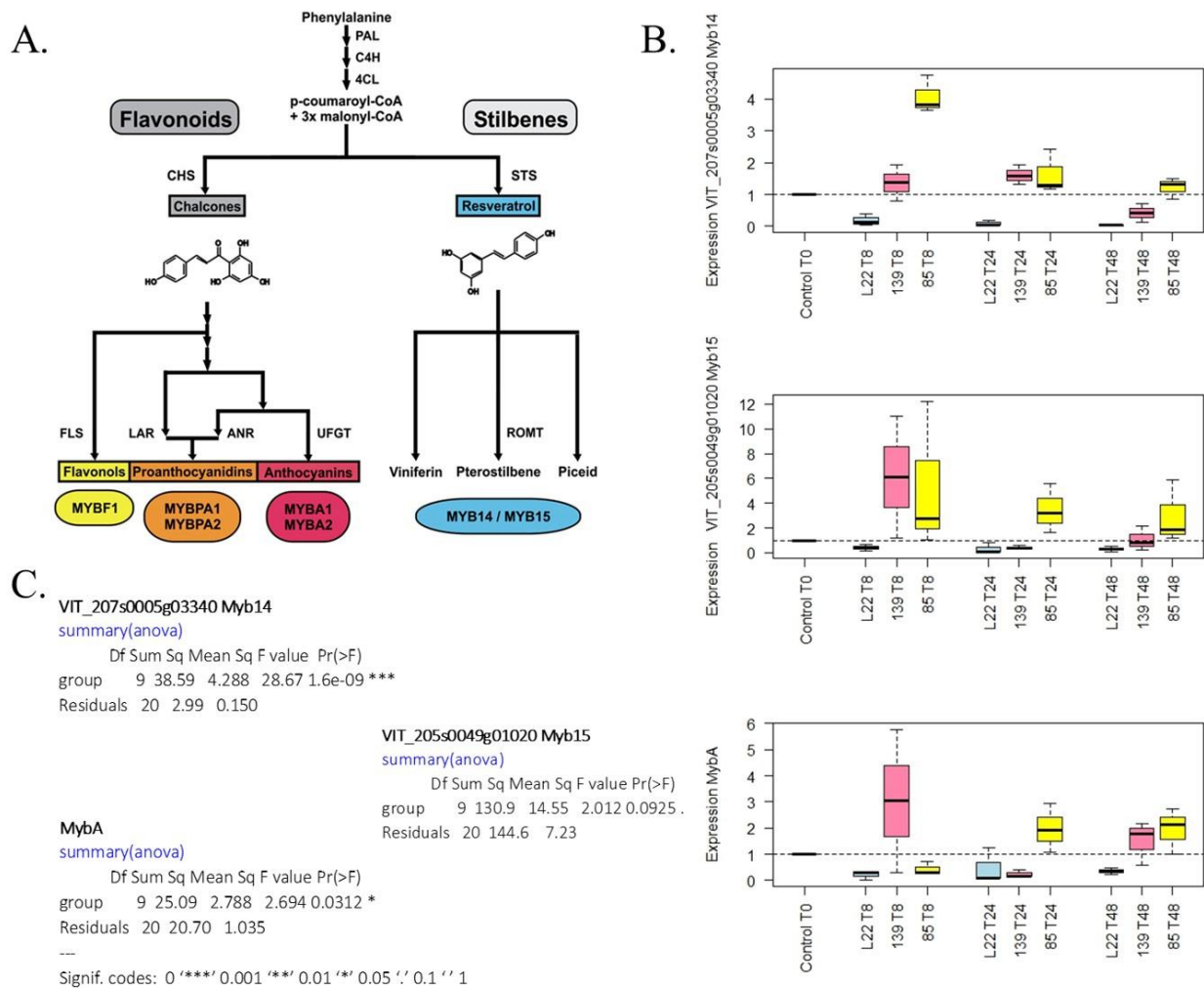


Figure 9 Box plot of gene expressions. A) Simplified representation of the grapevine Phe/Polymalonate pathway which leads to the biosynthesis of Flavonoids and Stilbenes [168]. B) Expression of VvMYB14, VvMYB15 and VvMYBA genes in response to DM infection. C) Summary of ANOVA test ($p \leq 0.1$, $* = p \leq 0.01$, $*** = p \leq 0$).

Discussion

Assessment of phenotype

Phenotypic evaluation was performed at 8 dpi both on leaf discs and on the whole plants treated with downy mildew. Leaf discs experiment allowed to define clearly the most tolerant accession (ID-85) comparing the sporulation rate at 8 dpi of the different genotypes, also supported by statistical analysis. On the other hand, we couldn't be able to reproduce the same clear result operating on the whole plants, inasmuch we didn't find any significant differences among the genotypes except for a few cases where we observed HR-like response on infected leaves of ID-85. Overall, we spotted an inconstant behavior among biological replicates which showed a wide phenotype variation, implicating a subsequent major effort to detect a significance across the gene expression analyses. Indeed, we discarded a lot of genes from our results because of the high values of standard deviations calculated on collected data, supported by the relative statistical test. However, despite the unstable phenotype, we were able to define the most tolerant accession (ID-85) validated also by the subsequent gene expression analysis. Moreover, we observed in all accessions a scattered sporulation which was characterized by the presence of fungal mycelium although not always defined by the presence of sporangia, indicating a probable delay of pathogen growth.

Responsiveness of candidate genes to pathogen treatment

Due to the lack of robust QTL results able to explain the tolerance to *P. viticola* in 'Mgaloblishvili N.', we studied the expression of candidate genes in other two accessions of the offspring which showed a different behavior across the year. This approach allowed us to better understand what kind of genes were mainly regulated after infection with the pathogen. The choice of candidate genes was essentially based on literature and QTL results.

According to our collected data, the most tolerant accession ID-85 showed a gene regulation related to Ethylene dependent signaling pathway. In the QTL range detected in 2014, we found VvWRKY13 involved in ethylene biosynthesis and VIT_201s0011g03470 gene encoding for an Ethylene Responsive Factor like protein, both upregulated in ID-85. Phytohormone crosstalk is crucial for plant defenses against pathogens in which salicylic acid (SA), jasmonic acid (JA), and ethylene (ET) play key roles. Over the past several years, it has become evident that the JA and SA pathways are mutually antagonistic, while the role of ET in plant defense is somewhat controversial. Interestingly, ethylene has been shown in certain cases to modulate programmed cell death (PCD) pathways necessary for growth, but also for survival in response to environmental stresses, acting as primary defense. A type of plant PCD is the hypersensitive response (HR) defined as a rapid and localized cell death associated with disease resistance. The unclear role of this hormone might be due to the fact that, during plant-pathogen interactions, ethylene regulates PCD which is observed both during the HR and disease development [174]. In agreement with phenotypic evaluation we detected HR-like response only in ID-85 where the genes related to ethylene resulted upregulated, suggesting a central role of ethylene in the activation of immune response. It's quite well known that the ERF subfamily proteins contain single AP2/ERF domain and mainly participate in responses to biotic stresses, such as pathogenesis, by binding the GCC-box present in the promoter of ET-inducible pathogenesis-related (PR) genes such as PR5 (thaumatin-like protein) that we found upregulated in ID-85 at 24 hpi.

In agreement with this evaluation, despite the very low expression of VvWRKY7 gene in ID-85 in the late stage of 48 hpi, we could suppose a negative regulation of plant immunity. Several studies suggested that expression of positive and negative regulators was fine-tuned and was dependent on the stage of disease and lifestyle of pathogens with a majority of positive WRKYs becoming active in the early stages of disease, whereas a majority of negative regulators becoming active during the later stages of disease. Indeed, VvWRKY7 TF, member of the WRKYIIId subfamily, was the first WRKY TF reported to bind CaM in a Ca²⁺-dependent manner [147], playing a role in plant defense responses. In particular, as reported in Kim et al., 2006 [146], plants downregulating WRKY7 showed a decrease susceptibility to the pathogen, suggesting a negative regulatory role for WRKY7 in plant defense responses against bacterial pathogens.

To complete the assessment, we focused the attention on VIT_201s0011g03730 gene detected in 2014 on chromosome 1 which, according to Devaiah et al., 2009 [145], was reported to be induced in *A. thaliana* in response to phosphate starvation. If the induction of MYB62, localized in the nucleus, was a specific response

in the leaves during Pi deprivation, on the other hand Pi starvation was known to induce anthocyanins production, useful for their antimicrobial activities. This could explain the overexpression of VvMYB62 in ID-85 in the later stages of infection at 24 hpi and 48 dpi, describing a first downregulation of this gene probably caused by an earlier activation of other defense genes such as stilbene synthases (STS) followed by a later increase of expression levels leading to the anthocyanins production.

‘Mgaloblishvili N.’ resilience: wild features as genetic resource

During the last years wild grapevine germplasm resources attracted the interest for disease-resistant traits, probably due to ancestral plant-pathogen coevolution and to resilience traits. Recent studies reported that the transcriptional regulation of the stilbene biosynthetic pathway was mediated by two R2R3-MYB-type transcription factors, MYB14 and MYB15 that were shown to activate the stilbene synthase promoter [168] and in Duan et al., 2015 [24] were described a few *V. sylvestris* genotypes found to be endowed with an elevated stilbene inducibility in response to inoculation with *P. viticola*. According to our analysis, both MYB14 and MYB15 were upregulated during the early stages of disease in the most tolerant accession ID-85 and downregulated in the parental line. Surprisingly, MYB15 was found overexpressed also in ID-139 despite the high standard deviation among biological replicates. In transient gene reporter assays [168], MYB14 and MYB15 were demonstrated to specifically activate the promoters of STS genes which, as previously described, are the central factors for the basal immunity of grapevine.

On the contrary, we detected an overexpression of MYBA gene, regulating UFGT (UDP-Glc:flavonoid-3-O-glucosyltransferase) enzyme responsible for the conversion of anthocyanidins to anthocyanins, in the susceptible ID-139 at 8 hpi, and a subsequent upregulation of the same in the later stage of disease at 24 hpi in ID-85. One possible scenario, able to explain these results, implied the competition for precursors between STS and CHS [173], indeed both CHS and STS use p-coumaroyl-CoA and malonyl-CoA as substrates and synthesize the same linear tetraketide intermediate, which is then converted in aromatic ring structures in clearly different steps. We could suppose that the primary defense which characterized the tolerance in ID-85 was defined by an early (8 hpi) strong induction of stilbene biosynthetic pathway leading to the accumulation of phytoalexins, such as resveratrol and viniferins, followed by a secondary (24 hpi) activation of CHS pathway, through the production of other antimicrobial transcripts, such as anthocyanins. This scenario bring back to the role of VIT_201s0011g03730 gene (VvMYB62), previously described as upregulated at 24 hpi in ID-85, determining a later accumulation of anthocyanins, consistent with these last obtained data and explaining the much higher levels of background activity of the STS promoters compared with the UFGT ones. Competition between the two branches of phenylpropanoid pathway with a differential regulation of the key enzymes CHS and STS was reported by Iriti et al., 2004 [175] therefore plant activators such as chemical compounds or, as in our case, the presence of the pathogen, could be able to reverse, to a certain degree, the inverse relationship between resveratrol and anthocyanin metabolic pathways, reducing CHS and STS competition for substrate binding and raising both anthocyanin and resveratrol synthesis.

On the other hand, we didn't observe any upregulation of defense genes in the parental line, except for VIT_201s0011g03470 gene (ERF118 like-protein) and this behavior probably mirrored the low LOD peaks detected in QTL analysis. These data suggested that there could be a small component in cultivar ‘Mgaloblishvili N.’ which define the tolerance to *P. viticola* infection and which is implied in basal immunity system, but it is mainly observed in some individuals of the offspring such as ID-85, obtained by a self-cross of the parental line. Overall, according to our phenotypic evaluation and gene expression analysis, the obtained data suggested a model similar to the ones described in Chang et al., 2011 [176], where resveratrol, in addition to its classical role as antimicrobial phytoalexin, represents an important regulator for initiation of HR-related cell death. Indeed, the overexpression of genes related to ethylene biosynthesis, to STS and CHS pathways, together with the accumulation of pathogenesis-related protein 5 (PR5) transcripts and the presence of HR like response in the most tolerant accession, summarized the probable defense mechanism which characterize the tolerance to *P.viticola* in ‘Mgaloblishvili N.’ cultivar.

Supplementary data

Table S1 Woody Plant Medium (WPM)

WPM basal salt mixture			WPM preparation	
Components	Concentrations [..]	Stock solution	Ingredients	1 liter
Macroelementi		[..] 10X (per 2l)	MilliQ water	Make up the volume
K ₂ SO ₄	990 mg l ⁻¹	19.8 g	WPM basal salt mixture	2.36 g
CaCl ₂ ×2H ₂ O	72.50 mg l ⁻¹	1.45 g	MS Vitamins (1000X)	1 ml
Ca(NO ₃) ₂	386.8 mg l ⁻¹	7.74 g	Myo-Inositol	100 mg
MgSO ₄	180.54 mg l ⁻¹	3.61 g	Sucrose	20 g
NH ₄ NO ₃	400 mg l ⁻¹	8.0 g		
KH ₂ PO ₄	170 mg l ⁻¹	3.4 g		
Microelementi		[..] 1000X (per 100 ml)	Adjust pH to 5.85 with NaOH 1M	
MnSO ₄ ×H ₂ O	22300 mg l ⁻¹	2.23 g	Phytigel 4,3 g/l	
ZnSO ₄ ×7H ₂ O	8600 mg l ⁻¹	0.86 g	Autoclave at 121°C for 20 min	
H ₃ BO ₃	6200 mg l ⁻¹	0.62 g		
CuSO ₄ ×5H ₂ O	250 mg l ⁻¹	0.025 g		
Na ₂ MoO ₄ ×2H ₂ O	250 mg l ⁻¹	0.025 g		
Ferro (come NN)		[..] 100X (per 100 ml)		
FeNaEDTA	36.7 mg l ⁻¹	0.367 g		

Table S2 MS Vitamins (Murashige&Skoog)[164]

MS Vitamins		
Vitamine		[..] 1000X (per 100 ml)
Myoinositol	100 mg l ⁻¹	Aggiunto separatamente
Thiamin×HCl	0.1 mg l ⁻¹	0.01 g
Nicotinic Acid	0.5 mg l ⁻¹	0.05 g
Pyridoxin×HCl	0.5 mg l ⁻¹	0.05 g
Glycine	2 mg l ⁻¹	0.2 g

Table S3 List of candidate genes. Description of genes tested in qRT-PCR assay.

Gene name	Gene ID	Genoscope	Annotation	Forward	Reverse
MYB14	VIT_207s0005g03340	GSVIVT00028596001	transcription factor myb14	TCTGAGGCCGGATATCAAAC	GGGACGCATCAAGAGAGTGT
MYB15	VIT_205s0049g01020	GSVIVT00020267001	transcription factor myb15	CAAGAATGAACAGATGGAGGAG	TCTGCGACTGCTGGGAAA
MYB62	VIT_201s0011g03730	GSVIVT01011872001	myb transcription factor	GCTTCGAAGAGGACCATGGAC	CTGCAACTCTTTCCAGTCCTC
MYBA1*	VIT_202s0033g00380	GSVIVT00038762001	transcription factor myba1	CTTTTCGGCTTCTGGAGAGA	CTGTGTTGCAGTTTCTTCTGTC
PAL	VIT_216s0039g01100	GSVIVT01024299001	Phenylalanine ammonia-lyase	TTGTCTCAGTGCTTGAACG	TTGAAAGCGTGACACAATC
VvSTS29	VIT_216s0100g00950,VIT_216s0100g00990, VIT_216s0100g01010	-	stilbene synthases	GGTTTTGGACCAGGCTTGACT	GAGATAAATACCTTACTCTATTCAAC
VvSTS41	VIT_216s0100g01130, VIT_216s0100g01160	-	stilbene synthases	GAGTACTATTTGGTTTTGGCCT	AACTCCTATTTGATACAAAACAACGT
PR10	VIT_05s0077g01530	GSVIVT01035055001	pathogenesis-related protein	GCACATCCCGATGCCTATTAAG	ACTTACTGAGACTGATAGATGCAATGAATA
PR5	VIT_202s0025g04290	GSVIVT01019842001	thaumatin-like protein	GATAGGTGTCCGGTGGCTTA	GGGCATGTAAAGGTGCTTGT
VIT_201s0011g03470	VIT_201s0011g03470	GSVIVT01011902001	ethylene-responsive transcription factor erf119	CCCTTTAGAGGTGTTTCGCGTC	GACAGCTACCGAGGAAGAAAC
WRKY13	VIT_207s0031g01840	GSVIVT01022259001	wrky transcription factor	CGACTCGTTTCTTTACGC	AGTGAGGTGGATGTTCTTG
WRKY33	VIT_206s0004g07500	GSVIVT01030258001	double wrky type transfactor	TTTGAGCCCTTTCATGC	GAGGCATTGTTGCCAGGTAT
WRKY57	VIT_201s0011g00720	GSVIVT01010525001	wrky transcription factor 57	GGGAATGGCCCTGTGTTT	AAATGAAATGAAATCAAACAACTGG
WRKY7	VIT_207s0031g00080	GSVIVT01022067001	wrky transcription factor	CAACTCCATGCTCTCCCTGT	CACCAACTCCACCATTTCTCT
UBQ			Ubiquitin C	GAGGGTCGTGAGGATTTGGA	GCCCTGCACCTACCATCTTTAAG
GADPH			Glycerinaldehyd-3-phosphat-Dehydrogenase	TCAAGGTCAAGGACTCTAACACC	CCAACAACGAACATAGGAGCA
ACTIN			Actin	TCCTTGCCTTGCCTCATCTAT	CACCAATCACTCTCTGCTAC

Table S4 ANOVA test and post-hoc Tukey HSD test.

VIT_207s0031g01840 WRKY13

`summary(anova)`

Df Sum Sq Mean Sq F value Pr(>F)

group 9 21.17 2.353 3.295 0.0126 *

Residuals 20 14.28 0.714

Signif. codes: 0 '***' 0.001 '**' 0.01 '*' 0.05 '.' 0.1 ' ' 1

`> TukeyHSD(anova, conf.level=.95)`

Tukey multiple comparisons of means

95% family-wise confidence level

Fit: aov(formula = data ~ group)

\$group	diff	lwr	upr	p adj
T24139-T0	0.52674883	-1.9163233	2.969821	0.9984208
T2485-T0	0.43675663	-2.0063155	2.8798288	0.9996364
T24L22-T0	-0.47738106	-2.9204532	1.9656911	0.9992631
T48139-T0	0.78217676	-1.6608954	3.2252489	0.9745782
T4885-T0	0.31290634	-2.1301658	2.7559785	0.999977
T48L22-T0	-0.72275303	-3.1658252	1.7203191	0.9847516
T8139-T0	2.39450393	-0.0485682	4.8375761	0.057626
T885-T0	1.26916503	-1.1739071	3.7122372	0.7051786
T8L22-T0	0.24935023	-2.1937219	2.6924224	0.9999967
T2485-T24139	-0.0899922	-2.5330643	2.3530799	1
T24L22-T24139	-1.00412989	-3.447202	1.4389422	0.8941908
T48139-T24139	0.25542793	-2.1876442	2.6985001	0.999996
T4885-T24139	-0.21384249	-2.6569146	2.2292296	0.9999991
T48L22-T24139	-1.24950186	-3.692574	1.1935703	0.7217629
T8139-T24139	1.8677551	-0.575317	4.3108272	0.2352
T885-T24139	0.7424162	-1.7006559	3.1854883	0.9818078
T8L22-T24139	-0.2773986	-2.7204707	2.1656735	0.9999918
T24L22-T2485	-0.91413769	-3.3572098	1.5289344	0.9357758
T48139-T2485	0.34542014	-2.097652	2.7884923	0.9999471
T4885-T2485	-0.12385029	-2.5669224	2.3192219	1
T48L22-T2485	-1.15950966	-3.6025818	1.2835625	0.7935041
T8139-T2485	1.95774731	-0.4853248	4.4008194	0.1890172
T885-T2485	0.8324084	-1.6106637	3.2754805	0.9626871
T8L22-T2485	-0.1874064	-2.6304785	2.2556657	0.9999997
T48139-T24L22	1.25955782	-1.1835143	3.70263	0.7133143
T4885-T24L22	0.7902874	-1.6527847	3.2333595	0.9728765
T48L22-T24L22	-0.24537197	-2.6884441	2.1977002	0.9999971
T8139-T24L22	2.871885	0.4288129	5.3149571	0.013565
T885-T24L22	1.74654609	-0.696526	4.1896182	0.309923
T8L22-T24L22	0.72673129	-1.7163408	3.1698034	0.9841874
T4885-T48139	-0.46927042	-2.9123426	1.9738017	0.9993561
T48L22-T48139	-1.50492979	-3.9480019	0.9381423	0.4982035

\$group	diff	lwr	upr	p adj
T8139-T48139	1.61232717	-0.830745	4.0553993	0.408909
T885-T48139	0.48698826	-1.9560839	2.9300604	0.9991386
T8L22-T48139	-0.53282653	-2.9758987	1.9102456	0.9982766
T48L22-T4885	-1.03565937	-3.4787315	1.4074128	0.8765961
T8139-T4885	2.0815976	-0.3614745	4.5246697	0.137594
T885-T4885	0.95625869	-1.4868135	3.3993308	0.9179118
T8L22-T4885	-0.06355611	-2.5066282	2.379516	1
T8139-T48L22	3.11725697	0.6741848	5.5603291	0.0062703
T885-T48L22	1.99191806	-0.4511541	4.4349902	0.1734793
T8L22-T48L22	0.97210326	-1.4709689	3.4151754	0.9104637
T885-T8139	-1.12533891	-3.568411	1.3177332	0.8184848
T8L22-T8139	-2.14515371	-4.5882258	0.2979184	0.1161315
T8L22-T885	-1.0198148	-3.4628869	1.4232573	0.8856311

VIT_207s0031g00080 WRKY7

> summary(anova)

```

      Df Sum Sq Mean Sq F value Pr(>F)
group   9  2.077  0.23080   2.885 0.0232 *
Residuals 20  1.600  0.08001

```

Signif. codes: 0 '***' 0.001 '**' 0.01 '*' 0.05 '.' 0.1 ' ' 1

> TukeyHSD(anova, conf.level=.95)

Tukey multiple comparisons of means

95% family-wise confidence level

Fit: aov(formula = data ~ group)

\$group	diff	lwr	upr	p adj
T24139-T0	-0.3856	-1.2034	0.43225	0.79925
T2485-T0	-0.1086	-0.9265	0.70919	0.99997
T24L22-T0	-0.5101	-1.3279	0.30772	0.48198
T48139-T0	-0.3711	-1.1889	0.44674	0.83022
T4885-T0	0.16013	-0.6577	0.97796	0.99925
T48L22-T0	-0.5531	-1.3709	0.26472	0.3778
T8139-T0	-0.2281	-1.0459	0.58973	0.98975
T885-T0	0.2264	-0.5914	1.04423	0.99026
T8L22-T0	-0.4259	-1.2438	0.3919	0.70246
T2485-T24139	0.27694	-0.5409	1.09477	0.96405
T24L22-T24139	-0.1245	-0.9424	0.69329	0.9999
T48139-T24139	0.01448	-0.8033	0.83231	1
T4885-T24139	0.5457	-0.2721	1.36353	0.39486
T48L22-T24139	-0.1675	-0.9854	0.6503	0.99893
T8139-T24139	0.15747	-0.6604	0.9753	0.99934
T885-T24139	0.61198	-0.2059	1.42981	0.25803
T8L22-T24139	-0.0404	-0.8582	0.77748	1

\$group	diff	lwr	upr	p adj
T24L22-T2485	-0.4015	-1.2193	0.41636	0.76273
T48139-T2485	-0.2625	-1.0803	0.55538	0.9742
T4885-T2485	0.26877	-0.5491	1.0866	0.97007
T48L22-T2485	-0.4445	-1.2623	0.37336	0.65449
T8139-T2485	-0.1195	-0.9373	0.69836	0.99993
T885-T2485	0.33504	-0.4828	1.15287	0.89593
T8L22-T2485	-0.3173	-1.1351	0.50054	0.92172
T48139-T24L22	0.13902	-0.6788	0.95685	0.99976
T4885-T24L22	0.67024	-0.1476	1.48807	0.16902
T48L22-T24L22	-0.043	-0.8608	0.77484	1
T8139-T24L22	0.28201	-0.5358	1.09984	0.95991
T885-T24L22	0.73652	-0.0813	1.55435	0.09995
T8L22-T24L22	0.08419	-0.7336	0.90202	1
T4885-T48139	0.53122	-0.2866	1.34905	0.42938
T48L22-T48139	-0.182	-0.9998	0.63581	0.99799
T8139-T48139	0.14299	-0.6748	0.96082	0.9997
T885-T48139	0.59749	-0.2203	1.41532	0.28473
T8L22-T48139	-0.0548	-0.8727	0.76299	1
T48L22-T4885	-0.7132	-1.5311	0.1046	0.12077
T8139-T4885	-0.3882	-1.2061	0.4296	0.79333
T885-T4885	0.06628	-0.7516	0.88411	1
T8L22-T4885	-0.5861	-1.4039	0.23178	0.30713
T8139-T48L22	0.325	-0.4928	1.14283	0.91106
T885-T48L22	0.77951	-0.0383	1.59734	0.06969
T8L22-T48L22	0.12718	-0.6907	0.94501	0.99988
T885-T8139	0.45451	-0.3633	1.27234	0.62802
T8L22-T8139	-0.1978	-1.0157	0.62001	0.99627
T8L22-T885	-0.6523	-1.4702	0.1655	0.19332

VIT_207s0005g03340 Myb14

[summary\(anova\)](#)

Df Sum Sq Mean Sq F value Pr(>F)

group 9 38.59 4.288 28.67 1.6e-09 ***

Residuals 20 2.99 0.150

Signif. codes: 0 '***' 0.001 '**' 0.01 '*' 0.05 '.' 0.1 ' ' 1

[> TukeyHSD\(anova, conf.level=.95\)](#)

Tukey multiple comparisons of means

95% family-wise confidence level

Fit: aov(formula = data ~ group)

\$group	diff	lwr	upr	p adj
T24139-T0	0.60087435	-0.51724467	1.71899338	0.6674751
T2485-T0	0.63794216	-0.48017686	1.75606119	0.5959186
T24L22-T0	-0.90773026	-2.02584928	0.21038877	0.1772636

\$group	diff	lwr	upr	p adj
T48139-T0	-0.58603249	-1.70415152	0.53208653	0.6955297
T4885-T0	0.23121546	-0.88690356	1.34933449	0.9988542
T48L22-T0	-0.97076444	-2.08888347	0.14735458	0.1238886
T8139-T0	0.36584579	-0.75227323	1.48396482	0.9708747
T885-T0	3.06686534	1.94874631	4.18498436	0.0000002
T8L22-T0	-0.81098226	-1.92910128	0.30713677	0.2930438
T2485-T24139	0.03706781	-1.08105122	1.15518684	1
T24L22-T24139	-1.50860461	-2.62672363	-0.39048558	0.0035542
T48139-T24139	-1.18690684	-2.30502587	-0.06878782	0.0319434
T4885-T24139	-0.36965889	-1.48777792	0.74846014	0.9689458
T48L22-T24139	-1.57163879	-2.68975782	-0.45351977	0.0022947
T8139-T24139	-0.23502856	-1.35314759	0.88309047	0.9987001
T885-T24139	2.46599098	1.34787196	3.58411001	0.0000063
T8L22-T24139	-1.41185661	-2.52997564	-0.29373758	0.0069462
T24L22-T2485	-1.54567242	-2.66379144	-0.42755339	0.0027479
T48139-T2485	-1.22397465	-2.34209368	-0.10585563	0.0249751
T4885-T2485	-0.4067267	-1.52484573	0.71139233	0.9452246
T48L22-T2485	-1.6087066	-2.72682563	-0.49058758	0.0017744
T8139-T2485	-0.27209637	-1.3902154	0.84602266	0.9960993
T885-T2485	2.42892317	1.31080415	3.5470422	0.0000078
T8L22-T2485	-1.44892442	-2.56704344	-0.33080539	0.0053757
T48139-T24L22	0.32169776	-0.79642126	1.43981679	0.9873409
T4885-T24L22	1.13894572	0.02082669	2.25706474	0.0437149
T48L22-T24L22	-0.06303419	-1.18115321	1.05508484	1
T8139-T24L22	1.27357605	0.15545702	2.39169507	0.017895
T885-T24L22	3.97459559	2.85647656	5.09271462	0
T8L22-T24L22	0.096748	-1.02137103	1.21486702	0.9999992
T4885-T48139	0.81724796	-0.30087107	1.93536698	0.2842208
T48L22-T48139	-0.38473195	-1.50285097	0.73338708	0.9604194
T8139-T48139	0.95187828	-0.16624074	2.06999731	0.1382329
T885-T48139	3.65289783	2.5347788	4.77101685	0
T8L22-T48139	-0.22494976	-1.34306879	0.89316926	0.9990742
T48L22-T4885	-1.2019799	-2.32009893	-0.08386088	0.0289117
T8139-T4885	0.13463033	-0.9834887	1.25274936	0.9999864
T885-T4885	2.83564987	1.71753085	3.9537689	0.0000007
T8L22-T4885	-1.04219772	-2.16031675	0.07592131	0.0806436
T8139-T48L22	1.33661023	0.21849121	2.45472926	0.0116536
T885-T48L22	4.03762978	2.91951075	5.1557488	0
T8L22-T48L22	0.15978218	-0.95833684	1.27790121	0.9999421
T885-T8139	2.70101954	1.58290052	3.81913857	0.0000015
T8L22-T8139	-1.17682805	-2.29494708	-0.05870902	0.0341363
T8L22-T885	-3.87784759	-4.99596662	-2.75972857	0

VIT_201s0011g03730 Myb-TF

summary(anova)

```

      Df Sum Sq Mean Sq F value Pr(>F)
group    9 27.926  3.1029  10.4 8.54e-06 ***
Residuals 20  5.969  0.2985

```

Signif. codes: 0 '***' 0.001 '**' 0.01 '*' 0.05 '.' 0.1 ' ' 1

> TukeyHSD(anova, conf.level=.95)

Tukey multiple comparisons of means

95% family-wise confidence level

Fit: aov(formula = data ~ group)

\$group	diff	lwr	upr	p adj
T24139-T0	-0.52813077	-2.1077027	1.0514411	0.9667249
T2485-T0	2.207429695	0.6278578	3.7870016	0.002444
T24L22-T0	-0.15565167	-1.7352236	1.4239202	0.9999976
T48139-T0	-0.05249397	-1.6320659	1.5270779	1
T4885-T0	1.775990446	0.1964186	3.3555623	0.019992
T48L22-T0	-0.77433146	-2.3539034	0.8052404	0.7640594
T8139-T0	0.081819467	-1.4977524	1.6613914	1
T885-T0	-0.18448082	-1.7640527	1.3950911	0.9999895
T8L22-T0	-0.76933174	-2.3489036	0.8102401	0.7701553
T2485-T24139	2.735560462	1.1559886	4.3151324	0.0001883
T24L22-T24139	0.372479102	-1.2070928	1.952051	0.9969048
T48139-T24139	0.475636794	-1.1039351	2.0552087	0.9828649
T4885-T24139	2.304121213	0.7245493	3.8836931	0.0015203
T48L22-T24139	-0.2462007	-1.8257726	1.3333712	0.999881
T8139-T24139	0.609950234	-0.9696217	2.1895221	0.9236671
T885-T24139	0.343649951	-1.2359219	1.9232218	0.9983087
T8L22-T24139	-0.24120098	-1.8207729	1.3383709	0.9998995
T24L22-T2485	-2.36308136	-3.9426533	-0.7835095	0.001139
T48139-T2485	-2.25992367	-3.8394956	-0.6803518	0.0018885
T4885-T2485	-0.43143925	-2.0110111	1.1481326	0.9911259
T48L22-T2485	-2.98176116	-4.5613331	-1.4021893	0.0000593
T8139-T2485	-2.12561023	-3.7051821	-0.5460383	0.0036533
T885-T2485	-2.39191051	-3.9714824	-0.8123386	0.0009892
T8L22-T2485	-2.97676144	-4.5563333	-1.3971895	0.0000607
T48139-T24L22	0.103157692	-1.4764142	1.6827296	0.9999999
T4885-T24L22	1.931642111	0.3520702	3.511214	0.0094395
T48L22-T24L22	-0.6186798	-2.1982517	0.9608921	0.9176218
T8139-T24L22	0.237471132	-1.3421008	1.817043	0.9999117
T885-T24L22	-0.02882915	-1.608401	1.5507427	1
T8L22-T24L22	-0.61368008	-2.193252	0.9658918	0.9211196
T4885-T48139	1.828484419	0.2489125	3.4080563	0.0155488

\$group	diff	lwr	upr	p adj
T48L22-T48139	-0.72183749	-2.3014094	0.8577344	0.8247488
T8139-T48139	0.13431344	-1.4452585	1.7138853	0.9999993
T885-T48139	-0.13198684	-1.7115587	1.4475851	0.9999994
T8L22-T48139	-0.71683777	-2.2964097	0.8627341	0.8301091
T48L22-T4885	-2.55032191	-4.1298938	-0.97075	0.0004579
T8139-T4885	-1.69417098	-3.2737429	-0.1145991	0.0294417
T885-T4885	-1.96047126	-3.5400432	-0.3808994	0.008203
T8L22-T4885	-2.54532219	-4.1248941	-0.9657503	0.0004691
T8139-T48L22	0.856150931	-0.723421	2.4357228	0.657608
T885-T48L22	0.589850647	-0.9897212	2.1694225	0.9364907
T8L22-T48L22	0.004999719	-1.5745722	1.5845716	1
T885-T8139	-0.26630028	-1.8458722	1.3132716	0.9997736
T8L22-T8139	-0.85115121	-2.4307231	0.7284207	0.6643776
T8L22-T885	-0.58485093	-2.1644228	0.994721	0.9394457

MybA

[summary\(anova\)](#)

Df Sum Sq Mean Sq F value Pr(>F)

group 9 25.09 2.788 2.694 0.0312 *

Residuals 20 20.70 1.035

Signif. codes: 0 '***' 0.001 '**' 0.01 '*' 0.05 '.' 0.1 ' ' 1

[> TukeyHSD\(anova, conf.level=.95\)](#)

Tukey multiple comparisons of means

95% family-wise confidence level

Fit: aov(formula = data ~ group)

\$group	diff	lwr	upr	p adj
T24139-T0	-0.75636651	-3.6976924	2.1849593	0.9941922
T2485-T0	0.97756521	-1.9637606	3.9188911	0.9679225
T24L22-T0	-0.52729527	-3.4686211	2.4140306	0.9996282
T48139-T0	0.51353427	-2.4277916	3.4548601	0.9996995
T4885-T0	0.95462347	-1.9867024	3.8959493	0.9723084
T48L22-T0	-0.65782532	-3.5991512	2.2835005	0.9979154
T8139-T0	2.03755176	-0.9037741	4.9788776	0.3479155
T885-T0	-0.57467821	-3.5160041	2.3666477	0.9992637
T8L22-T0	-0.7799224	-3.7212483	2.1614035	0.9927838
T2485-T24139	1.73393172	-1.2073941	4.6752576	0.554818
T24L22-T24139	0.22907124	-2.7122546	3.1703971	0.9999997
T48139-T24139	1.26990078	-1.6714251	4.2112266	0.8651808
T4885-T24139	1.71098998	-1.2303359	4.6523158	0.5717001
T48L22-T24139	0.09854119	-2.8427847	3.039867	1
T8139-T24139	2.79391827	-0.1474076	5.7352441	0.0712915
T885-T24139	0.1816883	-2.7596376	3.1230142	1
T8L22-T24139	-0.02355589	-2.9648817	2.91777	1
T24L22-T2485	-1.50486048	-4.4461863	1.4364654	0.7213957

\$group	diff	lwr	upr	p adj
T48139-T2485	-0.46403094	-3.4053568	2.4772949	0.9998685
T4885-T2485	-0.02294174	-2.9642676	2.9183841	1
T48L22-T2485	-1.63539053	-4.5767164	1.3059353	0.6274692
T8139-T2485	1.05998655	-1.8813393	4.0013124	0.9480804
T885-T2485	-1.55224342	-4.4935693	1.3890824	0.6879471
T8L22-T2485	-1.75748761	-4.6988135	1.1838383	0.5375615
T48139-T24L22	1.04082954	-1.9004963	3.9821554	0.9532914
T4885-T24L22	1.48191874	-1.4594071	4.4232446	0.7372055
T48L22-T24L22	-0.13053006	-3.0718559	2.8107958	1
T8139-T24L22	2.56484703	-0.3764788	5.5061729	0.1208495
T885-T24L22	-0.04738294	-2.9887088	2.8939429	1
T8L22-T24L22	-0.25262713	-3.193953	2.6886987	0.9999993
T4885-T48139	0.4410892	-2.5002367	3.3824151	0.9999135
T48L22-T48139	-1.17135959	-4.1126855	1.7699663	0.9100621
T8139-T48139	1.52401749	-1.4173084	4.4653434	0.7079905
T885-T48139	-1.08821248	-4.0295383	1.8531134	0.9397078
T8L22-T48139	-1.29345667	-4.2347825	1.6478692	0.8529369
T48L22-T4885	-1.61244879	-4.5537747	1.3288771	0.6443106
T8139-T4885	1.08292829	-1.8583976	4.0242542	0.9413392
T885-T4885	-1.52930168	-4.4706275	1.4120242	0.7042633
T8L22-T4885	-1.73454586	-4.6758717	1.20678	0.5543669
T8139-T48L22	2.69537708	-0.2459488	5.6367029	0.08981
T885-T48L22	0.08314712	-2.8581787	3.024473	1
T8L22-T48L22	-0.12209707	-3.0634229	2.8192288	1
T885-T8139	-2.61222997	-5.5535558	0.3290959	0.1086432
T8L22-T8139	-2.81747416	-5.7588	0.1238517	0.0674102
T8L22-T885	-0.20524419	-3.14657	2.7360817	0.9999999

VIT_201s0011g03470 ERF-TF

summary(anova)

Df Sum Sq Mean Sq F value Pr(>F)

group 9 12.032 1.3369 5.687 6e-04 ***

Residuals 20 4.702 0.2351

Signif. codes: 0 '***' 0.001 '**' 0.01 '*' 0.05 '.' 0.1 ' ' 1

> TukeyHSD(anova, conf.level=.95)

Tukey multiple comparisons of means

95% family-wise confidence level

Fit: aov(formula = data ~ group)

\$group	diff	lwr	upr	p adj
T24139-T0	0.22779416	-1.17410933	1.62969764	0.9998324
T2485-T0	0.06277283	-1.33913066	1.46467632	1
T24L22-T0	1.37568717	-0.02621632	2.77759065	0.0571452
T48139-T0	0.34747373	-1.05442976	1.74937722	0.9955423
T4885-T0	1.20267615	-0.19922734	2.60457964	0.132497

\$group	diff	lwr	upr	p adj
T48L22-T0	1.05077569	-0.3511278	2.45267918	0.2562284
T8139-T0	-0.45282636	-1.85472985	0.94907713	0.9731238
T885-T0	-0.32750415	-1.72940764	1.07439934	0.997112
T8L22-T0	-0.30360648	-1.70550997	1.09829701	0.9983665
T2485-T24139	-0.16502132	-1.56692481	1.23688216	0.9999888
T24L22-T24139	1.14789301	-0.25401048	2.5497965	0.1697812
T48139-T24139	0.11967957	-1.28222392	1.52158306	0.9999993
T4885-T24139	0.97488199	-0.4270215	2.37678548	0.3432002
T48L22-T24139	0.82298153	-0.57892195	2.22488502	0.5601382
T8139-T24139	-0.68062051	-2.082524	0.72128297	0.7731248
T885-T24139	-0.5552983	-1.95720179	0.84660518	0.9125696
T8L22-T24139	-0.53140064	-1.93330413	0.87050285	0.9310023
T24L22-T2485	1.31291433	-0.08898915	2.71481782	0.0782196
T48139-T2485	0.2847009	-1.11720259	1.68660438	0.9990041
T4885-T2485	1.13990332	-0.26200017	2.54180681	0.1758768
T48L22-T2485	0.98800286	-0.41390063	2.38990635	0.3269597
T8139-T2485	-0.51559919	-1.91750268	0.8863043	0.941691
T885-T2485	-0.39027698	-1.79218047	1.01162651	0.9898805
T8L22-T2485	-0.36637931	-1.7682828	1.03552417	0.9934851
T48139-T24L22	-1.02821344	-2.43011693	0.37369005	0.2803012
T4885-T24L22	-0.17301102	-1.5749145	1.22889247	0.9999832
T48L22-T24L22	-0.32491147	-1.72681496	1.07699201	0.9972776
T8139-T24L22	-1.82851352	-3.23041701	-0.42661004	0.0050352
T885-T24L22	-1.70319131	-3.1050948	-0.30128783	0.0100358
T8L22-T24L22	-1.67929365	-3.08119714	-0.27739016	0.0114365
T4885-T48139	0.85520242	-0.54670107	2.25710591	0.5108284
T48L22-T48139	0.70330196	-0.69860153	2.10520545	0.7415131
T8139-T48139	-0.80030009	-2.20220357	0.6016034	0.5952294
T885-T48139	-0.67497788	-2.07688136	0.72692561	0.7807494
T8L22-T48139	-0.65108021	-2.0529837	0.75082328	0.8118375
T48L22-T4885	-0.15190046	-1.55380395	1.25000303	0.9999945
T8139-T4885	-1.65550251	-3.057406	-0.25359902	0.0130203
T885-T4885	-1.5301803	-2.93208379	-0.12827681	0.025573
T8L22-T4885	-1.50628263	-2.90818612	-0.10437914	0.0290291
T8139-T48L22	-1.50360205	-2.90550554	-0.10169856	0.0294434
T885-T48L22	-1.37827984	-2.78018333	0.02362365	0.0563987
T8L22-T48L22	-1.35438217	-2.75628566	0.04752132	0.063632
T885-T8139	0.12532221	-1.27658128	1.5272257	0.999999
T8L22-T8139	0.14921988	-1.25268361	1.55112336	0.9999953
T8L22-T885	0.02389767	-1.37800582	1.42580115	1

PR5

summary(anova)

```

Df Sum Sq Mean Sq F value Pr(>F)
group    9 10.327  1.1474  2.758 0.0282 *
Residuals 20  8.322  0.4161

```

Signif. codes: 0 '***' 0.001 '**' 0.01 '*' 0.05 '.' 0.1 ' ' 1

> TukeyHSD(anova, conf.level=.95)

Tukey multiple comparisons of means

95% family-wise confidence level

Fit: aov(formula = data ~ group)

\$group	diff	lwr	upr	p adj
T24139-T0	-0.58967552	-2.4547047	1.2753536	0.9765165
T2485-T0	0.92268074	-0.9423484	2.7877099	0.7552704
T24L22-T0	-0.50086122	-2.3658904	1.3641679	0.9921112
T48139-T0	-0.6150001	-2.4800292	1.250029	0.9694373
T4885-T0	1.00108639	-0.8639428	2.8661155	0.6688183
T48L22-T0	-0.75393575	-2.6189649	1.1110934	0.9027882
T8139-T0	-0.25569923	-2.1207284	1.6093299	0.9999591
T885-T0	-0.15656294	-2.0215921	1.7084662	0.9999994
T8L22-T0	-0.34927725	-2.2143064	1.5157519	0.9994731
T2485-T24139	1.51235626	-0.3526729	3.3773854	0.1782864
T24L22-T24139	0.0888143	-1.7762148	1.9538434	1
T48139-T24139	-0.02532458	-1.8903537	1.8397046	1
T4885-T24139	1.59076191	-0.2742672	3.4557911	0.1367978
T48L22-T24139	-0.16426023	-2.0292894	1.7007689	0.9999991
T8139-T24139	0.33397629	-1.5310529	2.1990054	0.9996315
T885-T24139	0.43311258	-1.4319166	2.2981417	0.9972368
T8L22-T24139	0.24039827	-1.6246309	2.1054274	0.9999757
T24L22-T2485	-1.42354196	-3.2885711	0.4414872	0.2368767
T48139-T2485	-1.53768084	-3.40271	0.3273483	0.1638877
T4885-T2485	0.07840565	-1.7866235	1.9434348	1
T48L22-T2485	-1.67661649	-3.5416456	0.1884127	0.1010311
T8139-T2485	-1.17837997	-3.0434091	0.6866492	0.4652269
T885-T2485	-1.07924368	-2.9442728	0.7857855	0.5782788
T8L22-T2485	-1.27195799	-3.1369871	0.5930712	0.3672751
T48139-T24L22	-0.11413888	-1.979168	1.7508903	1
T4885-T24L22	1.50194761	-0.3630815	3.3669768	0.1844928
T48L22-T24L22	-0.25307453	-2.1181037	1.6119546	0.9999625
T8139-T24L22	0.24516199	-1.6198672	2.1101911	0.9999713
T885-T24L22	0.34429828	-1.5207309	2.2093274	0.99953
T8L22-T24L22	0.15158398	-1.7134452	2.0166131	0.9999996
T4885-T48139	1.61608649	-0.2489427	3.4811156	0.1252652
T48L22-T48139	-0.13893565	-2.0039648	1.7260935	0.9999998
T8139-T48139	0.35930087	-1.5057283	2.22433	0.9993409

\$group	diff	lwr	upr	p adj
T885-T48139	0.45843716	-1.406592	2.3234663	0.9958033
T8L22-T48139	0.26572285	-1.5993063	2.130752	0.9999436
T48L22-T4885	-1.75502214	-3.6200513	0.110007	0.0758247
T8139-T4885	-1.25678562	-3.1218148	0.6082435	0.3823577
T885-T4885	-1.15764933	-3.0226785	0.7073798	0.4883006
T8L22-T4885	-1.35036364	-3.2153928	0.5146655	0.2950611
T8139-T48L22	0.49823652	-1.3667926	2.3632657	0.9923958
T885-T48L22	0.59737281	-1.2676563	2.462402	0.9745075
T8L22-T48L22	0.4046585	-1.4603706	2.2696876	0.9983431
T885-T8139	0.09913629	-1.7658929	1.9641654	1
T8L22-T8139	-0.09357802	-1.9586072	1.7714511	1
T8L22-T885	-0.19271431	-2.0577435	1.6723148	0.9999964

WRKY33

summary(anova)

```

Df Sum Sq Mean Sq F value Pr(>F)
group    9  6.848  0.7609  2.554 0.0387 *
Residuals 20  5.958  0.2979

```

Signif. codes: 0 '***' 0.001 '**' 0.01 '*' 0.05 '.' 0.1 ' ' 1

> TukeyHSD(anova, conf.level=.95)

Tukey multiple comparisons of means

95% family-wise confidence level

Fit: aov(formula = data ~ group)

\$group	diff	lwr	upr	p adj
T24139-T0	-0.55938396	-2.13742289	1.018655	0.9528143
T2485-T0	0.45719405	-1.12084487	2.035233	0.9867345
T24L22-T0	-0.38144156	-1.95948049	1.1965974	0.9962867
T48139-T0	-0.5105442	-2.08858313	1.0674947	0.9728503
T4885-T0	0.09596532	-1.48207361	1.6740042	1
T48L22-T0	-0.62416239	-2.20220132	0.9538765	0.9132336
T8139-T0	-0.10953598	-1.68757491	1.468503	0.9999999
T885-T0	0.98005988	-0.59797905	2.5580988	0.487572
T8L22-T0	0.11132867	-1.46671026	1.6893676	0.9999999
T2485-T24139	1.01657802	-0.56146091	2.5946169	0.4400546
T24L22-T24139	0.1779424	-1.40009653	1.7559813	0.9999923
T48139-T24139	0.04883976	-1.52919917	1.6268787	1
T4885-T24139	0.65534928	-0.92268965	2.2333882	0.8885241
T48L22-T24139	-0.06477843	-1.64281736	1.5132605	1
T8139-T24139	0.44984798	-1.12819095	2.0278869	0.9881066
T885-T24139	1.53944385	-0.03859508	3.1174828	0.0595276
T8L22-T24139	0.67071263	-0.9073263	2.2487516	0.8750076
T24L22-T2485	-0.83863562	-2.41667455	0.7394033	0.680126
T48139-T2485	-0.96773826	-2.54577719	0.6103007	0.5039978

\$group	diff	lwr	upr	p adj
T4885-T2485	-0.36122874	-1.93926767	1.2168102	0.997518
T48L22-T2485	-1.08135645	-2.65939538	0.4966825	0.3613473
T8139-T2485	-0.56673003	-2.14476896	1.0113089	0.9491027
T885-T2485	0.52286583	-1.0551731	2.1009048	0.9685205
T8L22-T2485	-0.34586539	-1.92390432	1.2321735	0.9982109
T48139-T24L22	-0.12910264	-1.70714157	1.4489363	0.9999995
T4885-T24L22	0.47740688	-1.10063205	2.0554458	0.9823309
T48L22-T24L22	-0.24272083	-1.82075976	1.3353181	0.9998933
T8139-T24L22	0.27190559	-1.30613334	1.8499445	0.9997298
T885-T24L22	1.36150145	-0.21653748	2.9395404	0.1283559
T8L22-T24L22	0.49277023	-1.0852687	2.0708092	0.9783086
T4885-T48139	0.60650952	-0.97152941	2.1845484	0.9255791
T48L22-T48139	-0.11361819	-1.69165712	1.4644207	0.9999998
T8139-T48139	0.40100822	-1.17703071	1.9790472	0.9946645
T885-T48139	1.49060408	-0.08743485	3.068643	0.0739658
T8L22-T48139	0.62187287	-0.95616606	2.1999118	0.9149018
T48L22-T4885	-0.72012771	-2.29816664	0.8579112	0.8258383
T8139-T4885	-0.20550129	-1.78354022	1.3725376	0.9999735
T885-T4885	0.88409457	-0.69394436	2.4621335	0.6182757
T8L22-T4885	0.01536335	-1.56267558	1.5934023	1
T8139-T48L22	0.51462642	-1.06341251	2.0926653	0.971467
T885-T48L22	1.60422228	0.02618335	3.1822612	0.0443636
T8L22-T48L22	0.73549106	-0.84254787	2.31353	0.8089126
T885-T8139	1.08959586	-0.48844307	2.6676348	0.3519386
T8L22-T8139	0.22086465	-1.35717428	1.7989036	0.9999514
T8L22-T885	-0.86873121	-2.44677014	0.7093077	0.6393349

VIT_205s0049g01020 Myb15

summary(anova)

```

Df Sum Sq Mean Sq F value Pr(>F)
group    9  130.9   14.55   2.012 0.0925 .
Residuals 20  144.6    7.23

```

Signif. codes: 0 '***' 0.001 '**' 0.01 '*' 0.05 '.' 0.1 ' ' 1

> TukeyHSD(anova, conf.level=.95)

Tukey multiple comparisons of means

95% family-wise confidence level

Fit: aov(formula = data ~ group)

\$group	diff	lwr	upr	p adj
T24139-T0	-0.594301	-8.368422	7.17982	0.9999997
T2485-T0	2.47290528	-5.301216	10.247026	0.9755972
T24L22-T0	-0.6771042	-8.451225	7.097017	0.9999992
T48139-T0	0.05878927	-7.715332	7.83291	1
T4885-T0	1.97216073	-5.80196	9.746282	0.9947297

\$group	diff	lwr	upr	p adj
T48L22-T0	-0.71130707	-8.485428	7.062814	0.9999987
T8139-T0	5.10764671	-2.666474	12.881768	0.4146624
T885-T0	4.34706167	-3.427059	12.121183	0.6206123
T8L22-T0	-0.5762287	-8.35035	7.197892	0.9999998
T2485-T24139	3.06720629	-4.706915	10.841327	0.9143739
T24L22-T24139	-0.08280319	-7.856924	7.691318	1
T48139-T24139	0.65309027	-7.121031	8.427211	0.9999994
T4885-T24139	2.56646173	-5.207659	10.340583	0.9692221
T48L22-T24139	-0.11700606	-7.891127	7.657115	1
T8139-T24139	5.70194771	-2.072173	13.476069	0.2802835
T885-T24139	4.94136268	-2.832758	12.715484	0.4574607
T8L22-T24139	0.0180723	-7.756049	7.792193	1
T24L22-T2485	-3.15000948	-10.92413	4.624111	0.9016153
T48139-T2485	-2.41411602	-10.188237	5.360005	0.979071
T4885-T2485	-0.50074455	-8.274865	7.273376	0.9999999
T48L22-T2485	-3.18421235	-10.958333	4.589908	0.8960316
T8139-T2485	2.63474142	-5.139379	10.408862	0.9638677
T885-T2485	1.87415639	-5.899964	9.648277	0.9963583
T8L22-T2485	-3.04913398	-10.823255	4.724987	0.9170153
T48139-T24L22	0.73589346	-7.038227	8.510014	0.9999983
T4885-T24L22	2.64926493	-5.124856	10.423386	0.9626488
T48L22-T24L22	-0.03420287	-7.808324	7.739918	1
T8139-T24L22	5.7847509	-1.98937	13.558872	0.2641816
T885-T24L22	5.02416587	-2.749955	12.798287	0.4359128
T8L22-T24L22	0.1008755	-7.673245	7.874996	1
T4885-T48139	1.91337146	-5.860749	9.687492	0.9957642
T48L22-T48139	-0.77009633	-8.544217	7.004024	0.9999975
T8139-T48139	5.04885744	-2.725263	12.822978	0.4295758
T885-T48139	4.28827241	-3.485848	12.062393	0.6369709
T8L22-T48139	-0.63501797	-8.409139	7.139103	0.9999995
T48L22-T4885	-2.68346779	-10.457589	5.090653	0.9596642
T8139-T4885	3.13548598	-4.638635	10.909607	0.9039309
T885-T4885	2.37490095	-5.39922	10.149022	0.9811743
T8L22-T4885	-2.54838943	-10.32251	5.225731	0.9705381
T8139-T48L22	5.81895377	-1.955167	13.593075	0.2577259
T885-T48L22	5.05836874	-2.715752	12.83249	0.4271461
T8L22-T48L22	0.13507837	-7.639042	7.909199	1
T885-T8139	-0.76058503	-8.534706	7.013536	0.9999977
T8L22-T8139	-5.68387541	-13.457996	2.090245	0.2838867
T8L22-T885	-4.92329037	-12.697411	2.85083	0.4622211

Chapter 5

GENERAL DISCUSSION

General discussion

The recent introduction of international vine varieties has reduced the variety of vineyards and at the same time, despite the production of resistant hybrids, pathogens have managed to overcome the resistance, making the process of breeding and genetic improvement essential. For these reasons, in the last period, priority was given to the recovery, characterization, selection and valorization of indigenous or cultivated vines for a long time in narrow vine areas. Several studies have confirmed the existence of different degrees of tolerance to *P. viticola* in varieties of *V. vinifera* suggesting the presence of defense mechanisms of which nature needs to be deepened.

This chapter will discuss the major aspects dealt with this thesis. The reasoning of the chosen accessions, the potential approaches in breeding and the possible future perspectives to deepen the research.

In spite of the abundance of archaeological, historical and genetic data, the origins, historical biogeography, identity of ancient grapevine cultivars and mechanisms of domestication are still largely unknown. In this research work a pool of 25 Caucasian accessions has been studied under different point of views since their low susceptibility to *P. viticola* infection. This germplasm collection has been deepened by a comparative phylogenetic analysis which involved several accessions, both wild and cultivated, to better understand its genetic location worldwide. According to our results, all of these accessions, characterized by high genetic diversity and high number of private alleles, have originated in Georgia which is considered, from many years, the center of grapevine domestication. Furthermore, the chloroplast analysis inferred the presence of a niche with ancestral features which could represent a bridge between subsp. *sylvestris* and *sativa* suggesting the presence of undisclosed potential agronomical traits of interest. The characterization of few ancient varieties tolerant to downy mildew disease allowed to consider the existence of resilience characters which partially define this interesting trait.

In order to study the tolerance in this germplasm collection, 'Mgaloblishvili N.', the cultivar which show the most interesting trait across the years, has been mainly deepened by using integrative approaches. 'Mgaloblishvili N.' belonging to Georgian accessions, according to our analysis, has been classified among the ancestral varieties, considering the quality of wine, the genetic and plastid analysis and the phylogeny.

The aim of many plant researches is to explain natural phenotypic variation in terms of simple changes in DNA sequence and use these functional changes to improve the breeding programs. Conventionally, linkage mapping has been the most commonly implemented method to identify QTLs responsible for phenotypic variation. So far, no genetic maps based on Georgian cultivars have been realized and in this thesis, we constructed one map by self-crossing 'Mgaloblishvili N.'. We employed a self-fertilization in order to avoid the loss of the trait of interest since its relative tolerance. The map was essentially performed using SSRs and SNPs and despite the high homozygosity of the accessions used, we were able to obtain a map covering all the 19 LGs. The choice to use a self-crossed mapping population revealed two main aspects: the high segregation distortion in specific *hotspots* and the problem of inbreeding depression. There is a variety of mechanisms that can cause segregation distortion and in most systems acts in genetic factors including pollen tube competition, pollen lethal, preferential fertilization, sterility and chromosome translocation. According to our results, despite the well conserved order of markers compared with already published maps, we detected a few *hotspots* for SD present on chr 8 and 5, suggesting a balanced chromosome translocation. This results are partially confirmed by Fornasiero et al., 2016 (oral communication) [141] which reported, in a poster session of an International conference, that self-fertilization of *V. vinifera* cultivars leads to high levels of SD and to the emergence of several epistatic effects due to unfavorable combinations of alleles in essential genes. On the other hand, much attention has focused on self-fertilization, the most extreme form of inbreeding, which is widespread in plant populations. Inbreeding depression is often caused by a combination of nearly recessive

highly deleterious (lethal and semi-lethal) mutations and moderately recessive or nearly additive mildly deleterious mutations. This aspect could be the cause of the inconstant phenotypic behavior of the studied mapping population, together with the climate changes across the years which probably also influenced the pathogen aggressiveness. Indeed, inbreeding depression occurs when the parental line has spreads to the offspring traits that negatively influence their fitness, largely due to homozygosity. Additionally, the low coverage of obtained genetic map and the presence of gaps could also be influenced by presumably occurred double crossing over. However, the 'Mgaloblishvili N.' genetic map, has been useful to perform a preliminary QTL analysis, which allowed us to study the major regions of interest and analyze possible genes related to pathogen response. The limiting factor of QTL analysis was the lack of correlations of phenotypic data across the years which didn't allow to define a clear result, despite the presence of interesting LOD peaks. To solve this problem our approach provided for the study of obtained results separately, in order to understand if the single results could be comparable. With this approach we considered different regions of interest in which were detected several interesting genes to be deepened. Nevertheless, since the lack of data repeatability, we were not able to identify the putative alleles linked to the trait and we decided to study the tolerance trait with an integrative approach based on the gene expression of CGs.

The availability of modern techniques for in vitro propagation allowed us to set up, in a pretty short period, a gene expression experiment by using different replicas of the parental line and other two accessions of the offspring, employing a method based on the qRT-PCR by following the pathogen infection at different time points. The choice of CGs represented the most critical step. The choice has been done on the base of QTL analysis results together with literature records focused on ancestral varieties. The inconstant behavior of 'Mgaloblishvili N.' was confirmed also among the biological replicas of the chosen genotypes of the offspring, making more complex the study of the trait. Despite the high standard deviation we were able to define a few genes, strictly associated to phytoalexins pathway and related to ethylene production, highly expressed in the most tolerant accessions. Our results demonstrated that a few genes involved in ethylene biosynthesis as well as ethylene responsive factors appeared to be induced during the early stages of infection, despite, basically, JA and SA play a key role in plant immunity, and only a marginal function is assumed by ET. Moreover, MYB TFs, related to secondary metabolism and chosen for their key role in defense response to pathogen in ancestral and wild varieties, have been found more modulated in the resistant genotype.

In light of this, results obtained from QTL analysis could be partially comparable to the ones obtained with gene expression analysis, indicating that surely 'Mgaloblishvili N.' represents an interesting source of tolerance to downy mildew, presumably due to its ancestral features. Overall, it is strongly necessary to be aware that if the trait of interest is a tolerance then it might be difficult to be identified especially if it is highly influenced by environmental effects. The difficulty to reproduce the tolerant phenotype in our experiments could be due to the use of young seedlings, which presumably might not have a good fitness.

Perspectives

Considering our results together with phenotypic evaluation carried out from the colleagues of University of Milan, we could conclude that the experimental inoculations carried out on Mgaloblishvili N. and its progenies indicated a tolerance which seem to be caused by a recessive character since only the offspring deriving from self-pollination kept the phenotype of interest. On the other hand, we could not be able to detect a clear response to pathogen infection because of the inbreeding depression process which probably influenced the fitness of the seedlings. Presumably, more reliable results and phenotypic evaluation could be achieved on adult and more robust plants by transferring the entire mapping population in the field. This approach could allow a more stable environment for the successive analysis. Moreover, a more strict QTL analysis, could imply the search of new interesting CGs to be tested on the parental line and its offspring, improving our results. In the next future, our results could be partially validated by the RNA seq experiment, carried out from colleagues of University of Milan, by elucidating the genes involved in Mgaloblishvili N. response after *P. viticola* infection.

Appendix: Viticulture in Georgia and Mgaloblishvili N.

Grapevine regions of Georgia

Georgia has an 8,000 years history of continuous wine making tradition, which is supported by several archeological discoveries. The diverse natural conditions of this region create the best environment for the development of high quality viticulture-winemaking according to the peculiarities of which the country's territory is divided into different viticulture zones: Kakheti, Kartli, Meskheti, Imereti, Racha-Lechkhumi, and the Black sea Coastal zone (Adjara, Guria, Samgrelo and Abkhazeti). The remarkable variable of landscapes ranges from the subtropical Black Sea shores to the snowy Caucasian crest line. Western Georgia has a humid subtropical, maritime climate, while Eastern Georgia has a very wide range of climates. According to historical records, the leader region for viticulture is Kakheti, followed by Imereti, Kartli, Racha-Lechkhumi, Samgrelo, Guria, Adjara and Abkhazeti.

Origin	Accession name	Region	Berry colour	Code
Georgia	Rkatsiteli Tsiteli	Kakheti	b	
Georgia	Borchalo	Kartli	b	
Georgia	Mtsvivani Rachuli	Racha - Lechkhumi	w	
Georgia	Almura Tetri	Adzharia	w	
Georgia	Saperavi Khashmis	Khashmi	-	
Georgia	Gorula (clone)	Kartli	w	
Georgia	Dondghlabi Shavi	Imereti	b	
Georgia	Beglaris Kurdzeni	Racha	w	
Georgia	Mkvrivi Kurdzeni	Kartli	w	
Georgia	Chitistvala Acharuli	Adzharia	b	
Georgia	Kitsstisela	Adzharia	b	
Georgia	Kamuri Sciavi	Guria	b	
Georgia	Dzaghlarchama	Kakheti	w	
Georgia	Mgaloblishvili	Imereti	b	
Georgia	Zhghia Sagviano	Kakheti	b	
Georgia	Kapistoni Tsitsiliani	Guria	w	
Georgia	Pirghebula	Kartli		
Armenia	Rzgi	-		
Georgia	-	wild		
Georgia	-	wild		
Georgia	-	wild		
Georgia	-	wild		
Georgia	-	wild		
Georgia	-	wild		
Georgia	-	wild		



Figure 1 List of 25 Caucasian accessions which showed low susceptibility to downy mildew.

Kakheti is the most renowned winemaking region and wines from Kakhetian grape varieties are made using both European and traditional wine making technology, despite the Kakhetian traditional wine technology has no analogy in the world. Basically, the process consists in pressing grapes in a Satsnakheli (woody winepress) and pouring the grape must (badagi) in the quevri (amphora of fermentation used to preserved a stable temperature). After completion of alcoholic fermentation the "Chacha" (grape skins, stalks and pips) sinks to the bottom and after malolactic fermentation the quevris are closed hermetically. In March the first racking occurs and after that, wine is aged for about a year and systematically controlled. The most wide-spread grape variety in this region is Saperavi, which is made with both technologies. Saperavi is used to produce wonderful pink and sparkling wines. For centuries Kakheti has created and formed an original type of table wine which is characterized by high extraction, a high content of phenolic compounds and tannins, pleasant bouquet, sort-specific aroma and taste.

Imereti is the one of the most diverse regions of Georgia and since climatic conditions and soil composition are very different also the wines are affected. Traditional winemaking here as well as in other regions is linked

with qvevri, which is called Churi in Imereti. Unlike Kakhetian traditional wine here less must is added to chacha. After fermentation, the wine is left in Churi for about two months, and after the removal of the pulp, it is transferred to the barrels and processed. The wine of Imeretian type has beautiful yellow color, full, quite harmonious and cheerful.

Kartli is known for its classic European style and high quality sparkling wines. The vineyards are cultivated in extensive basins of the river Mtkvari and its tributaries Liakhvi and Ksani. Besides local varieties foreign others are also common in this region.

Racha-Lechkhumi is distinguished other regions by scarcity of vineyards and rare grape varieties and The vineyards here are grown mostly on the slopes of River Rioni gorge.

Viticulture and wine making of regions Adjara, Guria, Samgrelo and Abkhazeti is situated along the Black Sea coastal area, the vineyards are at 2-4 m above sea level and extend up to 500 meters. The climate is subtropical, humid, in some areas even wetland and therefore, the vine has a long vegetation period. Guria - Samegrelo region is probably one of the oldest center of winemaking in Georgia related to Colchis.

The vine is central to Georgian culture and tightly bound to their religious heritage and a great deal of attention has recently been falling on Georgia's ancient tradition of qvevri winemaking.

Mgaloblishvili N.

Mgaloblishvili N. is a local variety from the Imereti region of Georgia and its origin is unknown; in the Western Georgia there are mono-varietal vineyards of this grape. 'Mgaloblishvili' is a Georgian surname, probably it is the name of the person who first grew this variety. What is known is that this variety is part of Proles *pontica* subproles *georgica* Negr. provar *tomentosae* Tserts and there are not revealed phenotypic variations so far.

The mature leaf is large, rounded and three lobed. The lower leaf side is covered with felt hairs. The petiole is as long as the main vein. The bunch is medium size, cylindrical-conical or seldom cylindrical and dense or very dense. The berry is medium size, round or slightly ovate and dark red covered with thick wax-like coating. The skin is thick, the flesh is juicy. There are mostly two seeds per berry. The time of ripening begins in the end of September. The yield is medium and the flower is hermaphrodite. Mgaloblishvili varietal wine is slightly colored, simple, with low body and therefore it is blended with 'Otskhanuri Sapere' to get intensively colored youthful red table wine. It is also recommended for production of brandy spirits.

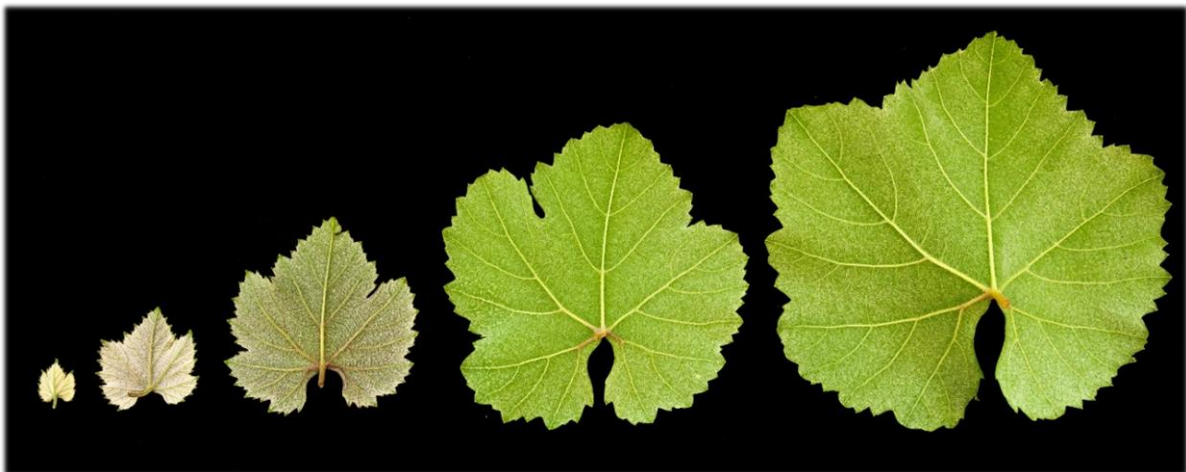


Figure 2 **Mgaloblishvili N. leaves at different stages.** Representation of abaxial surface of five leaves which show different degree of hairiness.

During the various seasons Mgaloblishvili N. has been observed in the field and it can be described under a phenologic and ampelographic point of view. From leaf fall to the beginning of growth in spring, grapevines are dormant and consist entirely of woody tissue. Time of bud burst begins on the first ten days of April, when temperatures warm in the spring and pruning wounds begin to "bleed". The newly emerged shots grow rapidly and soon cluster inflorescences become visible. After a few weeks, usually in the end of May depending from

weather conditions, inflorescences begin to swell and flowers open. The flowering period lasts for approximately two or three weeks and further flower cluster primordia begin to originate in buds and will continue to develop until veraison around the middle of August. Several weeks after fruit set, veraison begins followed by the time of ripening at the beginning of the second ten days of October.



Figure 3 **Phenological stages.** A) Bud burst B) Blooming C) Fruit set D) Veraison E) Ripening

Table 1 **Analytical results.** The followed data were obtained by chemical analysis supplied by Centro Trasferimento Tecnologico (CTT) of Edmund Mach Foundation

Mgaloblishvili N.	Fresh must
Brix (°)	18.21
pH	2.78
Total acidity (g/l) (as Tartaric acid)	15.6
Relative density at 20°C	1.0793
Tartaric acid (g/l)	6.75
Malic acid (g/l)	10.41
Potassium (mg/l)	1529
Available nitrogen (mg/l)	< 20

According to our previous phylogenetic analyses, 'Mgaloblishvili N.' showed several wild features which described it as a high homozygous cultivar, really closed to *V. vinifera* subsp. *sylvestris*, and characterized by the plastidial haplotype A, typical of the more ancient cultivars (ND).

Moreover, since the tolerance traits which characterized this cultivar, a genetic screening with markers linked to the already published RPV loci was performed as described in Chapter 2.

Table 2 **List of RPV and REN1 loci associated markers tested on 'Mgaloblishvili N.' accessions and relative sizes.** Sizes linked to resistant traits are in bold.

	Rpv12											
	<i>udv350</i>	<i>udv350</i>	<i>udv370</i>	<i>udv370</i>	<i>udv343</i>	<i>udv343</i>	<i>udv345</i>	<i>udv345</i>	<i>udv360</i>	<i>udv360</i>	<i>Gf14-28</i>	<i>Gf14-28</i>
Kumbarat											152	160
Monica	308	322	198	208	162	218	220	244	208	210		
Mgaloblishvili N.	306	308	188	196	192	192	214	220	194	194	154	168

	Rpv10							
	<i>Gf09-44</i>	<i>Gf09-44</i>	<i>Gf09-46</i>	<i>Gf09-46</i>	<i>Gf09-47</i>	<i>Gf09-47</i>	<i>Gf09-55</i>	<i>Gf09-55</i>
Solaris	230	246	410	420	294	296	248	260
Mgaloblishvili N.	230	242	402	418	290	294	238	260

	Rpv3				RPV1+RUN1				
	<i>vmc7f2</i>	<i>vmc7f2</i>	<i>Gf18-06</i>	<i>Gf18-06</i>	<i>wim11</i>	<i>wim11</i>	<i>vmc1g3.2</i>	<i>vmc1g3.2</i>	
Regent	206	210	384	390	BC4	270	292	118	136
Mgaloblishvili N.	206	206	382	384	Mgaloblishvili N.	270	270	128	136

REFERENCES

1. Toffolatti SL, Maddalena G, Salomoni D, Maghradz, D, Bianco PA., Failla O. **Evidence of resistance to the downy mildew agent *Plasmopara viticola* in the Georgian *Vitis vinifera* germplasm.** *Vitis - J. Grapevine Res.* 2016;**128**:121–8.
2. Jaillon O, Aury J-M, Noel B, Policriti A, Clepet C, Casagrande A, Choisne N, Aubourg S, Vitulo N, Jubin C, Vezzi A, Legeai F, Huguency P, Dasilva C, Horner D, Mica E, Jublot D, Poulain J, Bruyère C, Billault A, Segurens B, Gouyvenoux M, Ugarte E, Cattonaro F, Anthouard V, Vico V, Del Fabbro C, Alaux M, Di Gaspero G, Dumas V, et al. **The grapevine genome sequence suggests ancestral hexaploidization in major angiosperm phyla.** *Nature* 2007, **449**:463–7.
3. Velasco R, Zharkikh A, Troggio M, Cartwright DA, Cestaro A, Pruss D, Pindo M, FitzGerald LM, Vezzulli S, Reid J, Malacarne G, Iliev D, Coppola G, Wardell B, Micheletti D, Macalma T, Facci M, Mitchell JT, Perazzolli M, Eldredge G, Gatto P, Oyzerski R, Moretto M, Gutin N, Stefanini M, Chen Y, Segala C, Davenport C, Dematté L, Mraz A, et al. **A high quality draft consensus sequence of the genome of a heterozygous grapevine variety.** *PLoS One* 2007, **2(12)**: e13.
4. Jansen RK, Kaittanis C, Saski C, Lee B, Tomkins J, Alverson AJ, et al. **Phylogenetic analyses of *Vitis* (Vitaceae) based on complete chloroplast genome sequences : effects of taxon sampling and phylogenetic methods on resolving relationships among rosids.** *BMC Evolutionary Biology* 2006, **14**:1–14.
5. Rossetto M, Jackes BR, Scott KD, Henry RJ. **Intergeneric relationships in the Australian Vitaceae: New evidence from cpDNA analysis.** *Genet Resour Crop Evol* 2001, **48**:307–314.
6. Ingrouille MJ, Chase MW, Fay MF, Bowman D, Van Der Bank M, Bruijn ADE. **Systematics of Vitaceae from the viewpoint of plastid rbcL DNA sequence data.** *Bot J Linn Soc* 2002, **138**:421–432.
7. Soejima A, Wen J. **Phylogenetic analysis of the grape family (Vitaceae) based on three chloroplast markers.** *Am J Bot* 2006, **93**:278–287.
8. Wen J, Nie Z-L, Soejima A, Meng Y. **Phylogeny of Vitaceae based on the nuclear GAI1 gene sequences.** *Can J Bot* 2007, **85**:731–745.
9. Kubitzki K. **The Families and Genera of Vascular Plants.** Volume 53; 2007.
10. Wan Y, Schwaninger HR, Baldo AM, Labate JA, Zhong G-Y, Simon CJ. **A phylogenetic analysis of the grape genus (*Vitis* L.) reveals broad reticulation and concurrent diversification during neogene and quaternary climate change.** *BMC Evol Biol* 2013, **13**:141.
11. Hewitt G. **The genetic legacy of the Quaternary ice ages.** *Nature* 2000, **405**:907–913.
12. This P, Lacombe T, Thomas MR. **Historical origins and genetic diversity of wine grapes.** *Trends Genet* 2006, **22**:511–519.
13. Arroyo-García R, Ruiz-García L, Bolling L, Ocete R, López MA, Arnold C, Ergul A, Söylemezoğlu G, Uzun HI, Cabello F, Ibáñez J, Aradhya MK, Atanassov A, Atanassov I, Balint S, Cenis JL, Costantini L, Gorislavets S, Grandó MS, Klein BY, McGovern PE, Merdinoglu D, Pejic I, Pelsy F, Primikiriou N, Risovannaya V, Roubelakis Angelakis KA, Snoussi H, Sotiri P, Tamhankar S, et al. **Multiple origins of cultivated grapevine (*Vitis vinifera* L. ssp. sativa) based on chloroplast DNA polymorphisms.** *Mol Ecol* 2006, **15**:3707–3714.
14. De Andres MT, Benito A, Perez-River G, Ocete R, Lopez MA, Gaforio L, et al. **Genetic diversity of wild grapevine populations in Spain and their genetic relationships with cultivated grapevines.** *Mol. Ecol.* 2012, **21**:800–16.
15. Di Vecchi-Staraz M, Laucou V, Bruno G, Lacombe T, Gerber S, Bourse T, Boselli M, This P. **Low level of pollen-mediated gene flow from cultivated to wild grapevine: Consequences for the evolution of the endangered subspecies *Vitis vinifera* L. subsp. silvestris.** *J Hered* 2009, **100**:66–75.

16. Somers D, Lopes MS, Mendonça D, Rodrigues dos Santos M, Eiras-Dias JE, da Câmara Machado A. **New insights on the genetic basis of Portuguese grapevine and on grapevine domestication.** *Genome* 2009, **52**:790–800.
17. Zinelabidine LH, Haddioui A, Bravo G, Arroyo-García R, Zapater JMM, Martínez Zapater JM. **Genetic origins of cultivated and wild grapevines from morocco.** *Am. J. Enol. Vitic.* 2010, **1**:83–90.
18. Gómez A, Lunt DH. **Refugia within refugia: patterns of phylogeographic concordance in the Iberian Peninsula.** *Phylogeography of southern European refugia.* Springer Netherlands. 2007, 155-188.
19. De Blij, Harm J. **Wine : a geographic appreciation.** Rowman & Littlefield Pub Incorporated 1983.
20. Ellstrand NC. **Dangerous Liaisons?: when cultivated plants mate with their wild relatives.** JHU Press 2003.
21. Keller LF, Waller DM. **Inbreeding effects in wild populations.** *Trends Ecol. Evol.* 2002, **17**:230–41.
22. Boso S, Kassemeyer HH. **Different susceptibility of European grapevine cultivars for downy mildew.** *Vitis - J. Grapevine Res.* 2008, **47**:39–49.
23. Arroyo-García R, Revilla E: **The Current Status of Wild Grapevine Populations (*Vitis vinifera* ssp *sylvestris*) in the Mediterranean Basin.** *Mediterr Genet Code - Grapevine Olive* 2013, 51–72.
24. Duan D, Halter D, Baltenweck R, Tisch C, Tröster V, Kortekamp A, Hugueney P, Nick P. **Genetic diversity of stilbene metabolism in *Vitis sylvestris*.** *J Exp Bot* 2015, **66**:3243–3257.
25. Schenk PM, Kazan K, Wilson I, Anderson JP, Richmond T, Somerville SC, et al. **Coordinated plant defense responses in *Arabidopsis* revealed by microarray analysis.** *Proc. Natl. Acad. Sci.* 2000; **97**:11655–11660.
26. Brooks DM, Bender CL, Kunkel BN. **The *Pseudomonas syringae* phytotoxin coronatine promotes virulence by overcoming salicylic acid-dependent defences in *Arabidopsis thaliana*.** *Mol. Plant Pathol.* 2005, **6**:629–39.
27. Beckers GJM, Spoel SH. **Fine-tuning plant defence signalling: salicylate versus jasmonate.** *Plant Biol.* 2006, **8**:1–10.
28. Mur LAJ, Kenton P, Atzorn R, Miersch O, Wasternack C. **The outcomes of concentration-specific interactions between salicylate and jasmonate signaling include synergy , antagonism , and oxidative stress leading to cell death.** *Plant Physiology* 2006, **140(1)**: 249-262.
29. Robert-Seilaniantz A, Grant M, Jones JDG. **Hormone crosstalk in plant disease and defense: more than just jasmonate-salicylate antagonism.** *Annu. Rev. Phytopathol.* 2011, **49**:317–43.
30. Glazebrook J. **Contrasting mechanisms of defense against biotrophic and necrotrophic pathogens.** *Annu. Rev. Phytopathol.* 2005, **43**:205–27.
31. Bari R, Jones JDG. **Role of plant hormones in plant defence responses.** *Plant Mol. Biol.* 2009, **69**:473–88.
32. Berrocal-Lobo M, Molina A, Solano R. **Constitutive expression of ETHYLENE-RESPONSE-FACTOR1 in *Arabidopsis* confers resistance to several necrotrophic fungi.** *Plant J.* 2002, **29**:23–32.
33. Jones JD, Dangl J. L.. **The plant immune system.** *Nature* 2006, **444**:323–9.
34. Wrolstad RE. **Anthocyanins.** *Nat. Food Color.* Lauro GJ FF, editor. 2000, 237–52.
35. Federal S, Pezet R, Gindro K, Viret O, Richter H. **Effects of resveratrol, viniferins and pterostilbene on *Plasmopara viticola* zoospore mobility and disease development.** *Vitis - J. Grapevine Res.* 2004, **43**:145–8.
36. Malacarne G, Vrhovsek U, Zulini L, Cestaro A, Stefanini M, Mattivi F, Delledonne M, Velasco R, Moser C. **Resistance to *Plasmopara viticola* in a grapevine segregating population is associated with stilbenoid accumulation and with specific host transcriptional responses.** *BMC Plant Biol.* 2011, **11**:114.
37. Sbaghi M, Jeandet P, Bessis R, Leroux P. **Degradation of stilbene-type phytoalexins in relation to the pathogenicity of *Botrytis cinerea* to grapevines.** *Plant Pathol.* 1996, **45**:139–44.
38. Du H, Zhang L, Liu L, Tang X-F, Yang W, Wu Y, et al. **Biochemical and molecular characterization of plant MYB**

- transcription factor family. *Biochem.* 2009, **74**:1–11.
39. Boudet A. **Evolution and current status of research in phenolic compounds.** *Phytochemistry* 2007, **68**:2722–35.
40. Matus J, Aquea F, Arce-Johnson P. **Analysis of the grape MYB R2R3 subfamily reveals expanded wine quality-related clades and conserved gene structure organization across *Vitis* and *Arabidopsis* genomes.** *BMC Plant Biol.* 2008, **8**:83.
41. Armijo G, Schlechter R, Agurto M, Muñoz D, Nuñez C, Arce-Johnson P. **Grapevine pathogenic microorganisms: understanding infection strategies and host response scenarios.** *Front. Plant Sci.* 2016, **7**:382.
42. Yu Y, Zhang Y, Yin L, Lu J. **The mode of host resistance to *Plasmopara viticola* infection of grapevines.** *Phytopathology.* 2012, **102(11)**: 1094-1101.
43. Rafaila C. and Z. David. **Morphological modifications in the sporangia and sporangiophores of *P. viticola* in relation to Vine vars. and environmental conditions.** *Lucrarile Gradinii botanice din Bucuresti* 1963, **2**:983–992.
44. Gómez-Zeledón J, Zipper R, Spring O. **Assessment of phenotypic diversity of *Plasmopara viticola* on *Vitis* genotypes with different resistance.** *Crop Prot.* Elsevier Ltd 2013; **54**:221–8.
45. Dussert Y, Gouzy J, Richart-Cervera S, Mazet ID, Delière L, Couture C, et al. **Draft genome sequence of *Plasmopara viticola*, the grapevine downy mildew pathogen.** *Genome Announc.* 2016; **4**:e00987-16.
46. Yin L, An Y, Qu J, Li X, Zhang Y, Dry I, et al. **Genome sequence of *Plasmopara viticola* and insight into the pathogenic mechanism.** *Sci. Rep.* Nature Publishing Group. 2017, **7**:46553.
47. Grattapaglia D, Sederoff R, Carolina N. **Genetic linkage maps of *Eucalyptus grandis* and *Eucalyptus urophylla* using a pseudo-testcross: mapping strategy and RAPD markers.** *Genetics* 1994, **137(4)**:1121–37.
48. Williams JGK, Kubelik AR, Livak KJ, Rafalski JA, Tingey SV. **DNA polymorphisms amplified by arbitrary primers are useful as genetic markers.** *Nucleic acids research* 1990, **18(22)**: 6531-6535.
49. Zabeau M and Vos P, Zabeau M, Vos P. **Selective restriction fragment amplification: fingerprinting.** U.S. Patent No 6,045,994, 2000.
50. Gupta PK, Balyan IS, Sharma PC RB, Gupta PK, Balyan HS, Sharma PC, Ramesh B. **Microsatellites in plants: A new class of molecular markers.** *Curr. Sci.* 1996, **70**:45–54.
51. Merdinoglu D, Butterlin G, Bevilacqua L, Chiquet V, Adam-Blondon A-F, Decroocq S. **Development and characterization of a large set of microsatellite markers in grapevine (*Vitis vinifera* L.) suitable for multiplex PCR.** *Mol. Breed.* 2005, **15**:349–66.
52. Di Gaspero G, Cipriani G, Marrazzo MT, Andreetta D, Castro MJP, Peterlunger E, et al. **Isolation of (AC)_n-microsatellites in *Vitis vinifera* L. and analysis of genetic background in grapevines under marker assisted selection.** *Mol. Breed.* 2005,**15**:11–20.
53. Adam-Blondon AF, Roux C, Claux D, Butterlin G, Merdinoglu D, This P. **Mapping 245 SSR markers on the *Vitis vinifera* genome: A tool for grape genetics.** *Theor. Appl. Genet.* 2004, **109**:1017–27.
54. Doligez A, Adam-Blondon AF, Cipriani G, Di Gaspero G, Laucou V, Merdinoglu D, et al. **An integrated SSR map of grapevine based on five mapping populations.** *Theor. Appl. Genet.* 2006, **113**:369–82.
55. Doligez A, Bouquet A, Danglot Y, Lahogue F, Riaz S, Meredith CP, Edwards KJ, This P. **Genetic mapping of grapevine (*Vitis vinifera* L.) applied to the detection of QTLs for seedlessness and berry weight.** *Theor Appl Genet* 2002, **105**:780–795.
56. Riaz S, Dangl GS, Edwards KJ, Meredith CP. **A microsatellite marker based framework linkage map of *Vitis vinifera* L.** *Theor. Appl. Genet.* 2004, **108**:864–72.
57. Riaz S, Krivanek AF, Xu K, Walker MA. **Refined mapping of the Pierce’s disease resistance locus, PdR1, and Sex on an extended genetic map of *Vitis rupestris* × *V. arizonica*.** *Theor. Appl. Genet.* 2006, **113**:1317–29.

58. Troggio M, Malacarne G, Coppola G, Segala C, Cartwright DA, Pindo M, et al. **A dense single-nucleotide polymorphism-based genetic linkage map of grapevine (*Vitis vinifera* L.) anchoring pinot noir bacterial artificial chromosome contigs.** *Genetics*. 2007, **176**:2637–50.
59. Di Gaspero G, Cipriani G, Adam-Blondon A-F, Testolin R. **Linkage maps of grapevine displaying the chromosomal locations of 420 microsatellite markers and 82 markers for R-gene candidates.** *Theor. Appl. Genet.* 2007, **114**:1249–63.
60. Salmaso M, Malacarne G, Troggio M, Faes G, Stefanini M, Grando MS, et al. **A grapevine (*Vitis vinifera* L.) genetic map integrating the position of 139 expressed genes.** *Theor. Appl. Genet.* 2008, **116**:1129–43.
61. Costantini L, Battilana J, Lamaj F, Fanizza G, Grando M. **Berry and phenology-related traits in grapevine (*Vitis vinifera* L.): From Quantitative Trait Loci to underlying genes.** *BMC Plant Biol.* 2008, **8**:38.
62. Myles S. **Improving fruit and wine: what does genomics have to offer?** *Trends Genet.* 2013, **29**:190–6.
63. Merdinoglu D, Wiedeman-Merdinoglu S, Coste P, Dumas V, Haetty S, Butterlin G, et al. **Genetic analysis of downy mildew resistance derived from *Muscadinia rotundifolia*.** *Acta Hortic.* 2003, 451–6.
64. Peressotti E, Wiedemann-Merdinoglu S, Delmotte F, Bellin D, Di Gaspero G, Testolin R, et al. **Breakdown of resistance to grapevine downy mildew upon limited deployment of a resistant variety.** *BMC Plant Biol.* 2010, **10**:147.
65. Marguerit E, Boury C, Manicki A, Donnart M, Butterlin G, Némorin A, et al. **Genetic dissection of sex determinism, inflorescence morphology and downy mildew resistance in grapevine.** *Theor. Appl. Genet.* 2009, **118**:1261–78.
66. Bellin D, Peressotti E, Merdinoglu D, Wiedemann-Merdinoglu S, Adam-Blondon AF, Cipriani G, et al. **Resistance to *Plasmopara viticola* in grapevine “Bianca” is controlled by a major dominant gene causing localised necrosis at the infection site.** *Theor. Appl. Genet.* 2009, **120**:163–76.
67. Casagrande K, Falginella L, Castellarin SD, Testolin R, Di Gaspero G. **Defence responses in Rpv3-dependent resistance to grapevine downy mildew.** *Planta* 2011, **234**:1097–109.
68. Di Gaspero G, Copetti D, Coleman C, Castellarin SD, Eibach R, Kozma P, et al. **Selective sweep at the Rpv3 locus during grapevine breeding for downy mildew resistance.** *Theor. Appl. Genet.* 2012, **124**:277–86.
69. Blasi P, Blanc S, Wiedemann-Merdinoglu S, Prado E, Rühl EH, Mestre P, et al. **Construction of a reference linkage map of *Vitis amurensis* and genetic mapping of Rpv8, a locus conferring resistance to grapevine downy mildew.** *Theor. Appl. Genet.* 2011, **123**:43–53.
70. Schwander F, Eibach R, Fechter I, Hausmann L, Zyprian E, Töpfer R. **Rpv10: a new locus from the Asian *Vitis* gene pool for pyramiding downy mildew resistance loci in grapevine.** *Theor. Appl. Genet.* 2012, **124**:163–76.
71. Venuti S, Copetti D, Folia S, Falginella L, Hoffmann S, Bellin D, et al. **Historical introgression of the downy mildew resistance gene Rpv12 from the Asian species *Vitis amurensis* into grapevine varieties.** *PLoS One* Nelson JC, editor. 2013, **8**:e61228.
72. Williams SJ, Yin L, Foley G, Casey LW, Outram MA, Ericsson DJ, et al. **Structure and function of the TIR domain from the grape NLR protein RPV1.** *Front. Plant Sci.* 2016, **7**:1–13.
73. Kang MS. **Quantitative genetics, genomics and plant breeding.** CABI, 2002
74. Díez-Navajas AM, Wiedemann-Merdinoglu S, Greif C, Merdinoglu D. **Nonhost versus host resistance to the grapevine downy mildew, *Plasmopara viticola*, studied at the tissue level.** *Phytopathology* 2008, **98**:776–80.
75. Jürges G, Kassemeyer H-H, Dürrenberger M, Düggelin M, Nick P. **The mode of interaction between *Vitis* and *Plasmopara viticola* Berk. & Curt. Ex de Bary depends on the host species.** *Plant Biol.* 2009, **11**:886–98.
76. Eibach R, Zyprian E, Welter L, Töpfer R. **The use of molecular markers for pyramiding resistance genes in grapevine breeding.** *Vitis - J. Grapevine Res.* 2007, **46**:120–4.

77. Nelson RR. **Genetics of horizontal resistance to plant diseases.** *Annu. Rev. Phytopathol.* 1978, **16**:359–78.
78. Gray DJ, Li ZT, Dhekney SA. **Precision breeding of grapevine (*Vitis vinifera* L.) for improved traits.** *Plant Sci.* Elsevier Ireland Ltd 2014, **228**:3–10.
79. McGovern PE. **Stone age wine.** *Anc. Wine.* 2003, 1–15.
80. Olmo HP. **Breeding tetraploid grapes.** *Proc. Amer. Soc. Hort. Sci.* 1952, **59**:285–90.
81. Kighuradze T. **Georgia, the cradle of viticulture and winemaking.** *J. Vazi da Ghvino.* Tblisi 2000, 27–9.
82. Ramishvili R. **History of Georgian grapevine and wine.** 2001, 240.
83. Chilashvili L. **The Vine, Wine and the Georgians.** Tblisi Petite, 2004.
84. Costantini L, Kvavadze E RN. **The antiquity of grapevine cultivation in Georgia.** *J. Vazi da Ghvino.* Tblisi, 2006.
85. Chkhartishvili DM. **Viticulture and winemaking in Georgia.** Caucasus and Northern Black Sea Region 2012, 169-239.
86. Negrul AM. **Evolution of cultivated forms of grapes.** *CR Acad Sci URSS.* 1938, 585–8.
87. Olmo HP. **Selecting and breeding new grape cultivars.** *Calif. Agric.* 1980, 23–4.
88. Sefc KM, Lopes MS, Lefort F, Botta R, Roubelakis-Angelakis KA, Ibáñez J, et al. **Microsatellite variability in grapevine cultivars from different European regions and evaluation of assignment testing to assess the geographic origin of cultivars.** *Theor. Appl. Genet.* 2000, **100**:498–505
89. Shaw J, Small RL. **Chloroplast DNA phylogeny and phylogeography of the North American plums (*Prunus* subgenus *Prunus* section *Prunocerasus*, *Rosaceae*).** *Am. J. Bot.* 2005, **92**:2011–30.
90. Riaz S, Boursiquot J, Dangl GS, Lacombe T, Laucou V, Tenschler AC, et al. **Identification of mildew resistance in wild and cultivated Central Asian grape germplasm.** *BMC Plant Biol.* 2013, **13**:149.
91. Coleman C, Copetti D, Cipriani G, Hoffmann S, Kozma P, Kovacs L, et al. **The powdery mildew resistance gene *REN1* co-segregates with an NBS-LRR gene cluster in two Central Asian grapevines.** *BMC Genet.* 2009, **10**:89.
92. Hoffmann S, Di Gaspero G, Kovács L, Howard S, Kiss E, Galbács Z, et al. **Resistance to *Erysiphe necator* in the grapevine “Kishmish vatkana” is controlled by a single locus through restriction of hyphal growth.** *Theor. Appl. Genet.* 2008, **116**:427–38.
93. Amrine KCH, Blanco-Ulate B, Riaz S, Pap D, Jones L, Figueroa-Balderas R, et al. **Comparative transcriptomics of Central Asian *Vitis vinifera* accessions reveals distinct defense strategies against powdery mildew.** *Hortic. Res.* 2015, **2**:15037.
94. Lózsa R, Xia N, Deák T, Bisztray GD. **Chloroplast diversity indicates two independent maternal lineages in cultivated grapevine (*Vitis vinifera* L. subsp. *vinifera*).** *Genet. Resour. Crop Evol.* 2015, **62**:419–29.
95. Welter LJ, Göktürk-Baydar N, Akkurt M, Maul E, Eibach R, Töpfer R, et al. **Genetic mapping and localization of quantitative trait loci affecting fungal disease resistance and leaf morphology in grapevine (*Vitis vinifera* L.).** *Mol. Breed.* 2007, **20**:359–74.
96. Barker CL, Donald T, Pauquet J, Ratnaparkhe MB, Bouquet A, Adam-Blondon AF, et al. **Genetic and physical mapping of the grapevine powdery mildew resistance gene, *Run1*, using a bacterial artificial chromosome library.** *Theor. Appl. Genet.* 2005, **111**:370–7.
97. Laucou V, Lacombe T, Dechesne F, Siret R, Bruno J-P, Dessup M, et al. **High throughput analysis of grape genetic diversity as a tool for germplasm collection management.** *Theor. Appl. Genet.* 2011, **122**:1233–45.
98. Sefc KM, Regner F, Turetschek E, Glössl J, Steinkellner H. **Identification of microsatellite sequences in *Vitis riparia* and their applicability for genotyping of different *Vitis* species.** *Genome.* 1999, **42**:367–73.
99. Maul E, Sudharma KN, Kecke S, Marx G, Müller C, Audeguin L, et al. **The European *Vitis* Database ([101](http://www.eu-</p>
</div>
<div data-bbox=)**

- vitis. de)—a technical innovation through an online uploading and interactive modification system. *Vitis - J. Grapevine Res.* 2012, **51**:79–85.
100. Peakall R, Smouse PE. **GenAlEx 6.5: genetic analysis in Excel. Population genetic software for teaching and research—an update.** *Bioinformatics* 2012, **28**:2537–9.
101. X. Perrier JPJ-C. **DARwin software** 2006.
102. Pritchard JK, Wen X, Falush D. **Documentation for structure software : Version 2.3.** Univ. Chicago. 2010, **6**:321–6.
103. Pritchard JK, Stephens M, Donnelly P. **Inference of population structure using multilocus genotype data.** *Genetics.* 2000, **155**:945–59.
104. Price AL, Patterson NJ, Plenge RM, Weinblatt ME, Shadick NA, Reich D. **Principal components analysis corrects for stratification in genome-wide association studies.** *Nat. Genet.* 2006, **38**:904–9.
105. Earl DA, VonHoldt BM. **STRUCTURE HARVESTER: a website and program for visualizing STRUCTURE output and implementing the Evanno method.** *Conserv. Genet. Resour.* 2012, **4**:359–61.
106. Evanno G, Regnaut S, Goudet J. **Detecting the number of clusters of individuals using the software STRUCTURE: a simulation study.** *Mol. Ecol.* 2005, **14**:2611–20.
107. Boutin-Ganache I, Raposo M, Raymond M DC. **M13-tailed primers improve the readability and usability of microsatellite analyses performed with two different allele-sizing methods.** *Biotechniques.* 2001
108. Emanuelli F, Lorenzi S, Grzeskowiak L, Catalano V, Stefanini M, Troggio M, et al. **Genetic diversity and population structure assessed by SSR and SNP markers in a large germplasm collection of grape.** *BMC Plant Biol.* 2013, **13**:39.
109. Marrano A, Grzeskowiak L, Moreno Sanz P, Lorenzi S, Prazzoli ML, Arzumanov A, et al. **Genetic diversity and relationships in the grapevine germplasm collection from Central Asia.** *Vitis - J. Grapevine Res.* 2015, **54**:233–7.
110. Drori E, Rahimi O, Marrano A, Henig Y, Brauner H, Salmon-Divon M, et al. **Collection and characterization of grapevine genetic resources (*Vitis vinifera*) in the Holy Land, towards the renewal of ancient winemaking practices.** *Sci. Rep.* Nature Publishing Group 2017, **7**:44463.
111. Templeton AR. **Population Genetics and Microevolutionary Theory.** Hoboken, NJ, USA: John Wiley & Sons, Inc., 2006.
112. Allendorf FW, Luikart G. **Conservation and the genetics of populations.** John Wiley & Sons, 2009.
113. Lomouri N. **Greek colonization of Colchian coastal region.** 1962
114. Lortkipanidze M, Muskhelishvili D, Metreveli R. **History of Georgia.** 2012, **2**.
115. Karataş DD, Karataş H, Laucou V, Sarikamiş G, Riahi L, Bacilieri R, This P. **Genetic diversity of wild and cultivated grapevine accessions from southeast Turkey.** *Hereditas.* 2014, **151**:73–80.
116. Grassi F, Labra M, Imazio S, Spada A, Sgorbati S, Scienza A, et al. **Evidence of a secondary grapevine domestication centre detected by SSR analysis.** *Theor. Appl. Genet.* 2003, **107**:1315–20.
117. Imazio S, Maghradze D, de Lorenzis G, Bacilieri R, Laucou V, This P, et al. **From the cradle of grapevine domestication: molecular overview and description of Georgian grapevine (*Vitis vinifera* L.) germplasm.** *Tree Genet. Genomes.* 2013, **9**:641–658.
118. Marrano A, Birolo G, Prazzoli ML, Lorenzi S, Valle G, Grando MS. **SNP-discovery by RAD-sequencing in a germplasm collection of wild and cultivated grapevines (*V. vinifera* L.).** *PLoS One* 2017, **12**:e0170655.
119. Bitsadze N, Aznarashvili M, Vercesi A, Chipashvili R, Failla O **Screening of Georgian grapevine germplasm for susceptibility to downy mildew (*Plasmopara viticola*).** *Vitis - J. Grapevine Res.* 2015, **54**: 193-196.

120. Pfender WF, Saha MC, Johnson EA, Slabaugh MB. **Mapping with RAD (restriction-site associated DNA) markers to rapidly identify QTL for stem rust resistance in *Lolium perenne***. *Theor. Appl. Genet.* 2011, **122**:1467–80.
121. Wang S, Meyer E, McKay JK, Matz M V. **2b-RAD: a simple and flexible method for genome-wide genotyping**. *Nat. Methods.* 2012, **9**:808–10.
122. Doyle JJ. **Isolation of DNA from small amounts of plant tissues**. *BRL Focus.* 1990, 12.
123. Thomas MR, Cain P, Scott NS. **DNA typing of grapevines: A universal methodology and database for describing cultivars and evaluating genetic relatedness**. *Plant Mol. Biol.* 1994, **25**:939–49.
124. Bowers JE, Meredith CP. **The parentage of a classic wine grape, Cabernet Sauvignon**. *Nat. Genet.* 1997, **16**:84–7.
125. Cipriani G, Marrazzo M, Di Gaspero G, Pfeiffer A, Morgante M, Testolin R. **A set of microsatellite markers with long core repeat optimized for grape (*Vitis* spp.) genotyping**. *BMC Plant Biol.* 2008, **8**:127.
126. Scott KD, Eggler P, Seaton G, Rossetto M, Ablett EM, Lee LS, et al. **Analysis of SSRs derived from grape ESTs**. *Theor. Appl. Genet.* 2000, **100**:723–726.
127. Fechter I, Hausmann L, Zyprian E, Daum M, Holtgräwe D, Weisshaar B, et al. **QTL analysis of flowering time and ripening traits suggests an impact of a genomic region on linkage group 1 in *Vitis***. *Theor. Appl. Genet.* 2014, **127**:1857–72.
128. Bonfield JK, Smith KF, Staden R. **A new DNA sequence assembly program**. *Nucleic Acids Res.* 1995, **23**:4992–9.
129. Van Ooijen JW. **JoinMap 4. Software for the calculation of genetic linkage maps in experimental populations**. Kyazma BV, Wageningen, the Netherlands. 2006.
130. Kosambi DD. **The estimation of map distances from recombination values**. *Ann. Eugen.* 1943, **12**:172–5.
131. Voorrips RE. **MapChart: Software for the Graphical Presentation of Linkage Maps and QTLs**. *J. Hered.* 2002, **93**:77–78.
132. Hubert SH, Ilott TW, Legg EJ, Lincoln SE, Lander ES, Michelmore RW. **Genetic analysis of the fungus, *Bremia lactucae*, using restriction fragment length polymorphisms**. *Genetics* 1988, **120**(4): 947-958.
133. Lowe KM, Walker MA. **Genetic linkage map of the interspecific grape rootstock cross Ramsey (*Vitis champinii*) × Riparia Gloire (*Vitis riparia*)**. *Theor. Appl. Genet.* 2006, **112**:1582–1592.
134. Toffolatti S, Venturini G, Maffi D, Vercesi A. **Phenotypic and histochemical traits of the interaction between *Plasmopara viticola* and resistant or susceptible grapevine varieties**. *BMC Plant Biol.* 2012, **12**:124.
135. Van Ooijen JW. **MapQTL 6, software for the mapping of quantitative trait loci in experimental populations of diploid species**. Wageningen, The Netherlands 2009.
136. Lander ES, Botstein S. **Mapping mendelian factors underlying quantitative traits using RFLP linkage maps**. *Genetics.* 1989, **121**:185–199.
137. Fischer BM, Salakhutdinov I, Akkurt M, Eibach R, Edwards KJ, Topfer R, et al. **Quantitative trait locus analysis of fungal disease resistance factors on a molecular map of grapevine**. *Theor. Appl. Genet.* 2004, **108**:501–15.
138. Poehlman JM and Sleper DA. **Breeding field crops**. Springer Science & Business Media, 2013.
139. Fehr, WR. **Principles of cultivar development**. Volume 1.Theory and technique. Macmillan publishing company. 1987.
140. Duchêne E, Butterlin G, Claudel P, Dumas V, Jaegli N, Merdinoglu D. **A grapevine (*Vitis vinifera* L.) deoxy-d-xylulose synthase gene colocates with a major quantitative trait loci for terpenol content**. *Theor. Appl. Genet.*

2009, **118**:541–52.

141. Fornasiero A, Marroni F, Magris G, Di Gaspero G, Morgante M. **Identification and mapping of loci controlling viability in *Vitis vinifera* self-crosses.** Proceedings of the LX SIGA Annual Congress, 2006 Oral Communication

142. Wang C, Zhu C, Zhai H, Wan J. **Mapping segregation distortion loci and quantitative trait loci for spikelet sterility in rice (*Oryza sativa* L.).** *Genet. Res.* 2005, **86**:97.

143. Xu S. **Quantitative trait locus mapping can benefit from segregation distortion.** *Genetics* 2008, **180**:2201–2208.

144. Zhang L, Wang S, Li H, Deng Q, Zheng A, Li S, et al. **Effects of missing marker and segregation distortion on QTL mapping in F2 populations.** *Theor. Appl. Genet.* 2010, **121**:1071–82.

145. Devaiah BN, Madhuvanthi R, Karthikeyan AS, Raghothama KG. **Phosphate starvation responses and gibberellic acid biosynthesis are regulated by the MYB62 transcription factor in *Arabidopsis*.** *Mol. Plant* The Authors 2009. All rights reserved. 2009, **2**:43–58.

146. Kim KC, Fan B, Chen Z. **Pathogen-induced *Arabidopsis* WRKY7 is a transcriptional repressor and enhances plant susceptibility to *Pseudomonas syringae*.** *Plant Physiol.* 2006, **142**:1180–92.

147. Park CY, Lee JH, Yoo JH, Moon BC, Choi MS, Kang YH, et al. **WRKY group IId transcription factors interact with calmodulin.** *FEBS Lett.* 2005, **579**:1545–1550.

148. Xiao J, Cheng H, Li X, Xiao J, Xu C, Wang S. **Rice WRKY13 regulates cross talk between abiotic and biotic stress signaling pathways by selective binding to different cis-elements.** *Plant Physiol.* 2013, **163**:1868–1882.

149. Gao QM, Venugopal S, Navarre D, Kachroo A. **Low oleic acid-derived repression of jasmonic acid-inducible defense responses requires the WRKY50 and WRKY51 proteins.** *Plant Physiol.* 2011, **155**:464–76.

150. Matsuo M, Johnson JM, Hieno A, Tokizawa M, Nomoto M, Tada Y, et al. **High redox responsive transcription factor1 levels result in accumulation of reactive oxygen species in *Arabidopsis thaliana* shoots and roots.** *Mol. Plant* 2015, **8**:1253–73.

151. Etchells JP, Provost CM, Turner SR. **Plant vascular cell division is maintained by an interaction between PXY and ethylene signalling.** *PLoS Genet.* 2012, **8**.

152. Bahieldin A, Atef A, Edris S, Gadalla NO, Ali HM, Hassan SM, et al. **Ethylene responsive transcription factor ERF109 retards PCD and improves salt tolerance in plant.** *BMC Plant Biology* 2016, **16**:216.

153. Wang F, Muto A, Van de Velde J, Neyt P, Himanen K, Vandepoele K, et al. **Functional analysis of *Arabidopsis* tetraspanin gene family in plant growth and development.** *Plant Physiol.* 2015, **169**:01310

154. Zyprian, E. and Topfer R. Unpublished.

155. Goto-Yamamoto, N., Mouri, H., Azumi, M. and Edwards KJ. Unpublished.

156. Mejía N, Gebauer M, Muñoz L, Hewstone N, Muñoz C, Hinrichsen P. **Identification of QTLs for seedlessness, berry size, and ripening date in a seedless x seedless table grape progeny.** *Am. J. Enol. Vitic.* 2007, **58**:499–507.

157. Sevini, F., Marino, R., Lacombe, T. and Grando MS. **Development and transferability of grape EST-SSR markers suitable for mapping in *Vitis* spp.** Unpublished.

158. Arroyo-García R, Martínez-Zapater JM. **Development and characterization of new microsatellite markers for grape.** *Vitis - J. Grapevine Res.* 2004, **43**:175–8.

159. Pellerone FI, Edwards KJ, Thomas MR. **Grapevine microsatellite repeats: Isolation, characterisation and use for genotyping of grape germplasm from southern Italy.** *Vitis - J. Grapevine Res.* 2001, **40**:179–86.

160. Decroocq V, Favé MG, Hagen L, Bordenave L, Decroocq S. **Development and transferability of apricot and grape EST microsatellite markers across taxa.** *Theor. Appl. Genet.* 2003, **106**:912–22.

161. Olmo HP. **The origin and domestication of the Vinifera grape.** *Orig. Anc. Hist. wine.* Gordon and Breach, Amsterdam 1995, 31-43
162. Vannozzi A, Dry IB, Fasoli M, Zenoni S, Lucchin M. **Genome-wide analysis of the grapevine stilbene synthase multigenic family: genomic organization and expression profiles upon biotic and abiotic stresses.** *BMC Plant Biol.* 2012, **12**:130.
163. Lloyd G, McCown B. **Commercially-feasible micropropagation of mountain laurel, *Kalmia latifolia*, by use of shoot-tip culture.** *Proc. Int. Plant Propagators Soc.* 1981, **30**: 421-427.
164. Murashige T, Skoog F. **A revised medium for rapid growth and bioassays with tobacco tissue cultures.** *Physiol. Plant.* 1962, **15(3)**:473–497.
165. Strober W. **Trypan Blue Exclusion Test of Cell Viability.** *Curr. Protoc. Immunol.* Hoboken, NJ, USA: John Wiley & Sons, Inc. 2001.
166. Peressotti E, Duchêne E, Merdinoglu D, Mestre P. **A semi-automatic non-destructive method to quantify grapevine downy mildew sporulation.** *J. Microbiol. Methods Elsevier B.V.* 2011, **84**:265–271.
167. Merz PR, Moser T, Höll J, Kortekamp A, Buchholz G, Zyprian E, et al. **The transcription factor VvWRKY33 is involved in the regulation of grapevine (*Vitis vinifera*) defense against the oomycete pathogen *Plasmopara viticola*.** *Physiol. Plant.* 2015, **153**:365–380.
168. Holl J, Vannozzi A, Czemplin S, D’Onofrio C, Walker AR, Rausch T, et al. **The R2R3-MYB Transcription Factors MYB14 and MYB15 Regulate Stilbene Biosynthesis in *Vitis vinifera*.** *Plant Cell* 2013, **25**:4135–4149.
169. Moser T. **Untersuchung der transkriptionellen Regulation von Kandidatengenen der Pathogenabwehr gegen *Plasmopara viticola* in der Weinrebe.** 2014, Ph.D thesis deposited in KIT (Karlsruhe Institute of Technology); electronic library.
170. Monteiro F, Sebastiana M, Pais MS, Figueiredo A. **Reference Gene Selection and Validation for the Early Responses to Downy Mildew Infection in Susceptible and Resistant *Vitis vinifera* Cultivars.** *PLoS One.* 2013, **8**.
171. Hellemans J, Mortier G, De Paepe A, Speleman F, Vandesompele J. **qBase relative quantification framework and software for management and automated analysis of real-time quantitative PCR data.** *Genome Biol.* 2007, **8**:R19.
172. Ma Q, Zhang G, Hou L, Wang W, Hao J, Liu X. ***Vitis vinifera* VvWRKY13 is an ethylene biosynthesis-related transcription factor.** *Plant Cell Rep.* Springer Berlin Heidelberg 2015, **34**:1593–1603.
173. Fischer R, Budde I, Hain R. **Stilbene synthase gene expression causes changes in flower colour and male sterility in tobacco.** *The Plant Journal* 1997, **11**:489–498.
174. Greenberg JT. **Programmed cell death in plant-pathogen interactions.** *Annual review of plant biology* 1997, **48(1)**: 525-545
175. Iriti M, Rossoni M, Borgo M, Faoro F. **Benzothiadiazole enhances resveratrol and anthocyanin biosynthesis in grapevine, meanwhile improving resistance to *Botrytis cinerea*.** *J. Agric. Food Chem.* 2004, **52**:4406–13.
176. Chang X, Heene E, Qiao F, Nick P. **The phytoalexin resveratrol regulates the initiation of hypersensitive cell death in *Vitis* cell.** *PLoS One.* 2011, **6**:e26405.

ACKNOWLEDGEMENTS

«It's the time you spent on your rose that makes your rose so important...People have forgotten this truth, but you mustn't forget it. You become responsible for what you've tamed. You're responsible for your rose» is a famous quote of Antoine de Saint-Exupéry, in 'The Little Prince'.

However, it is not just a quote, it is the mainstay of my Ph.D. experience during which I never gave up and I dedicated myself to my project as well as my duties, trying to face problems as best as I could. Everyone has their own experiences, which can be used as a way to face future situations and learn from them. Over the last few years, many people have left and taken a piece of me. Because of that, it is quite difficult to find the right words to express my gratitude to the people that I should, I must and I would like to acknowledge.

Firstly, I would like to sincerely thank my supervisors Dr. Maria Stella Grando and Dr. Osvaldo Failla for the continuous support during my Ph.D. studies and related research. They helped me in every possible way to face and overcome the troubles which I encountered, leaving me the freedom to learn through all the experiences I lived during these years. Thanks to both of you for the time, suggestions, precious advice and teaching.

I wish to express my appreciation and thanks to Dr. Eva Zyprian and Dr. Reinhard Töpfer to have hosted me in their laboratories at JKI. They gave me the opportunity to join their team as an intern and gave me access to their research facilities. A special thanks must go to Dr. Zyprian for the support, encouragement and for the kind hospitality which made me feel at home.

I greatly appreciate the support received through the collaborative work done with the staff of FEM (Fondazione E. Mach), UNIMI (Università di Milano) and JKI (Julius Kühn-Institut) during the different phases of my research and during my field work. Moreover, I would like to thank the FIRST program and the University of Milan for the financial support.

I would like to thank the "FEMily" and the "JKI Ph.D. community" with whom I have shared unforgettable moments. My Ph.D. experience was not just a scientific and educational investment, but mostly a personal growth. A special thanks goes to Annarita, Daniele, Silvia, Paula, Florian, Daniel and Nicolai which have been more than co-workers, they have been good friends. I cannot mention all of the people to whom I feel grateful both professionally and personally.

A special word of thanks to Matteo, the man who has made all the difference in my life. I am thankful for your love, confidence, optimism and tolerance. But you already know that, no other words are needed.

Finally, I would like to dedicate this thesis to my parents who love me unconditionally. Mum and Dad, I could never have done this without your faith, support and constant encouragement. Thank you for teaching me to believe in myself, in God and in my dreams.

Maria Lucia Protti